# SUMO and SUMO-targeted Ubiquitin Ligases in Protein Quality Control


Dissertation

zur

Erlangung des Doktorgrades

der Mathematisch-Naturwissenschaftlichen Fakultät

der Universität zu Köln

vorgelegt von

Friederike Profe-Austermann

2025

# Table of Contents

# List of Figures

# List of Tables

# Abstract

The **s**mall **u**biquitin-like **mo**difier (SUMO) is a posttranslational modification involved in various cellular processes, such as the regulation of the cell cycle and genome stability. Through so-called **S**UMO-**t**argeted **U**biquitin **l**igases (STUbLs), SUMOylation can also lead to the degradation of proteins. STUbLs recognize SUMO chains via their **S**UMO-**i**nteracting **m**otifs (SIMs) and recruit ubiquitin conjugating enzymes using their RING domain. This leads to the ubiquitylation of the SUMO chain and subsequent targeting of the substrate for proteasomal degradation. One STUbL system in *S. cerevisiae* is the heterodimer Slx5-Slx8 (Uls2), which has predominantly been described in the targeting of nuclear proteins involved in DNA-related processes.

In this study, it was shown that Uls2 is part of a quality control mechanism for cytosolic proteins. In this thesis, the working hypothesis was developed that, upon stress or absence of an interaction partner, a hidden SIM or SUMOylation site of a protein is exposed triggering its polySUMOylation. PolySUMOylation of the protein then leads to nuclear localization and subsequent targeting for degradation through Uls2.

In light of this hypothesis, it was shown that two proteins - Nis1 and Fir1 – are targeted by Uls2 upon their overexpression. Both proteins are targeted to the nucleus upon overexpression, where they accumulate in aggregates. For Fir1 it was demonstrated that SUMOylation is essential for nuclear localization whereas SUMO-chain formation is not required for the nuclear localization but greatly enhances the formation of Fir1 aggregates. Additionally, it was observed that the SIM of Fir1 is required for aggregate formation. Colocalization experiments revealed that SUMO is part of the Fir1 aggregates itself. A whole cell proteome approach comparing wild-type cells with Uls2-deficient cells (*slx5Δ*) under non-stress and oxidative stress conditions revealed further promising candidates that might undergo Uls2-mediated quality control.

In conclusion, the results of this thesis point toward a quality control mechanism involving the STUbL Uls2 for proteins with hidden SIMs or SUMOylation sites. This deepens our understanding of quality control of cytosolic proteins involving their relocalization to the nucleus. Further research should focus on elucidating the mechanism of nuclear import of the Uls2 targets as well as on investigating the proteins found in the proteomic approach.

# 1 Introduction

## 1.1 Protein Quality Control

Living cells depend on the presence of correct proteins at the correct place and the correct time. Deviations disturb the homeostasis of the cells. Aberrant proteins interfere with the cell cycle, disturb genome integrity and can lead to cell death (Hegde & Zavodszky, 2019; Moreno-Gonzalez & Soto, 2011). Therefore, it is essential that mechanisms are in place to remove unwanted proteins. Those mechanisms are collectively referred to as quality control. Two major quality control systems in the cell are autophagy and the ubiquitin-proteasome system (Cohen-Kaplan et al., 2016). Autophagy is involved in the removal of damaged organelles or protein aggregates as well as in the removal of soluble proteins. Under starvation conditions, the overall turnover of cellular material including soluble proteins by autophagy is massively induced.

The ubiquitin-proteasome system predominantly removes misfolded, soluble proteins as well as short lived proteins (Cohen-Kaplan et al., 2016) (Pohl & Dikic, 2019). Various quality control sites, such as JUNQs, INQs, and IPODs, exist that support these degradation processes. JUNQ and INQ stand for **ju**xta**n**uclear **q**uality control sites or **i**ntra**n**uclear **q**uality control sites, respectively. In JUNQs and INQs, the sequestrases Btn2 and Hsp42 recruit misfolded proteins to the quality control site. Then proteins are degraded by the proteasome (Kumar et al., 2022). IPOD stands for **i**nsoluble **pro**tein **d**eposit. Here, sequestrases deposit the misfolded proteins next to the vacuole where they are degraded through autophagic mechanisms (Rothe et al., 2018). These quality control mechanisms involve posttranslational modifications specifically ubiquitylation.

## 1.2 Posttranslational Modifications

To organize and regulate proteins after their translation, cells employ a myriad of **p**ost**t**ranslational **m**odifications (PTMs). PTMs can activate or deactivate proteins, lead to their degradation and coordinate proteins during the cell cycle and upon stress (Zhong et al., 2023). Posttranslational modifications can be small chemical groups such phosphor groups or methyl groups to phosphorylate or methylate proteins,

respectively (Ramazi & Zahiri, 2021). However, also small proteins such as ubiquitin and proteins belonging to the ubiquitin family can be attached to proteins and serve as PTMs (Finley et al., 2012; Sengupta & Pick, 2023).

## 1.3 The Ubiquitin Proteasome System

To remove proteins that are damaged or superfluous, quality control systems are in place to degrade those proteins. One of these systems is the previously mentioned ubiquitin-proteasome system. Here, proteins are ubiquitylated through a cascade of enzymes. Then, the ubiquitin modification is recognized by the proteasome which degrades the proteins while ubiquitin is recycled. Key components are ubiquitin, ubiquitylating enzymes and the proteasome. Together they form a major system for protein quality control (Finley et al., 2012; Liao et al., 2024).

### 1.3.1 Ubiquitin and Ubiquitylation

The first component of the ubiquitin-proteasome system is ubiquitin. Ubiquitin is a small protein which consists of 76 amino acids and is highly conserved across species showing 96% identity between *S. cerevisiae* and humans. Structurally, ubiquitin consists of a β-grasp fold with a five-stranded β-sheet and a central α-helix (Agrata & Komander, 2025; Sengupta & Pick, 2023).

Ubiquitin is attached to its substrates in a cascade of three enzymes: E1 activating enzyme, E2 conjugating enzyme and an E3 ligase (Finley et al., 2012). The E1 activating enzyme forms a thioester bond with the C-terminal glycine of ubiquitin. This process requires ATP and a cysteine residue in the active site of the E1 enzyme. First, the C-terminal glycine of ubiquitin is adenylated using the ATP. Then using the produced energy, it forms a thioester bond with the cysteine in the active site of the E1 enzyme. *S. cerevisiae* harbors only one E1 enzyme, namely Uba1, which is making it essential for viability (McGrath et al., 1991). After the activation of ubiquitin, it undergoes a trans-thioesterfication. In this reaction, ubiquitin is transferred from the E1 onto a E2 conjugating enzyme, resulting in ubiquitin being linked to an E2 cysteine residue again via a thioester bond. Yeast cells harbor 11 distinct ubiquitin-conjugating enzymes (Ubcs) (Finley et al., 2012).

The role of E3 ligases is to convey the substrate specificity and promote the ubiquitin transfer onto the substrate. There are a multitude of E3 ligases which are attributed to multiple classes. The two main classes of E3 ligases are the RING ligases and the HECT ligases. They are named after the domain they carry to recruit the E2 enzyme. The HECT ligase class has five members in *S. cerevisiae* whereas RING ligases are more dominant with up to 100 members. The two classes employ distinct mechanisms of transferring the ubiquitin onto the target. RING ligases transfer the ubiquitin directly from the E2 enzyme onto the substrate. In contrast, the HECT ligases first transfer the ubiquitin onto a cysteine in their HECT domains and subsequently onto a target. In both cases, ubiquitin is usually transferred onto a lysine residue of the target protein forming an isopeptide bond (Finley et al., 2012).

Once a protein is ubiquitylated with one ubiquitin (monoubiquitylation), ubiquitylation of this ubiquitin can occur enabling polyubiquitylation of proteins. Since ubiquitin harbors seven lysine residues, polyubiquitin chains with different topology can occur. The topology of the ubiquitin chain depends on the E2 or the E2-E3 combination which can force the usage of certain lysine residues through their positioning in the interaction with the substrate (French et al., 2021). The most prominent ubiquitin chain linkages are K48-linked chains, K11-linked chains, and K63-linked chains with an abundance of 29%, 28%, and 16%, respectively (Xu et al., 2009). Different chain topologies facilitate different signals in the cells. K48 chains are the most common signal for proteasomal degradation, but most other chain-linkages except K63 can mediate proteasomal degradation as well (Xu et al., 2009). In contrast, K63 chains play a role in non-proteolytic processes such as DNA repair, protein trafficking, and translation (Pickart & Fushman, 2004).

### 1.3.2 26S Proteasome

As described above, polyubiquitylation can lead to proteasomal degradation, which involves a large multi-subunit complex: the 26S proteasome. This high molecular weight protease complex consists of a 20S core particle (CP) and two 19S regulatory particles (RP), one on top of the 20S core particle and one on the bottom (Huang et al., 2016; Matias et al., 2010). However, one 19S RP is sufficient to degrade proteins. The RP mediates the recognition of the substrates. Then it confers their deubiquitylation and their unfolding. Lastly, the 19S RP translocates the target protein

into the 20S CP (Saeki & Tanaka, 2012). The 19S RPs consist of the 19 distinct subunits which form a base and a lid. The base consists of a ring of six AAA+ ATPases and four non-ATPase subunits. In *S. cerevisiae* the ATPases of the 19S RP are Rpt1-Rpt6 and the non-ATPase subunits are Rpn1, Rpn2, 10 and 13 (Glickman et al., 1998). The lid consists of the nine non-ATPase subunits Rpn3, Rpn5-9, Rpn11, Rpn12, and Sem1 (Lander et al., 2012).

The 20S CP harbors the active sites of the protease, which mediate degradation of substrates into small peptides. CPs consist of two inner β-rings surrounded by two outer α-rings. The rings consist of seven subunits, β1-7 and α1-7, respectively. Three β-subunits convey the catalytic activity of the proteasome: β1, β2, β5 (Matias et al., 2010). After assembly, the propeptides of these β-subunits become the first target of the proteasome and are cleaved off (Kunjappu & Hochstrasser, 2014). Upon maturation of the propeptides, the threonine of their active site is exposed, and the proteasome is ready to degrade its substrates.

The majority of proteasome substrates are ubiquitylated proteins, especially proteins with K48-linked ubiquitin chains. However, proteins can also be targeted by the proteasome ubiquitin-independently. Such substrates are also referred to as intrinsic proteasome substrates and are usually proteins that are natively disordered, or proteins which become unfolded upon oxidization and exposure to chemicals (Baugh et al., 2009). The disordered structure results in recognition by the proteasome. A study from 2009 suggests that roughly 20% of proteins are targeted through this pathway (Baugh et al., 2009). Signals for degradation might also involve more intricate targeting mechanisms. For example, ubiquitylation of a protein may be dependent on other factors or posttranslational modifications e.g. SUMOylation. SUMOylation of a protein can trigger its ubiquitylation and subsequently its degradation through the proteasome (Sriramachandran & Dohmen, 2014).

## 1.4 SUMO

Next to ubiquitin, a family of **Ub**iquitin-**l**ike proteins (Ubls) has evolved. This family contains proteins such as SUMO, Rub1, or ATG8 (Sengupta & Pick, 2023). The **s**mall **u**biquitin-related **mo**difier (SUMO) is one of the major ubiquitin-like proteins and has reportedly over 1000 substrates. SUMO plays an important role in the cell and, like ubiquitin, is essential. It regulates the cell cycle, is involved in stress responses and genome stability. In *S. cerevisiae,* a single isoform of SUMO exists: Smt3 (Johnson et al., 1997). Smt3 was first found as a **s**uppressor of **M**if1 **t**emperature sensitive phenotype, thus the name Smt3 (Meluh & Koshland, 1995). In mammals, SUMO has five isoforms: SUMO1-SUMO5. SUMO2 and SUMO3 are closely related, sharing 95% of their sequence and are often referred to as SUMO2/3. SUMO4 shares 86% of the sequence with SUMO2, unlike SUMO1, which only shares 45% identity with SUMO2. The SUMO4 isoform is only present in liver tissue (Bohren et al., 2004; Kamitani et al., 1998). A notable difference between these isoforms is their ability to form chains. Like ubiquitin, SUMO can form chains on internal lysine residues. The attachment of SUMO to another SUMO occurs favorably on lysines embedded in a SUMO consensus site (ΨKxD/E with Ψ being V, I or L) (Johnson, 2004). Yeast SUMO (Smt3) has three lysines located in its N-terminal extension embedded in such motifs (K11, K15, K19). SUMO2/3 and SUMO4, on the other hand, have only one lysine residue located in a SUMO consensus site. SUMO1 does not have a lysine residue in such a motif and accordingly does not form chains efficiently *in vivo* (Tatham et al., 2001).

So far, numerous proteins have been found to be SUMOylated. Some of the most prominent targets of SUMOylation are RanGAP1, PML, Sp100 and Top2 (Bachant et al., 2002; Mahajan et al., 1997; Matunis et al., 1996; Sternsdorf et al., 1997).

### 1.4.1 SUMO Structure and SUMO Interaction Motifs

All SUMO isoforms share structural similarities with ubiquitin. SUMO and ubiquitin alike form a β-sheet and an α-helix where one strand of the β -sheet and the α -helix form a hydrophobic grove (Cappadocia & Lima, 2018). For SUMO, this grove is involved in interaction with the SUMO machinery as well as in interaction with SUMO targets (Lascorz et al., 2022). Notably, SUMO has an N-terminal extension which ubiquitin lacks. Similar to ubiquitin, SUMO is initially synthesized as a precursor. The SUMO precursor has three residues after its C-terminal Gly-Gly motif. These residues

need to be cleaved off to mature SUMO before it can be attached to substrates. In yeast, this maturation is performed by the **u**b**l** specific **p**rotease 1 (Ulp1) (Li & Hochstrasser, 1999).

The before-mentioned hydrophobic grove of SUMO interacts with so-called SUMO-interacting motifs (SIMs). SIMs are short sequences consisting of hydrophobic residues followed by acidic residues, which can be divided into multiple categories. The first one is the SIM type a or short 'SIMa'. It consists of three hydrophobic residues, then any residue followed by multiple acidic residues namely glutamic acid, aspartic acid or serine [ΨΨxΨAcAcAcAcAC]. The second type is the reverse SIMa or short 'SIMr'. The SIMr has the same residues as the SIMa just in opposite order [AcAcAcAcAcΨxΨΨ]. Lastly, the SIM type b ('SIMb') has a stricter sequence. It consists of two hydrophobic residues followed by the amino acids glutamic acid, leucine and threonine [ΨΨDLT] (Praefcke et al., 2012). Usually, functional SIMs are parts of unstructured regions that are located in loops between structured regions. They interact with the hydrophobic grove of SUMO through hydrophobic interactions. When a SIM is embedded in the hydrophobic grove of SUMO, it adopts the characteristics of an extended β-like conformation (Lascorz et al., 2022). Importantly, the SUMO-SIM interaction is not covalent and does not require a covalent attachment of SUMO to a target (Kerscher, 2007). In addition to the previously discussed SIMs, non-canonical SIMs, exist which do not have a defined hydrophobic core. Here, predictions are not as well established. Furthermore, posttranslational modifications such as phosphorylation can contribute to a SIMs function. The phosphorylation near the hydrophobic core increases the binding affinity of a SIM to SUMO. Such SIMs are also referred to as 'phosphoSIMs'. A prominent example for phosphorylation increasing SUMO-SIM binding is the E3 ligase PIAS1. PIAS1 can be phosphorylated on a serine residue adjacent to a SIM increasing its interaction with SUMO1 (Mascle et al., 2013; Stehmeier & Muller, 2009).

SUMO-SIM interactions can have different effects and purposes, for example increasing the affinity between two interaction partners. PolySUMOylated proteins can be recognized by proteins with multiple SIMs leading to their deSUMOylation or their targeting for degradation (Sriramachandran & Dohmen, 2014). Furthermore, SUMO-SIM interactions can stabilize protein complexes such as in DNA repair factors. In the case of PML, SUMO-SIM interaction can lead to the formation of non-membranous subcellular organelles, namely PML-nuclear bodies (Lascorz et al., 2022)

## 1.4.2 SUMOylation Cascade

The process of SUMOylation is similar to ubiquitylation and performed by a cascade of three enzymes: E1 activating enzyme, E2 conjugating enzyme and E3 ligase (**Fig. 1 A)**. Before SUMO can be conjugated to any substrate, it needs to be matured. The maturation of SUMO is performed by the **u**b**l** specific **p**rotease 1 (Ulp1) in yeast. In humans, SENPs perform this step. Ulp1 cleaves off three C-terminal residues to expose the Gly-Gly motif of SUMO. After the maturation, the SUMOylation cascade can begin (Li & Hochstrasser, 1999). The first step is performed by the E1 enzyme. In *S. cerevisiae*, the E1 enzyme is a heterodimer, Uba2-Aos1 (SAE1-SAE2 in humans). Both subunits are essential. In an ATP-dependent manner, a cysteine residue in the active center of Uba2 forms a thioester bond with the Gly-Gly motif of SUMO. As previously described for ubiquitin, first the C-terminal glycine forms an adenylate intermediate with AMP with release of PPi. Then the thioester bond can be formed (Dohmen et al., 1995; Johnson et al., 1997).

In the next step, SUMO is transferred onto the cysteine residue of the E2 conjugating enzyme Ubc9. Ubc9 is the only SUMO-specific E2 enzyme in *S. cerevisiae* (UBE2I in humans) (Johnson & Blobel, 1997; Shen et al., 1996). Therefore, it is essential. Upon deletion cells arrest at the G2 or early M-phase. It has been shown that, *in vitro*, a SUMO E3 ligase is not required to SUMOylate a substrate, but that SUMO-charged Ubc9 is sufficient. This has yet to be shown *in vivo* (Melchior, 2000).

Opposed to the E1 and E2 enzyme, there are multiple E3 ligases that can convey SUMOylation. E3 ligases confer the substrate specificity. They interact with the substrate and with SUMO-charged Ubc9 (Gareau & Lima, 2010). E3 ligases mediate the transfer from Ubc9's cysteine residue onto a lysine residue of the substrate. Here, SUMO's C-terminal glycine forms an isopeptide bond with the ε-amino group of the lysine. SUMO is now covalently attached to its substrate (Gareau & Lima, 2010). E3 ligases can be divided into multiple categories, the largest one being the **S**iz-**P**IAS-**RING** (SP-RING) family. This family contains the PIAS family (**p**rotein **i**nhibitor of **a**ctivated **S**TAT) in humans as well as all established E3 ligases from yeast. Members of the PIAS family are PIAS1-4 and Nse2 (Rytinki et al., 2009). The E3 ligases in *S. cerevisiae* are Siz1, Siz2, Mms21/Nse2, and Zip3 (Cheng et al., 2006; Johnson & Gupta, 2001; Takahashi et al., 2001; Zhao & Blobel, 2005). The name giving SP-RING

domain, which is harbored by all E3s in this family, has similarities to the ubiquitin RING domain (Gareau & Lima, 2010). Opposed to the SP-RING containing E3 ligases stands the human E3 ligase RanBP2. RanBP2 does not contain an SP-RING or HECT domain, instead it harbors an IR1-M-IR2 domain that has E3 ligase activity. RanBP2 binds Ubc9 and alters its properties enabling SUMOylation of its substrates (Pichler et al., 2002; Pichler et al., 2004). Its most famous target is **G**TPase **a**ctivating **p**rotein for **Ran** (RanGAP1)**.** RanBP2 binds SUMO and Ubc9 in an optimal orientation for conjugation of SUMO to RanGAP1 (Reverter & Lima, 2005).

Once a protein has been SUMOylated, it can be further SUMOylated. Here, either SUMO gets attached to another lysine on the substrate, resulting in so-called multiSUMOylation or the SUMO on the substrate gets SUMOylated resulting in polySUMOylation. After the polySUMOylation, a SUMO chain can be removed or processed by deSUMOylating enzymes. In yeast, these are **U**b**l**-specific **p**roteases 1 and 2 (Ulp1 and Ulp2). However, SUMO chains can also be recognized by **S**UMO-**t**argeted **u**biquitin **l**igases (STUbLs) which recruit the ubiquitylation machinery leading to the degradation of a substrate by the proteasome (Sriramachandran & Dohmen, 2014).

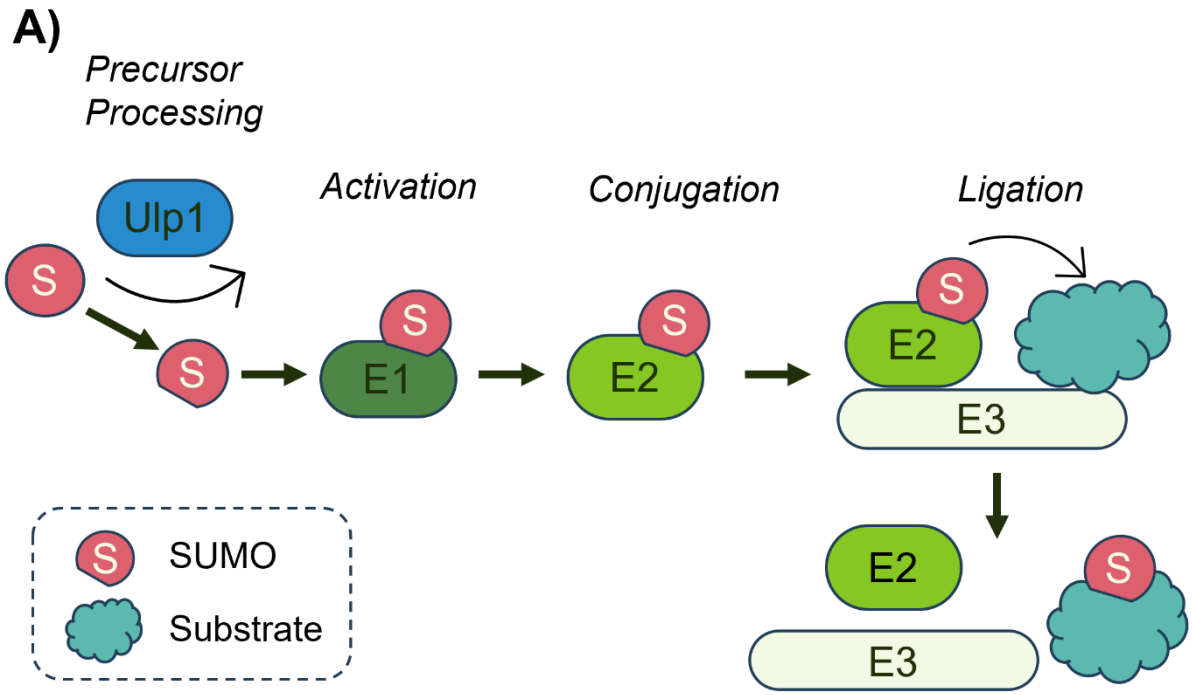


B)

| | *S. cerevisiae* | *Homo sapiens* |
|---|---|---|
| E1 | Aos1-Uba2 | SAE1-SAE2 |
| E2 | Ubc9 | Ubc9 |
| E3 | Siz1, Siz2, Mms21 | PIAS1-4, Nse2, RanBP2 |

**Figure 1 Overview of the SUMOylation cascade**. **A)** SUMOylation cascade starting with the processing of the SUMO precursor by Ulp1 followed by the activation through the E1 activating enzyme. The activation is followed by the transfer of SUMO onto the E2 conjugating enzyme. Lastly, SUMO is transferred from the E2 enzyme onto the substrate mediated by an E3 ligase. **B)** List of enzymes involved in the SUMOylation cascade in *S. cerevisiae* and humans.

## 1.4.3 DeSUMOylating Enzymes

In yeast, there are two SUMO-specific proteases or deSUMOylating enzymes namely Ulp1 and Ulp2 (**Fig. 2 A)**. Ulp1 and Ulp2 have distinct functions in the cell as well as distinct localizations. Ulp1 is a 72 kDa protein and localizes to the nuclear pore (Schwienhorst et al., 2000). Its deletion arrests cells in the G2/M-phase and it is essential, whereas cells can survive Ulp2 deletion. Ulp1 has two distinct functions. First, the previously discussed processing of the SUMO precursor. Second, the deconjugation of SUMO chains and SUMO from its substrates (Li & Hochstrasser,

1999). In its C-terminus Ulp1 carries a ~200 residue Ulp domain (UD). This domain harbors the active cysteine of Ulp1 and therefore its deSUMOylating qualities. The UD is sufficient to rescue a *ulp1Δ* phenotype (Li & Hochstrasser, 2003).

Ulp2 is a large 117 kDa protein which localizes in the nucleoplasm (Schwienhorst et al., 2000). Ulp2 is not involved in processing the SUMO precursor but in the deconjugation of SUMO chains (Bylebyl et al., 2003). The C-terminal domain of Ulp2 is required for deconjugation of SUMO chains, and the N-terminal domain is involved in the localization of Ulp2 in the nucleoplasm (Kroetz et al., 2009). Even though Ulp2 is not essential, deletion of Ulp2 causes severe defects such as temperature-sensitive growth, abnormal cell morphology and decreased chromosome stability (Schwienhorst et al., 2000) (Li & Hochstrasser, 2000). Notably, Ulp2 cleaves SUMO of the SUMO chain of the distal end from the substrate. It leaves two SUMO moieties on the substrates which are required for efficient binding (Eckhoff & Dohmen, 2015). This mode of cleavage is referred to as *exo* cleavage mode. Compared to Ulp2, Ulp1 displays an *endo* cleavage mode, where it is able to cleave anywhere in the SUMO chain as well as all SUMO from the substrate (Eckhoff & Dohmen, 2015).

Ulp1 and Ulp2 facilitate the removal of SUMO chains from proteins. An opposing mechanism involves STUbLs. STUbLs recognize SUMO chains, mediate the ubiquitylation of so modified substrates and thereby their degradation by the proteasome.

## 1.5 SUMO-targeted Ubiquitin Ligases

**S**UMO-**t**argeted **ub**iquitin ligases (STUbLs), also referred to as E3 **u**biquitin **l**igases for **S**UMOylated proteins (Uls), connect the SUMO system with the ubiquitin-proteasome system. STUbLs carry SIMs to interact with a SUMO chain on their substrates, and a RING domain to interact with an E2 ubiquitin conjugating enzyme. The SIMs characterize STUbLs as SUMO interactors and the RING-domain as E3 ligases (Sriramachandran & Dohmen, 2014). Ultimately, SUMO-SIM interaction between the SUMO on the substrate and the SIMs of the STUbL leads to the ubiquitylation of the SUMO chain. Ubiquitylation of the SUMO chain ends in degradation of the substrate by the proteasome (**Fig. 2 A**). In *S. cerevisiae*, three STUbL or STUbL-like systems have been identified: Uls1, Slx5-Slx8 (Uls2), and Rad18. In *S. pombe* Rfp1, Rfp2 and Slx8 form a STUbL system. Humans have the

STUbLs Rnf4, which is homologous to Slx5-Slx8 in *S. cerevisiae*, and Rnf111/Arkadia (Sriramachandran & Dohmen, 2014).

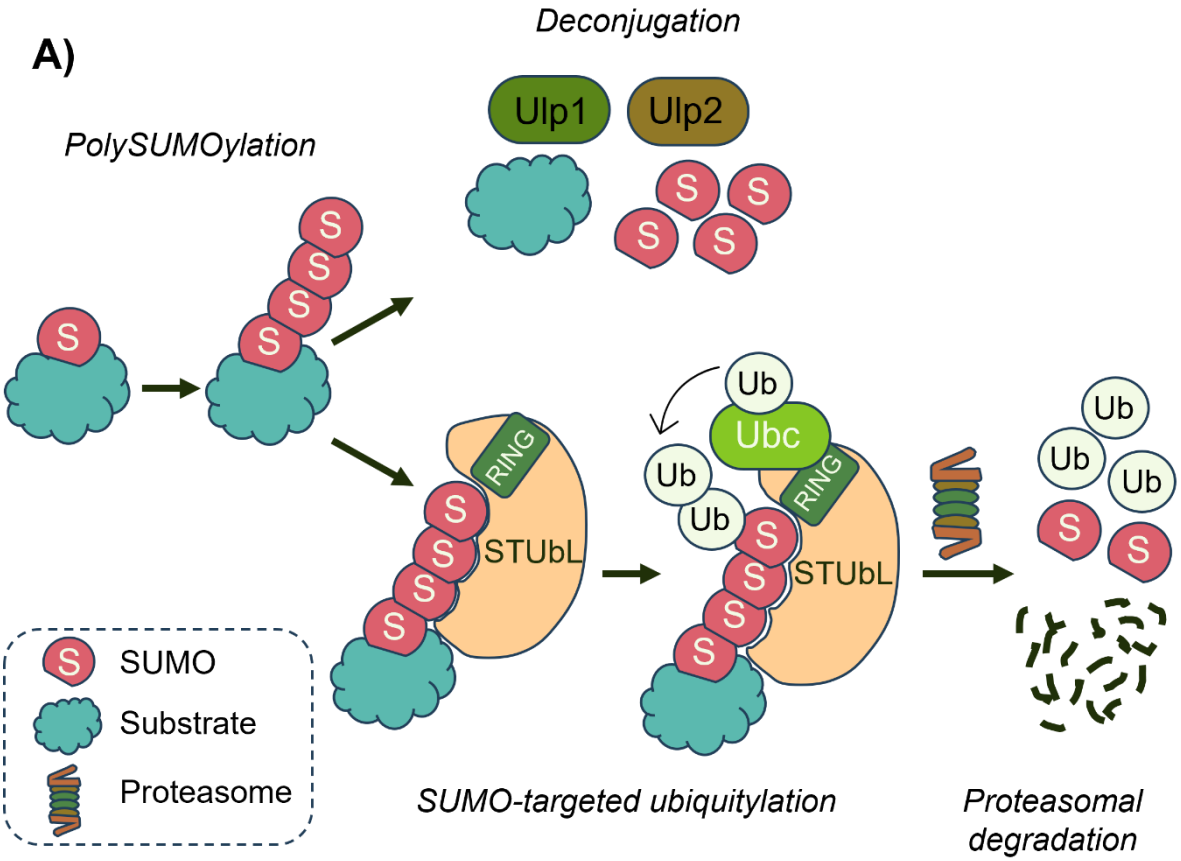


**B)**

| | *S. cerevisiae* | *Homo sapiens* |
|---|---|---|
| *DeSUMOylating enzymes* | Ulp1<br>Ulp2 | SENP1,2,3,5<br>SENP6,7 |
| *SUMO-targeted ubiquitin ligases* | Uls1<br>Uls2 (Slx5-Slx8)<br>Rad18 | RNF111/ARKADIA<br>RNF4 |

**Figure 2 Schematic overview of the targeting of polySUMOylated proteins. A)** After polySUMOylation, deconjugation by the Ubl-specific proteases Ulp1 and Ulp2 can occur or SUMO chains can be recognized by SUMO-targeted Ubiquitin ligases (STUbLs). STUbLs recognize SUMO chains and recruit ubiquitin-charged E2-conjugating enzymes (Ubc). Subsequently, the SUMO chain is ubiquitylated tagging it for degradation by the proteasome while recycling ubiquitin and SUMO. **B)** List of deSUMOylating enzymes and STUbL systems in *S. cerevisiae* and humans.

### 1.5.1 Uls1

One STUbL in *S. cerevisiae* is Uls1, also known as Ris1, Dis1 or Tid4. Uls1 is a large 184 kDa protein. It is involved in various processes such as chromatin remodeling, homologous recombination and inhibition of non-homologous end joining. Uls1 carries four SIMs: two SIMa and two SIMb. Uls1 also has a SWI2/SNF2-like ATPase domain and a RING domain (Sriramachandran & Dohmen, 2014). In the context of Uls1's connection to SUMO, Uls1 was discovered as an interactor of Smt3 in a yeast-two hybrid screen (Hannich et al., 2005; Uzunova et al., 2007). Deletion of Uls1 resulted in the accumulation of HMW-SUMO conjugates, indicating that Uls1 targets HMW-SUMO conjugates. This points towards its role as a STUbL (Uzunova et al., 2007).

Uls1 belongs to the family of SWI/SNF ATPases. The SWI/SNF family remodels chromatin using ATP and plays a role in transcriptional regulation, DNA repair and mitotic chromosome segregation. Uls1's SWI/SNF domain has a negative regulatory role in DNA silencing. It makes DNA more accessible, which is otherwise silenced by organized packing in higher order chromatin (Zhang & Buchman, 1997). In addition, Uls1 shows genetic interaction with multiple genes involved in homologous recombination. Here, Uls1's DNA translocase activity is involved (Bauer et al., 2019). Uls1, together with Rad54 and Rdh54, removes Rad51 from undamaged chromatin. Rad51 is a recombinase and is involved in the repair of double strand breaks or single stranded DNA gaps. Translocases, such as Uls1, are necessary to remove Rad51 from undamaged DNA, otherwise Rad51 will accumulate on chromatin leading to genome instability and chromosome loss (Shah et al., 2010).

Deletion of Uls1 causes telomere-telomere fusions suggesting that Uls1 is involved in the inhibition of **n**on-**h**omologous **e**nd **j**oining (NHEJ). The master regulator of inhibiting NHEJ is Rap1. Rap1 has several ways of mediating the inhibition of NHEJ. It was proposed that Uls1 supports the inhibition of NHEJ by targeting polySUMOylated Rap1 at the telomeres. Clearance of polySUMOylated Rap1 ensures continuous NHEJ inhibition (Lescasse et al., 2013). Uls1 also plays a role in DNA damage control by targeting SUMOylated Srs2. **P**roliferating **c**ell **n**uclear **a**ntigen (PCNA) forms a ring around DNA and enables binding of DNA polymerases and replication-associated proteins. PCNA is controlled by ubiquitylation as well as SUMOylation. Upon SUMOylation of PCNA, the Srs2 helicase is recruited, which inhibits certain homologous recombination repair pathways. In contrast, if Srs2 itself is SUMOylated,

its interaction with PCNA is downregulated. Uls1 interacts with PCNA and Srs2, and reduces SUMOylated Srs2 level ensuring that PCNA is not downregulated. (Kramarz et al., 2017).

### 1.5.2 Uls2

Another STUbL in *S. cerevisiae* is Uls2. Uls2 is a heterodimer consisting of the subunits Slx5 (Hex3) and Slx8. Slx5 and Slx8 were initially found in a genetic screen searching for genes which were necessary for viability in a mutated Top3 strain. Thus their name: **S**ynthetic **l**ethal of unknown function (Slx) (Mullen et al., 2001). Both subunits carry a RING domain, Slx8 has one SIM type a, whereas Slx5 has a total of four SIMs, two SIMa, one SIMb and one SIMr. Together Slx5 and Slx8 act as a STUbL system. As a complex Slx5 and Slx8 are involved in stress tolerance, DNA repair and maintaining genome stability (Hopfler et al., 2019; Sun et al., 2020; Zhang et al., 2006). In accordance, targets of Slx5-Slx8 include DNA-associated proteins such as Cse4, Kar9, and Bir1 (Ohkuni et al., 2016; Schweiggert et al., 2016; Thu et al., 2016) as well as transcription factors such as Mot1 and Matα2 (Wang & Prelich, 2009; Xie et al., 2010). Interestingly, a mutant gene of Mot1, namely *mot1-301,* encodes a Mot variant that displays stronger targeting through Uls2 than the wild type Mot1 suggesting Uls2 might act in quality control mechanism (Wang & Prelich, 2009). Notably, SUMOylation of a protein is not always required for its targeting through Uls2. This is the case for the transcription factor Matα2. Matα2 achieves this by mimicking SUMOs structure and interacting directly with the SIMs of Uls2 (Xie et al., 2010). Further substrates of Uls2 include the nuclease Yen1 and the nuclear pool of the SUMO E3 ligase Siz1 (Talhaoui et al., 2018; Westerbeck et al., 2014).

Uls2 contributes to stress tolerance by formation of ubiquitin hot spots on chromatin. Uls2 is recruited to chromatin by SUMOylated Euc1 leading to ubiquitin hotspots. Then Cdc48 extracts ubiquitylated proteins from chromatin, thus clearing the DNA from protein aggregates (Hopfler et al., 2019). Uls2 is also involved in DNA repair in its function as a STUbL. Usually, the topoisomerases Top1 and Top2 form transient cleavage complexes with the DNA. Under stress conditions, these cleavage complexes can remain undissolved. Here, Top1 or Top2 are SUMOylated by Siz1 and subsequently targeted by Uls2. Uls2 ubiquitylates the cleavage complex leading to its degradation and ensuring repair of the DNA lesion (Sun et al., 2020).

Another significant aspect of Uls2 is its role in genome stability. In S-phase, it is necessary that replication forks move through the genome uninterrupted. Stalling can be caused by toxins and radiation damage, or through secondary structures and DNA-protein complexes. This stalling contributes to genome instability and promotes mutations. The RecQ pathway contributes to the stability of replication forks. In *S. cerevisiae,* the DNA helicase Sgs1 assists in keeping damaged replication forks clean. Sgs1 plays a major role in suppressing genomic instability during normal S-phase progression. In the absence of Sgs1, Slx5 and Slx8 become essential (Zhang et al., 2006). During an unperturbed cell cycle, Slx5 and Slx8 are important for suppression of gross chromosomal arrangements (GCRs) as well as suppression of mutations and accumulation of spontaneous DNA lesions (Zhang et al., 2006) (Albuquerque et al., 2013) (Ii et al., 2007).

### 1.5.3 Rad18

The third STUbL in *S. cerevisiae* is Rad18 a 487 amino acids protein with an N-terminal RING domain. Interestingly, it has only one SIM which is a SIM type r. So far, only one substrate has been identified for Rad18: the sliding clamp protein PCNA. PCNA builds a homotrimer around the DNA and serves as a platform for various proteins involved in replication and DNA repair (Maga & Hubscher, 2003). Upon replication stalling through DNA damage, PCNA becomes ubiquitylated. This ubiquitylation is mediated by Rad18 together with the E2 enzyme Rad6. Interestingly, this ubiquitylation is not entirely dependent on SUMOylation but strongly increased by it (Parker & Ulrich, 2012).

To summarize, SUMO-targeted ligases are involved in genome maintenance. They add a layer of regulation in diverse events in genome control such as regulation of NHEJ or DNA repair. What remains to be elucidated is if STUbLs target non-nuclear proteins. Previous results showed that a reporter with artificial SUMO chains is targeted by overexpressed Uls2. Interestingly, the reporter appeared to be targeted to the nucleus by the attachment of the SUMO chains (Doering Thesis, 2022). Based on this observation it would be of interest to further investigate if cytosolic proteins are targeted by Uls2 when they undergo nuclear translocation mediated by SUMOylation. This question was tackled in this thesis.

## 1.6 Cell cycle

Cell division is a highly orchestrated process. It is regulated by a plethora of proteins, checkpoints, and posttranslational modifications. Cell cycle checkpoints verify that the current phase of the cell cycle is successfully completed before moving to the next phase, ensuring the well-being of mother and daughter cell. Every aspect of the yeast cell cycle is organized and needs to be timed correctly from the choice of the next bud site to the degradation of the septum and cytokinesis (Brace et al., 2019; Meitinger et al., 2014). SUMOylation is highly involved in the cell cycle. Deletion of the SUMO E2 conjugating Ubc9 leads to an arrest in G2 or early M-phase emphasizing the necessity of SUMO for completion of the cell cycle (Johnson & Blobel, 1997). One of the most prominent examples for SUMOylation during the cell cycle are the septins at the bud neck, which become SUMOylated during mitosis (Johnson & Blobel, 1999).

The tight connection of SUMO and the cell cycle prompted the question whether Uls2 targets cell-cycle dependent proteins. The two proteins Nis1 and Fir1 were chosen for closer investigation because they are involved in the cell cycle, carry SIMs and interact with SUMO in a yeast-two-hybrid screen (Uzunova et al., 2007).

### 1.6.1 Nis1

One mechanism to ensure smooth cell division is dedicated to ensuring that cells do not divide at the same site twice. Reusing an old bud site has negative effects such as increased replicative aging (Wedlich-Soldner, 2014). One protein involved in inhibiting re-establishment of the old bud site is the **n**eck protein **i**nteracting with **s**eptins **1** (Nis1) (Meitinger et al., 2014). The other proteins involved in this mechanism are the scaffold protein Aim44/Gps1, the transcription factor Nap1, transmembrane proteins Rax1 and Rax2, and Nba1 (**Fig. 3**). During cell division, these proteins are sequentially recruited to the bud neck. First, Aim44 arrives. It serves as a scaffold for the other proteins. Then Nap1 and Nba1 are recruited. Lastly, Nis1 arrives at the complex. After cell division, Nis1-Nba1 are transferred via Nap1 onto the transmembrane proteins Rax1/Rax2. Nis1 serves as an anchor for Nba1, and Nba1 locally inhibits the **g**uanine **e**xchange **f**actor (GEF) Cdc24 (Meitinger et al., 2014). Cdc24 is the GEF for Cdc42, the master regulator for cell polarity (Johnson & Pringle, 1990).

The bud neck localization of each protein depends on the previous protein. For example, if Nba1 is deleted, Nis1 is unable to localize to the Aim44 complex at the bud neck leading to an accumulation of Nis1 in the nucleus (Meitinger et al., 2014). Interestingly, the nuclear localization of Nis1 can also be triggered by its overexpression of Nis1 (Perez & Thorner, 2019). This might be because the correct stoichiometry between Nis1 and Nba1 molecules no longer persists. As a consequence, a large fraction of Nis1 cannot localize at the bud neck.

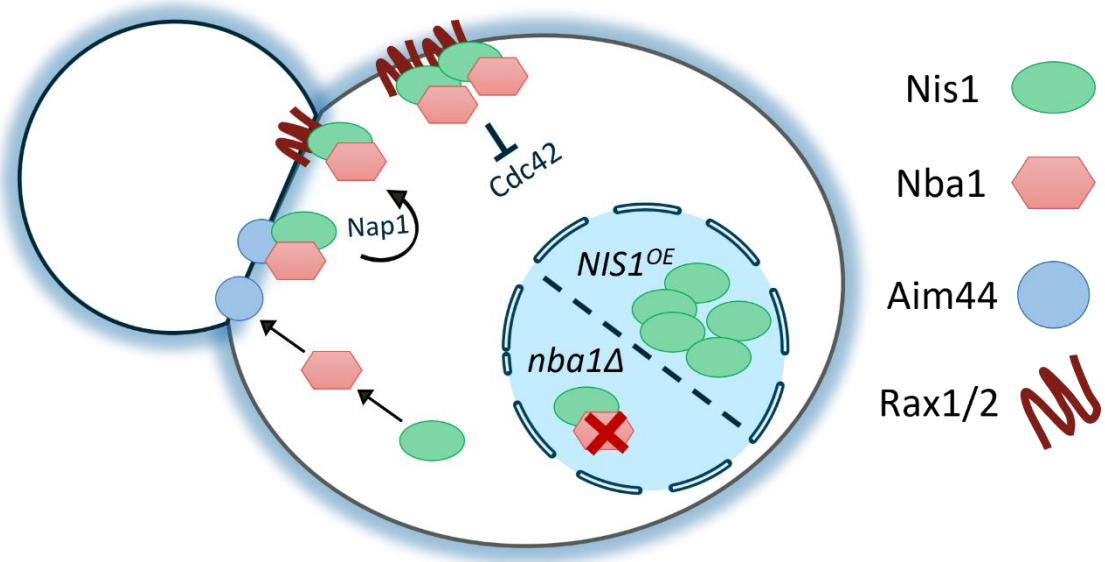


**Figure 3 Schematic overview of Nis1 function and localization**. During the cell cycle, Aim44, Nba1, Nap1 and Nis1 localize to the bud neck where Aim44 serves as platform for the other proteins. After cytokinesis, Nap1 transfers Nis1-Nba1 onto the transmembrane proteins Rax1/Rax2, which anchor the duplex at the old bud site. Nba1 locally inhibits the master regulator for cell polarity Cdc42 by inhibiting its guanine exchange factor Cdc24 (Meitinger et al., 2014; Perez & Thorner, 2019). *NIS1*$^{OE}$ = Overexpressed *NIS1*.

In the context of this thesis, Nis1 became relevant because multiple factors pointed towards Nis1 being a substrate of SUMOylation. Initially, Nis1 was found as an interactor of septins in a yeast two hybrid screen (Iwase & Toh-e, 2001). Septins are highly SUMOylated during mitosis (Johnson & Gupta, 2001). Furthermore, Nis1 was found as an interactor of Smt3 in a yeast-two-hybrid screen. Subsequently, a SIM in the C-terminal domain of Nis1 was identified (IIIPDSQDD) (Uzunova et al., 2007). SIMs are a good indicator for potential SUMOylation of proteins as they promote the interaction with SUMO or with SUMO-charged Ubc9 (Lascorz et al., 2022). Interestingly, upon overexpression of Nis1, high-molecular weight SUMO conjugates

accumulate, which disappear upon mutation of Nis1's SIM. This further pointed towards polySUMOylation of Nis1 (Uzunova et al., 2007). Therefore, Nis1 was investigated as a putative substrate of Uls2 in this thesis.

### 1.6.2 Fir1

Accurate cell division is essential for survival of cells. Multiple mechanisms are in place to ensure the correct order of events. A final checkpoint to ensure that cytokinesis can take place involves the **f**actor **i**nteracting with ***R****EF2* **1** (Fir1). Fir1 is part of the **e**nforcement of **c**ytokinesis **o**rder (ECO) pathway, which ensures that all cytokinetic processes are finished before cell separation takes place (Brace et al., 2019). As part of the ECO pathway, Fir1 localizes at the bud neck. Here, it inhibits a separation specific exocytosis function of the **c**ell wall **b**iosynthesis **k**inase **1** (Cbk1). Cbk1 induces mother-daughter cell separation as part of the "hippo" signaling pathway (Weiss, 2012). Fir1's localization at the bud neck is driven by two forces: SUMO-SIM interaction and Fir1 binding to Spa2 (**Fig. 4**). Hence, Fir1 localizes at the bud neck in two phases. In phase I, SUMOylated septins recruit Fir1 via its SIM to the septin hourglass. In phase II, Spa2 mediates the localization of Fir1 into the split double septin ring. The second phase can also occur if Fir1 does not undergo a phase I localization due to the lack of septin localization or mutation of its SIM. In phase II, Fir1 carries Skt5, the activator of Chs3, into the split double ring (Müller et al., 2024). Here, the Fir1-Skt5 complex promotes chitin synthesis by acting as a receptor for Chs3. Recruitment of Chs3 increases chitin synthesis for the secondary septum (Müller et al., 2024). In parallel, Fir1 also inhibits Cbk1 activity and therefore inhibits degradation of the primary septum (Brace et al., 2019). After cytokinesis, the APC/C ubiquitin ligase degrades Fir1 (Ostapenko et al., 2012). Interestingly, apart from its localization at the bud neck, Fir1 also displays a nuclear localization in the *spa2Δ cdh1Δ* mutant (personal communication, Nils Johnson, University of Ulm).

In the context of this thesis, Fir1 is especially interesting because of its connection to SUMOylation. First, it was shown that Fir1 interacts with septins in a SUMO-dependent manner (Müller et al., 2024). Second, Fir1 was identified in a yeast-two-hybrid screen as an interactor of Smt3. Third, Fir1 carries a SIM (Uzunova et al., 2007). Lastly, Fir1 was found to be SUMO-modified on its K715 residue in a proteomics study investigating SUMOylation during meiosis (Bhagwat et al., 2021). Interestingly, the

same lysine residue was found in another proteomics study to be ubiquitylated phosphorylation-dependently (Swaney et al., 2013). Fir1's connections to SUMOylation and its localization pattern were the reason why Fir1 was investigated as a putative substrate of Uls2 in this thesis.

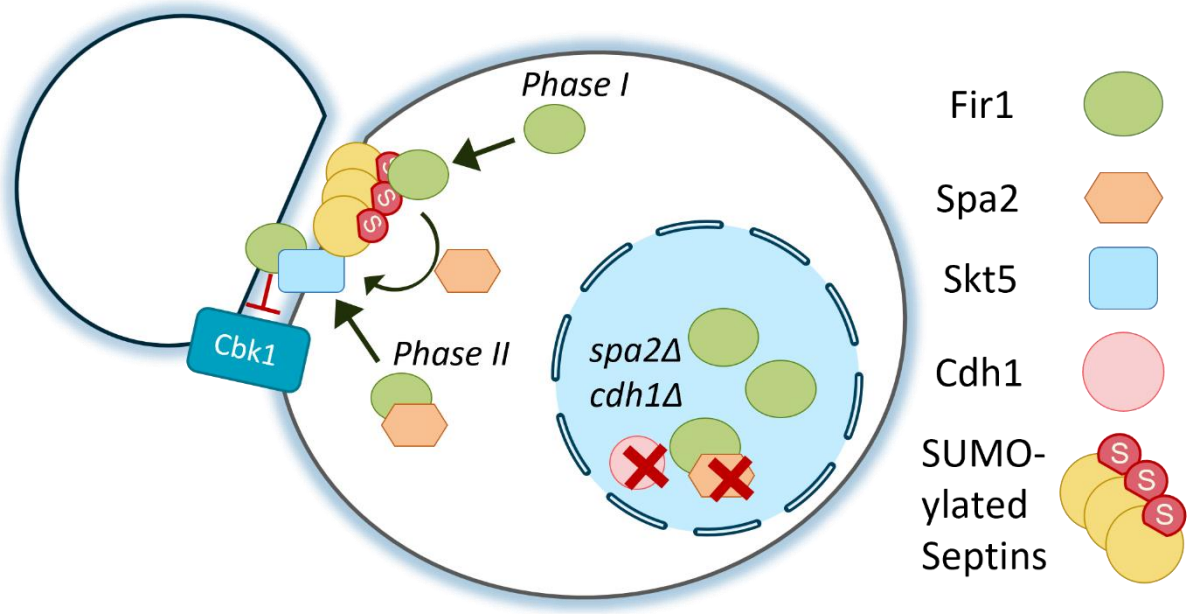


**Figure 4 Schematic overview of Fir1 function and localization.** During the cell cycle, Fir1 localizes in two phases to the bud neck. In phase I, it localizes to the SUMOylated septins. In phase II, it translocates from the SUMOylated septins into the split double septin ring mediated by its partner Spa2. This can also occur without previous localization at the septins. Fir1 carries Skt5 into the split double septin ring where they inhibit Cbk1 activity as part of the ECO pathway (Brace et al., 2019; Müller et al., 2024). Upon deletion of Spa2 and Cdh1, Fir1 localizes in the nucleus (personal communication, Nils Johnsson, University of Ulm).

## 1.7 Proteins from proteomic approach

In this study, a proteomics approach was used to identify targets of Uls2 under stress and non-stress conditions. The following paragraphs provide a brief background for four proteins found in this proteomic approach. The selected proteins are Hsp90, *YBR053C*/regucalcin, Pam16 and Sod2. They were selected from the proteomics data, because they showed significant increase in protein levels in a *slx5Δ* strain either independently of stress or dependent on stress treatment.

### 1.7.1 Hsp90

Chaperones play a crucial role in the cell. They assist proteins in folding, structure maintenance, support cellular processes, and contribute to cellular stress resistance (Buchner, 2019). One chaperone family is the Hsp90 family. In *S. cerevisiae* two isoforms exist which stem from whole genome duplication*:* Hsp82 and Hsc82 (Girstmair et al., 2019). Both share a sequence identity of 97% and are indistinguishable by antibody. Despite their high sequence similarity, they differ distinctly in expression and function. Hsp82 is stress-inducible, whereas Hsc82 is constitutively expressed. Usually, the expression of Hsc82 is tenfold higher than the expression of Hsp82. Under heat shock the levels of both Hsp90 chaperones become equal (Borkovich et al., 1989). Structurally, Hsp90 chaperones form homodimers. The homodimer usually persists in an open conformation. ATP-dependently, the homodimer can switch to a closed conformation. This conformational change promotes folding and stability of proteins (Krukenberg et al., 2011).

In the context of this thesis, Hsp82 is of interest, because a proteomics approach identified it as one protein, levels of which were increased in cells lacking a functional Slx5-Slx8 STUbL. Furthermore, it was reported earlier that Hsp90 is SUMOylated both in yeast (K178) and in humans (K191) (Mollapour et al., 2014).

### 1.7.2 *YBR053C*

Even though the whole genome of *S. cerevisiae* has been sequenced, not every protein has been functionally characterized. One such protein is the product of the gene *YBR053C*. Regarding literature about *YBR053C*, there are only two primary

papers cited in the Saccharomyces Genome Database SGD. One describes a transcriptome analysis of cell well perturbations. This study showed that *YBR053C* is stabilized upon cell wall stress induced by zymolyase or calcofluor white (Boorsma et al., 2004). The second paper profiled the yeast proteome in the *ybr053cΔ* strain. Based on the proteins correlating with *YBR053C* deletion, they postulate a role for *YBR053C* in yeast budding (Liu et al., 2022). Secondary literature, investigating the yeast phosphoproteome, provides evidence that the *YBR053C* gene product is phosphorylated (Lanz et al., 2021; Leutert et al., 2023). Furthermore, *YBR053Cs* gene product has been identified as an interactor of the chaperone Hsp90 (Girstmair et al., 2019; Kolhe et al., 2023).

According to SGD, *YBR053C* has similarities to regucalcin proteins in different species. Databases such as Alliancegenome.org or marrvel.org consider them as orthologues even though reviews do not (Danish & Ahmad, 2023). Nevertheless, *YBR053C* harbors multiple similarities to regucalcin proteins. Regucalcin, also known as **S**enescence **m**arker **p**rotein-30 (SMP30) is a calcium binding protein. As a regulator of Ca+ it has pleiotropic functions such as suppression of protein phosphatases, protein kinases, as well as DNA and RNA synthesis (Danish & Ahmad, 2023). Structurally, regucalcin consists of six β-sheets which form a six bladed β-propellor fold (Boorsma et al., 2004). Prediction of yeast's *YBR053C* gene product using AlphaFold V2 reveals a similar structure.

In this thesis, *YBR053C* was investigated because a proteomic approach identified it as a protein, levels of which were increased upon deletion of *Slx5*.

### 1.7.3 Pam16

Pam16 (or Tim16) is an essential protein and part of the **p**resequence translocase-**a**ssociated **m**otor (PAM) complex. As part of the PAM complex, Pam16 is localized in the inner mitochondrial membrane. Pam16 has a size of 16 kDa and carries an N-terminal degenerate J-domain, that is crucial for its function (Frazier et al., 2004). The J-like domain, however, does not have the ability to stimulate the ATPase function of the chaperone mtHsp70, which forms the core of the PAM complex. Instead, Pam16's J-like domain ensures the perfect positioning of its partner Pam18. Pam18 itself has a functional J-domain and can stimulate mtHsp70 (D'Silva et al., 2005). As part of the PAM complex, Pam16 is essential and conditional mutants display growth deficits and

accumulate unprocessed precursor proteins (Frazier et al., 2004). So far, Pam16 has not been described as a substrate of SUMOylation or a target of a STUbL.

In this thesis, Pam16 was found in a proteomic approach because it showed a strong increase in protein level in the *slx5Δ* strain upon exposure to stress.

### 1.7.4 Sod2

**S**uper**o**xide **d**ismutase **2** (Sod2) also known as manganese-dependent dismutase, is a key player in protecting mitochondria from oxidative stress. Sod2 is a 26 kDa protein and forms homotetramers. In the center of the homotetramere, the four Sod2 molecules bind a manganese ion with their active centers (Kang et al., 2011). At its N-terminus Sod2 carries a mitochondrial targeting signal (MTS). Sod2 localizes in the mitochondrial matrix. There it converts the superoxide radicals ($O_2^-$) from the electron transport chain into the less reactive $H_2O_2$ and $O_2$. This protects the mitochondria from oxidative stress and helps to maintain the integrity of mitochondria (Palma et al., 2020). Sod2 was found to be SUMOylated during meiosis in a proteomic approach (Bhagwat et al., 2021). In this thesis study, Sod2 protein level was found to be increased in *slx5Δ* under both stress and non-stress conditions.

## 1.8 Aim

The initial aim of this PhD thesis was to elucidate the mechanism of SUMO-targeted ubiquitylation. Previous results had shown that SUMO chains can target a reporter to the nucleus. This effect is stronger with increasing chain length. Interestingly, a reporter with SUMO chains is targeted by overexpressed Uls2 (Doering Thesis, 2022). Based on these observations, possible natural substrates of Uls2 that undergo a relocalization to the nucleus and are subsequently targeted by Uls2 were investigated. Here, the proteins Nis1 and Fir1 were chosen based on their reported connections to SUMOylation (HMW-SUMO conjugates, SIM, Interactor of Smt3 in Y2H) and based on their dual localization at the bud neck and in the nucleus under certain circumstances.

The work of this thesis can be divided into four parts, the third of which develops a hypothesis based upon the results described in the first two parts, and the fourth of which summarized the results of a proteomic approach aimed at testing this hypothesis.

- Investigation of Nis1 as a substrate Uls2 (2.1)
- Investigation of Fir1 as a substrate of Uls2 (2.2)
- Hypothesis based on the results obtained in Nis1 and Fir1 (2.3)
- Proteomics approach to identify further substrates of Uls2 (2.4)

# 2 Results

## 2.1 Nis1

To identify substrates of the STUbL Uls2 and investigate its mechanism of substrate selection, Nis1 was chosen as the first potential substrate. Nis1 harbors multiple qualities that qualify it as a target of SUMOylation and a potential STUbL target. Firstly, Nis1 interacts with Smt3 in a yeast-two-hybrid screen. Secondly, it carries a SUMO-interacting motif. Lastly, upon overexpression of Nis1 HMW-SUMO-conjugates accumulate (Uzunova et al., 2007). Apart from its connection to SUMO, Nis1 was chosen, because it has been observed that upon its overexpression or deletion of its partner Nba1, Nis1 accumulates in the nucleus, where Uls2 is located (Cook et al., 2009; Perez & Thorner, 2019). Nis1 was investigated regarding its targeting by Uls2, its posttranslational modifications, and localization by employing western blots and fluorescence microscopy.

### 2.1.1 Endogenous Nis1 is not targeted by Uls2

First, endogenous Nis1 was investigated as a substrate of Uls2. Therefore, two Nis1 constructs were used. First, a strain expressing HA-tagged Nis1 was used for western blot analysis. Second, a strain with neongreen-tagged Nis1 (Nis1-NG) was used in microscopy. Both tags were introduced at the *NIS1* locus such that the modified genes were expressed from the endogenous $P_{NIS1}$ promoter (**Fig. 5 A**). To compare Nis1 levels, in presence and absence of Uls2, a strain with inducible Uls2 was used. Here, the genes encoding both subunits of Uls2, Slx5 and Slx8, were under control of the galactose-inducible promoter $P_{GAL1}$. In this strain, transcription of both genes could either be shut off by adding glucose to the medium or induced by adding galactose. To ensure a swift induction of *SLX5* and *SLX8* expression, overnight cultures were grown in medium containing raffinose. Raffinose served as an intermediate carbon source which neither inhibits nor induces the promoter (Stockwell et al., 2015).

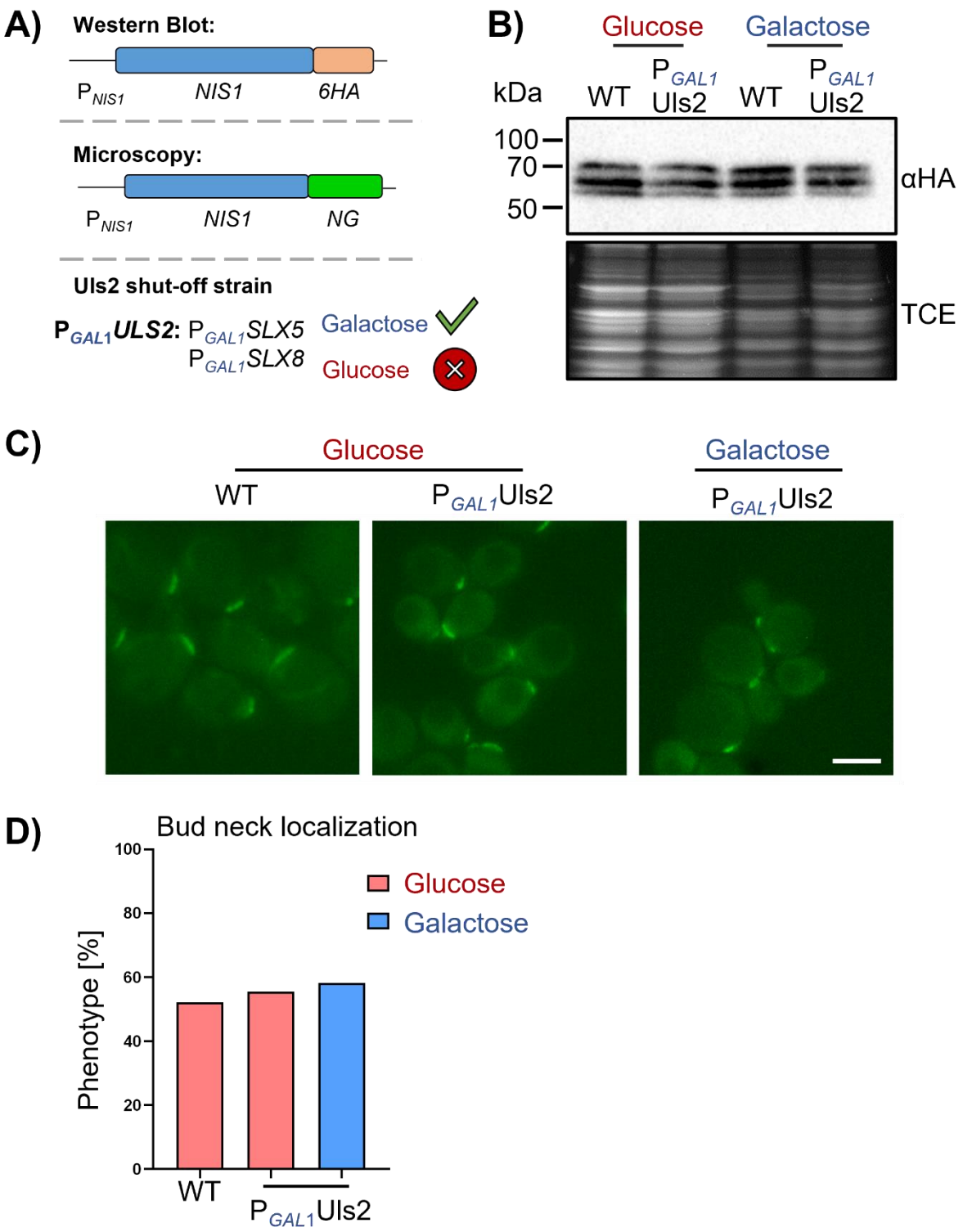


**Figure 5 Endogenous Nis1 is not targeted by Uls2. A)** Constructs used in B) and C) **B)** Western blot of Nis1-6HA in wild type and P$_{GAL1}$*ULS2* strains. After overnight preculture in YP-Raffinose, the cells were grown 5 h in YP-Glucose or YP-Galactose. Boiled extracts were loaded on a 10% SDS-Gel with TCE, blotted for 1 h at 400 mA, 100 V at 4 °C on nitrocellulose using wet blot. Blots were incubated with anti-HA (αHA) antibody (3F10-rat at 1:2,000) overnight at 4°C and with anti IGG coupled to fluorophore (680 nm emission peak) for 2 h at room temperature. Strains used were: yFP2, yFP21 **D)** Microscope images of Nis1-NG in WT and P$_{GAL1}$*ULS2*. After overnight

preculture in YP-Raffinose, cells were grown for 4 h in YP-Glucose or YP-Galactose. Acquisition: FITC: 2 s. Strains used were: yFP45, yFP14 + pFP5. **Scale: 5 µM**.

To investigate if Nis1 is targeted by Uls2, Nis1 levels were compared under Uls2 shut off and overexpression conditions by western blotting. Interestingly, Nis1 displayed a characteristic band pattern under all conditions (**Fig. 5 B**) running in three distinct bands with apparent size differences of roughly 10-15 kDa. The bands varied in abundance, with the middle band being the most abundant followed by the upper band and lastly the lowest band. This band pattern did not change in the $P_{GAL1}$*ULS2* strain compared to the wild type neither on glucose nor on galactose. It can be concluded that neither overexpression nor shut off of Uls2 had any apparent effects on endogenous Nis1 detectably on western blot. A likely explanation for the formation of the different bands could be posttranslational modifications which alter the electrophoretic mobility of Nis1.

To further investigate the possible influence of Uls2, Nis1 localization was studied in the $P_{GAL1}$*ULS2* strain. Under its endogenous promotor, Nis1 had been shown by others to localize predominantly at the bud neck or in the cytosol (Meitinger et al., 2014; Perez & Thorner, 2019). This could be confirmed in our wild-type background using the Nis1-NG construct (**Fig. 5 C**). Nis1 bud neck localization was examined during Uls2 overexpression and shut off conditions revealing that the localization of Nis1 at the bud neck was not influenced by Uls2 levels. Quantification of Nis1 bud neck localization supports these observations (**Fig. 5 D**). Here, the percentage of cells that displayed bud neck-localized Nis1 was determined. There was no significant difference between the wildtype (52%) and the Uls2 strain (55% on glucose and 58% in galactose). The microscopic analysis thus supports the western blot result. Endogenous Nis1 is either not targeted by Uls2, or the targeting was not detectable with the applied methods. In conclusion, Nis1 showed an interesting band pattern which may be attributed to posttranslational modifications. This encouraged further investigation of Nis1.

So far, Nis1 could not be identified as a target of Uls2, but investigation under different conditions could provide valuable insights into its regulation. The abovementioned absence of an apparent effect of Uls2 on endogenous Nis1, which localizes mainly in the cytosol and at the bud neck, was consistent with the fact that Uls2 itself is localized in the nucleus (Cook et al., 2009). Therefore, it would be best to investigate the nuclear fraction of Nis1.

## 2.1.2 Nuclear Localization of Nis1

The previous results prompted the question of which experimental set up would be best to investigate the nuclear fraction of Nis1. Nis1 undergoes nuclear localization mostly under two conditions: First, upon deletion of its interaction partner Nba1 and second upon overexpression (Perez & Thorner, 2019). Both conditions were investigated to determine which would be more suitable for further experiments.

In the *nba1Δ* strain, *NIS1* was expressed from its endogenous promoter (**Fig. 6**). Here, Nis1-NG was localized to the nucleus and to the cytoplasm while the bud neck localization was abolished. This is consistent with a previous study (Perez & Thorner, 2019). However, even though Nis1 could be observed in the nucleus, the intensity of nuclear Nis1 was low. To investigate overexpressed *NIS1*, the gene was put under the control of the *TDH3 (GPD)* promoter and integrated at the *LEU2* locus in the otherwise wild-type background. Here, Nis1 localized to the nucleus and to the cytoplasm as well as the bud neck. Notably, the nuclear staining was more pronounced in cells overexpressing *NIS1* compared to endogenous Nis1 in the *nba1Δ* mutant (**Fig. 6**). This becomes especially clear considering the notably higher exposure time necessary for the visualization of Nis1-NG was more than doubled for the *nba1Δ* mutant. Additionally, in the *nba1Δ* mutant Nis1 was tagged with neongreen whereas the overexpressed Nis1 was tagged with GFP. Reportedly, neongreen is more sensitive than GFP when working with low expression (Hostettler et al., 2017). The doubled exposure time as well as the improved fluorophore did still not achieve a similar detection of Nis1 in the *nba1Δ* background.

To summarize, both expression in a *nba1Δ* mutant and overexpression of *NIS1* lead to a detectable fraction of nuclear Nis1. However, overexpression of *NIS1* leads to a more intense nuclear localization and subsequently a better detection. Based on these findings, it was decided that in experiments investigating the targeting through Uls2 the nuclear fraction of Nis1 will be investigated under overexpression conditions.

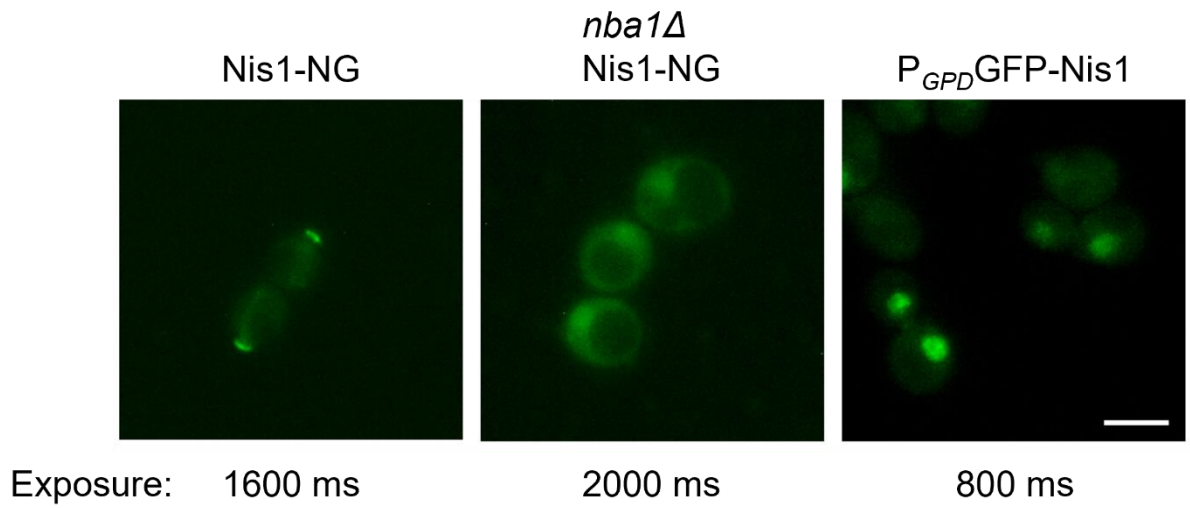


**Figure 6 Effect of *nba1Δ* and overexpression of *NIS1* on Nis1 localization**. Microscope images of Nis1-neongreen (NG) in wild-type and *nba1Δ* cells and overexpressed Nis1 ($P_{GPD}$GFP-NIS1) in wild-type cells. Cells were grown in YP-Glucose into exponential phase. Microscope images were acquired using different exposure times as indicated below the images. The images with NG were acquired using the FITC channel (excitation: 490 nm) and the GFP image was acquired using the GFP channel (excitation: 470 nm). **Scale: 5 µM.**

## 2.1.3 Nis1s Band Pattern Correlates with its Localization

The distinct band pattern of Nis1 prompted further investigation. Previous studies showed that Nis1 localization at the bud neck depends on the cell cycle and on its partner protein Nba1 (Meitinger et al., 2014; Perez & Thorner, 2019). Therefore, it is likely that western blot bands and potential PTMs depend on the cell cycle. To study this, cell cycle arrests and deletion of the partner protein Nba1 were studied. As before, cell extracts from an asynchronous wild-type culture displayed the distinct band pattern (**Fig. 7 C**). Here, the middle band was the strongest followed by the other two bands, which were of similar intensity. Arresting cells in the mitotic metaphase by the spindle poison nocodazole did not change the band pattern. By contrast, when extracts from cells arrested in S-phase with hydroxyurea were analyzed, the band pattern was changed. The lowest band was noticeably weaker, whereas the upper band was stronger compared to the extracts from the asynchronous culture. It can be concluded that the upper band is a form of Nis1 that is more prominent in cells arrested in S-phase of the cell cycle by hydroxyurea treatment. Deletion of Nba1 revealed a starkly different band pattern. Here, the lowest band was the most prominent form. The middle

band was weak and ran slightly lower compared to the wild type. Strikingly, the upper band was absent in the *nba1Δ* strain.

In addition to the western blot analysis, the localization of Nis1 under the same conditions was examined by fluorescence microscopy (**Fig. 7 D**). In the asynchronous wild-type culture, Nis1 was distributed in the cytoplasm. Depending on the cell cycle stage of the individual cells, Nis1 was localized either at the bud neck (M-phase, cytokinesis), localized at the bud neck and the bud scar (M-phase, cytokinesis), or found exclusively at the old bud site (G1/S/G2-phase). Therefore, in the asynchronous culture, Nis1 had three major localizations: cytoplasm, bud neck, bud scar. Upon arrest in the S-phase by addition of hydroxyurea, Nis1 was not yet localized at the bud neck, but it could be observed at the newest bud scar. Furthermore, it was distributed throughout the cytoplasm. In the *nba1Δ* strain, Nis1 did not localize at the bud neck or the bud scars (Perez & Thorner, 2019). Instead, it localized mostly to the nucleus where it was evenly distributed in most cells. Even though, it formed small aggregates in some cells.

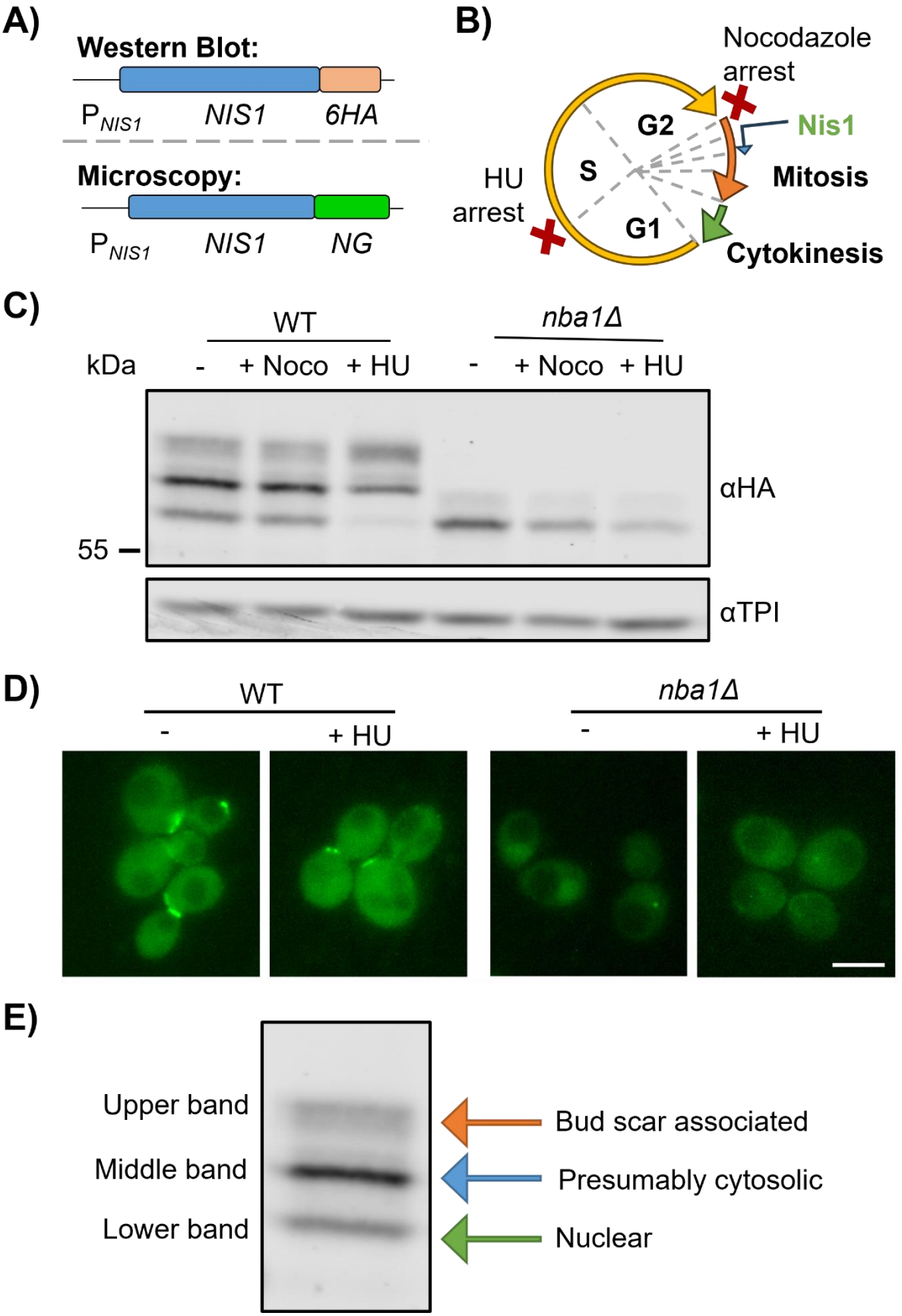


**Figure 7 Nis1s band pattern correlates with its localization. A)** Constructs used in C) and D). **B)** Overview over cell cycle arrests and Nis1 bud neck localization. Hydroxyurea inhibits the cells at the G1/S-phase border whereas nocodazole inhibits

the cells between late G2-phase and early M-phase (Day et al., 2004). Nis1 arrives at the bud neck at the on-set of mitosis (Meitinger et al., 2014). **C)** Western blot of Nis1-6HA in wild type and *nba1Δ* cells either unsynchronized, nocodazole arrested or hydroxyurea arrested. Arrests were performed by adding 15 µg/ml nocodazole or 100 µM hydroxyurea to the culture for 2 h. Boiled extracts were loaded on a 10% SDS-PAGE, blotted for 1 h at 400 mA, 100 V at 4 °C on nitrocellulose using wet blot. Blots were incubated with anti-HA (αHA) antibody (3F10-rat at 1:2,000) overnight at 4°C and with anti IGG coupled to fluorophore (680 nm emission peak) for 2 h at room temperature. Strains used were: yKU5, yFP28 **D)** Microscope images of Nis1-NG in hydroxyurea arrested cells in WT and *nba1Δ* strains. Arrest was performed for 2 h with 100 µM hydroxyurea. Acquisition time: 2 s. Strains used were: yFP45, yFP47. **E)** Overview of the band pattern of Nis1 and its attributed localization. **Scale: 5 µM**

Aside from the predominant nuclear localization, weak Nis1 signals were also distributed in the cytoplasm. Hydroxyurea arrest of *nba1Δ* cells shifted Nis1 localization from the nucleus to the cytoplasm. Since Nba1 was deleted, Nis1 could not be detected at the newest bud scar but also did not display the distinct nuclear localization it had in the asynchronous *nba1Δ* strain.

Combining western blot results with fluorescence microscopy observations, one can attribute certain bands to Nis1s localization. The lower band was the most dominant form in the *nba1Δ* strain but was reduced upon hydroxyurea arrest. Since, under both conditions, Nis1 was not located at the bud neck, it can be concluded that the lower band is a bud neck-independent form. Furthermore, the predominantly nuclear localization in the asynchronous *nba1Δ* strain compared to the hydroxyurea arrested *nba1Δ* strain, suggests that the lower band might be nuclear Nis1. The upper band of Nis1 did not occur in the *nba1Δ* strain. This suggests that the upper band is either bud neck- or bud scar-localized Nis1, since both localizations are abolished in *nba1Δ* cells. Upon hydroxyurea arrest, the upper band was stronger compared to the asynchronous culture. This suggests that the upper band most likely represents bud scar-localized Nis1, because, in the hydroxyurea arrest, Nis1 was not yet at the bud neck. The middle band might be cytoplasmic Nis1 but cannot be clearly attributed to a localization.

Linking the different bands to Nis1s localization implies that Nis1s molecular weight is different at that localization. This is most likely due to posttranslational modifications which are linked to the localization. Nis1 could either be modified locally, or the modification causes the localization at the site. These findings prompted a further investigation of Nis1 posttranslational modifications.

## 2.1.4 Posttranslational Modifications of Nis1

The distinct band pattern of Nis1 suggests that Nis1 is heavily posttranslationally modified. One of the most common PTMs is phosphorylation. In yeast, approximately over 40,000 phosphorylation sites on 3,000 proteins are estimated (Vlastaridis et al., 2017). Furthermore, Nis1 has 15 identified phosphorylation sites which were found in large proteome studies (Albuquerque et al., 2008; Holt et al., 2009; Leutert et al., 2023; Swaney et al., 2013; Zhou et al., 2021). Therefore, it was investigated whether the distinct running behavior of one of the Nis1 bands is caused by phosphorylation. The other two posttranslational modifications that were investigated were SUMOylation and ubiquitylation. Both are involved in the targeting mechanism of STUbL enzymes. First, the protein is polySUMOylated and then the SUMO chain is ubiquitylated (see Introduction). SUMOylation is especially interesting, because of Nis1's previously discussed connection to SUMO (Y2H, SIM). Ubiquitylation was investigated because it is an essential part of the degradation mediated by STUbL enzymes (Sriramachandran & Dohmen, 2014). In addition, it is a widely spread PTM (Blaszczak et al., 2024). For those reasons, phosphorylation, SUMOylation and ubiquitylation of Nis1 were investigated.

## 2.1.5 Nis1 is Phosphorylated

To investigate if one of the bands corresponds to phosphorylated Nis1, a dephosphorylation assay was employed. Here, yeast extracts were treated with $\lambda$-phosphatase. The resulting samples were probed on western blots and the band pattern was analyzed. For the $\lambda$-phosphatase treatment, a native lysis needed to be performed. Here, a glass bead lysis in native buffer was chosen. This had the downside that not all bands could be detected after lysis. The upper band could not be recovered after application of this lysis method. Various optimizations such as addition of triton or prior treatment with zymolyase could not resolve this issue. Also, addition of N-ethylamide (NEM), which inhibits DUBs, could not stabilize this band (data not shown). A likely explanation is that the upper band is lost during the centrifugation step in the glass bead lysis, where it remains in the pellet. Loading of the pellet onto an SDS-PAGE revealed that the upper band is indeed present in the pellet, although not more prominent than the lower or middle band, both of which are detectable after glass bead lysis (data not shown). The issue could not be resolved in the context of a native lysis.

Therefore, only the lower and middle band were analyzed in a dephosphorylation assay.

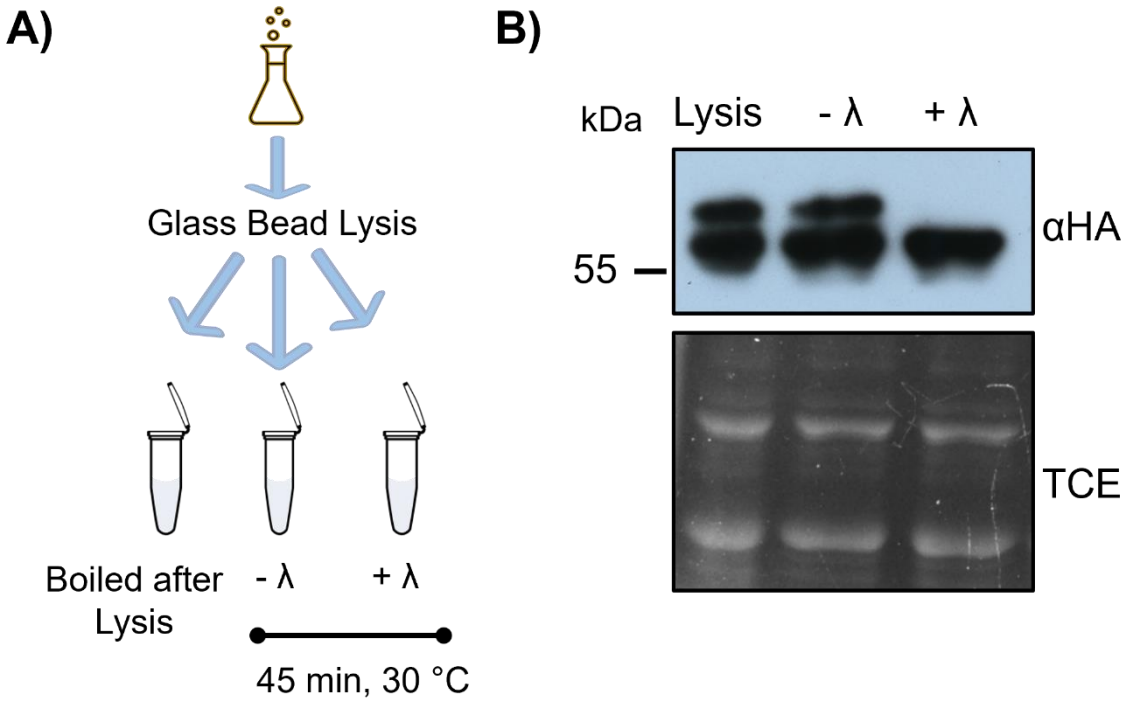


**Figure 8 Nis1 is phosphorylated. A)** Scheme of the performed dephosphorylation assay. **B)** Western blot of Nis1-6HA dephosphorylation assay. The assay was performed with extracts from native lysis. Samples were loaded on a 10% SDS-Gel with TCE, blotted for 1 h at 400 mA, 100 V at 4 °C overnight on nitrocellulose using wet blot. Blots were incubated with anti-HA (αHA) antibody (α3F10-rat used at 1:2,000) overnight at 4°C and with αrat-POD for 2h at room temperature. The film was developed for 2 h. Strain used: yFP2

For the dephosphorylation assay, three samples were analyzed by SDS-PAGE (**Fig. 8 A**). The *Lysis* sample was denatured immediately after the glass bead lysis. The *Control* sample was incubated alongside the λ-phosphatase sample with the same buffer but without λ-phosphatase. Finally, the *λ-phosphatase* sample was incubated with buffers (according to the user manual) and 1.5 µl λ-phosphatase. The first two samples showed the lower and middle band without any notable differences (**Fig. 8 B**). In the *λ-phosphatase* sample the middle band completely disappeared. The absence of the middle band in the dephosphorylation assay indicates that the protein forming this band had been dephosphorylated and therefore shifted down in the western blot. This suggests that the middle band corresponds to phosphorylated Nis1.

## 2.1.6 Nis1 is Ubiquitylated

To investigate if Nis1 is ubiquitylated, two methods were employed. First, a ubiquitin shift assay where ubiquitin was tagged with a small peptide to induce a band shift. Second, a pulldown assay where ubiquitin was pulled and Nis1 was detected.

For the ubiquitin shift assay, a myc-tagged ubiquitin expressed under the control of a copper-regulated promoter ($P_{CUP1}$) was used. Cultures were grown with and without copper sulfate. In the samples without myc-ubiquitin, Nis1 displayed a band pattern similar to the three bands (**Fig. 9 A**). Here, to achieve a higher sensitivity, western blots were developed using peroxidase (POD) coupled antibodies and films instead of fluorescent antibodies and the Odyssey scanner. This caused the middle band to overshadow the other bands; hence the band pattern appeared slightly different compared to previous blots (**Fig. 7 C**). In samples with myc-ubiquitin, but without copper induction, a weak smear upwards was already detectable. This was expected because the copper promoter $P_{CUP1}$ is leaky in comparison to the $P_{GAL1}$ promoter (Peng et al., 2015). Upon induction with copper sulfate, the smear signal increased immensely. This showed that Nis1 undergoes ubiquitylation. Since a strong smear appeared above the endogenous Nis1 bands, ubiquitylation could not be pinpointed to a specific band. But instead, it seemed that upon ubiquitin overexpression more Nis1 was ubiquitylated. It is possible that the overexpression of ubiquitin causes increased ubiquitylation of Nis1. Another explanation could be that overexpression causes the overload of the ubiquitin-proteasome system leading to a stabilization and therefore accumulation of ubiquitylated Nis1. Either way, the ubiquitin shift assay demonstrated that Nis1 is ubiquitylated.

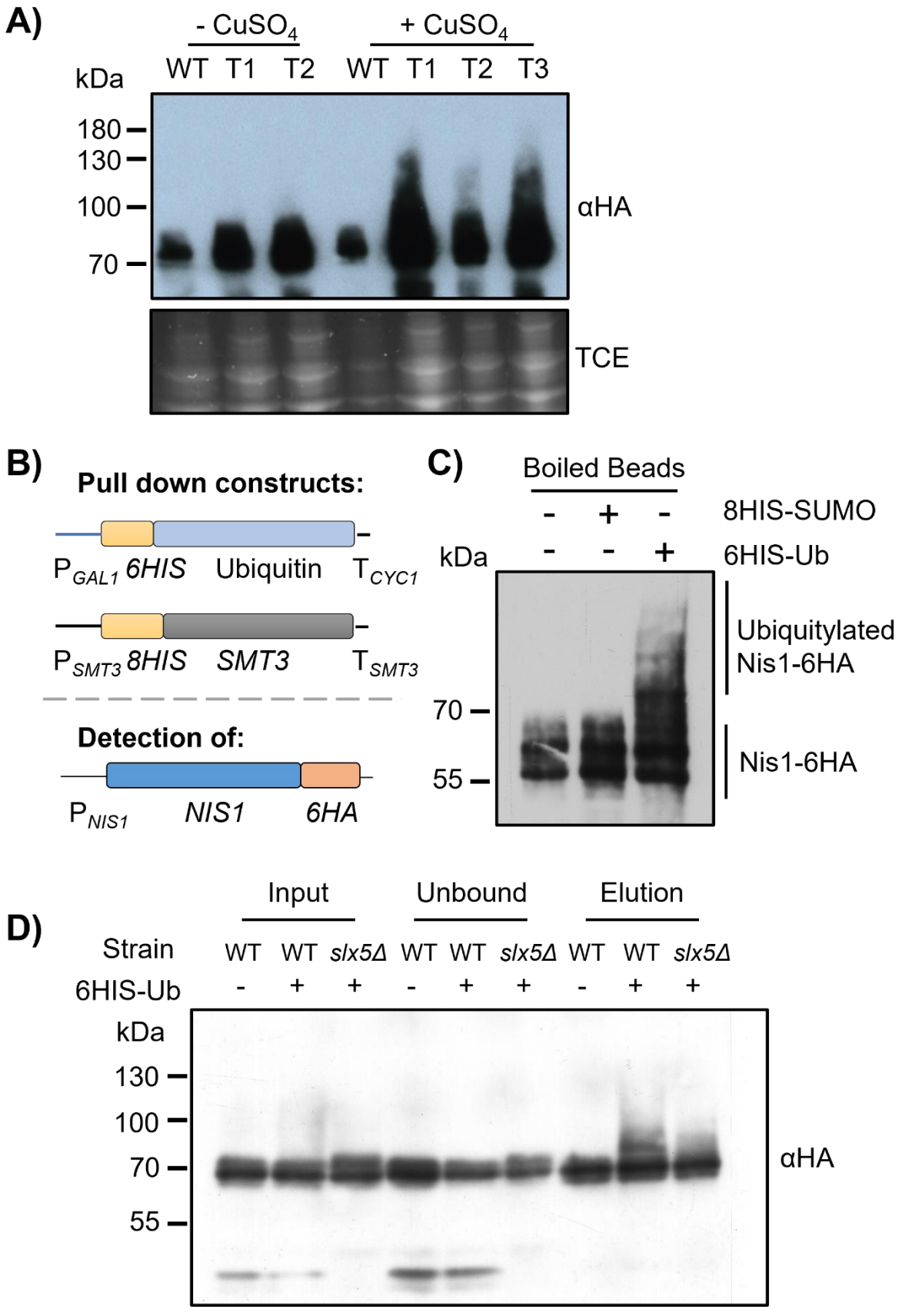


**Figure 9 Nis1 is ubiquitylated. A)** Western blot of the Nis1-6HA ubiquitin shift assay. The induction of myc-ubiquitin with 100 µM $CuSO_4$ was performed for 4 h using 100 µM $CuSO_4$. Boiled extracts were loaded on a 10% SDS-Gel with TCE, blotted for 1 h at 400 mA, 100 V at 4 °C on nitrocellulose using wet blot. Blots were incubated

with anti-HA (αHA) antibody (3F10-rat at 1:2,000) overnight at 4°C and with anti IGG coupled to HRP (αrat-POD) for 2 h at room temperature. Strains used were: yFP105 with pRB240. **B)** Schematic representation of the constructs used in the pull downs in C) and D) **C)** Western blot of 6HIS-ubiquitin and 8HIS-SUMO pulldown detecting Nis1-6HA. 50 µl of the supernatant of boiled bead samples were loaded on a 10% SDS-PAGE with TCE, blotted for 1 h at 400 mA, 100 V at 4 °C on nitrocellulose using wet blot. Blots were incubated with anti-HA (αHA) antibody (3F10-rat at 1:2,000) overnight at 4°C and with anti IGG coupled to HRP (αrat-POD) for 2 h at room temperature. Strains used were: yFP105 with pKU103. **D)** Western blot of 6HIS-Ubiquitin and 8HIS-SUMO pulldown detecting Nis1-6HA. 50 µl samples were loaded on a 10% SDS-Gel with TCE, blotted for 1 h at 400 mA, 100 V at 4 °C on nitrocellulose using wet blot. Blots were incubated with anti-HA (αHA) antibody (3F10-rat at 1:2,000) overnight at 4°C and with anti IGG coupled to HRP (αrat-POD) for 2 h at room temperature. Film was developed for 30 min. Strains used were: yFP105; yFP105 with pKU103, yKU87 with pFP3 & pKU103.

In parallel to the shift assay, ubiquitin and SUMO pulldowns were performed. Here, ubiquitin and SUMO were tagged with 6HIS and 8HIS, respectively. A denaturing lysis using 8 M UREA buffer was performed to ensure that only covalently bound Nis1 was pulled. This is crucial to show the SUMOylation of SIM-containing proteins as SIMs promote the non-covalent interaction with SUMO under native conditions. This problem can be circumvented by using denaturing conditions. Here, a HIS pulldown was chosen. HIS pulldowns are based on metal-chelate interaction and not on antibody - antigen interaction such as the HA or FLAG pulldown. Therefore, HIS pulldowns can be performed under denaturing conditions. The downside is that they are comparably less specific, because many proteins carry multiple histidine residues and may also bind the resin in absence of a HIS-tag.

The western blot of the boiled magnetic cobalt-coated beads of the SUMO and ubiquitin pulldown of Nis1-6HA can be found in Fig. 9 C. Notably, Nis1 in the pulldown control, without HIS tagged SUMO or ubiquitin, had already some affinity to the HIS-beads. This is not surprising considering the abovementioned downside of HIS-pulldowns. So, to determine if Nis1 is SUMOylated or ubiquitylated, the pulled Nis1 needed to be above the background level in the pulldown control. In the SUMO pulldown, the detectable amount of Nis1 was not above the background level. Therefore, SUMOylation of Nis1 could not be detected in this assay. In contrast, elution of HIS-tagged ubiquitin pulled down higher molecular weight forms of Nis1-HA way above the background level. Therefore, the pulldown supports the result of the ubiquitin shift assay and shows that Nis1 is ubiquitylated.

In the context of SUMO-targeted ubiquitin ligases, the question occurred if the observed ubiquitylation is promoted by STUbL enzymes. Therefore, the pulldown was repeated in the *slx5Δ* background. Deletion of Slx5, one of the Uls2 subunits, renders Uls2 non-functional. As a control, a Nis1-6HA strain without HIS-tagged ubiquitin was used, as well as the strain expressing 6HIS-ubiquitin and untagged Nis1 (**Fig. 9 D**). In the elution of the sample from the wild type, a smear above the background level of Nis1 could be detected as previously described (**Fig. 9 C**). This smear was reduced in the *slx5Δ* background. This points to a role of Slx5 in the ubiquitylation of Nis1, although it does not seem to be fully dependent on Slx5. One must note that this result is still preliminary and requires further investigation.

To summarize, it could be shown that Nis1 is ubiquitylated. This ubiquitylation might be linked to Uls2. So far, however, there is no direct evidence for SUMOylation of Nis1. This could be explained by the fact that only a small fraction of a protein is SUMOylated, estimated 5-10%, which makes the detection of SUMOylation difficult (Xiao et al., 2015).

### 2.1.7 Reporter Construct with Nis1 C-terminal Domain

Previous studies showed that Nis1 has a SUMO-interacting motif in its C-terminal domain (Uzunova et al., 2007). Since SIMs promote the interaction with SUMO or the SUMOylation machinery, this prompted further investigation. To study the role of this Nis1 SIM, the C-terminal domain of Nis1, which includes the last 55 amino acids, was attached to a reporter construct. The reporter protein was a FLAG- and HIS-tagged version of the fluorescent protein neongreen (NG). The gene encoding this reporter protein was placed under the copper-inducible promoter $P_{CUP1}$. (**Fig. 10 A**). Different variants of the C-terminal Nis1 domain were attached to the reporter (**Fig. 10 C**). As a control, a reporter without any part of the Nis1 C-terminal domain was designed.

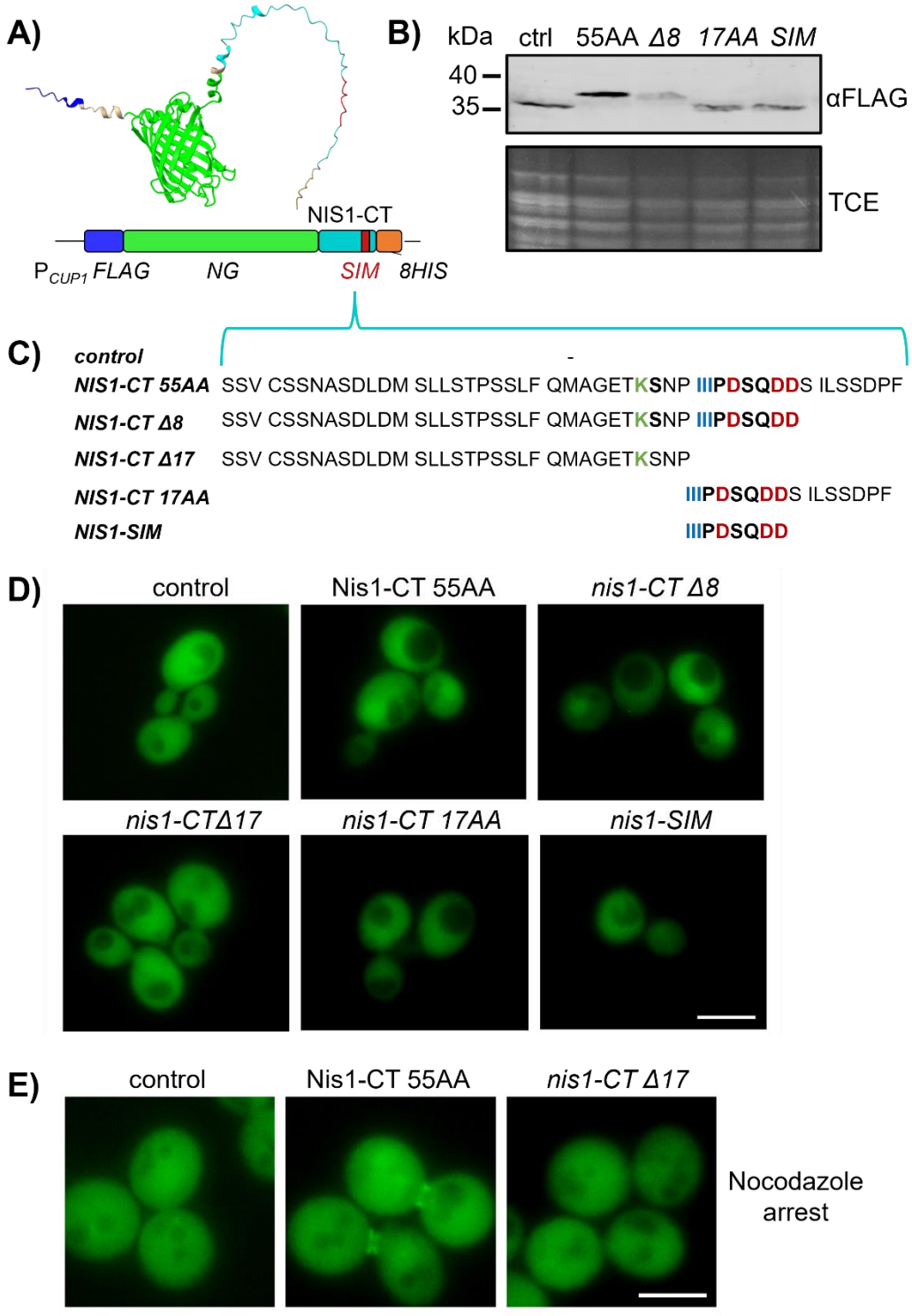


**Figure 10 C-terminal domain of Nis1 targets reporter to the nucleus. A)** AlphaFold model of Nis1 C-terminal domain reporter construct Nis1-CT 55AA (Abramson et al., 2024). **B)** Western blot of different Nis1 C-terminal domain reporter proteins. Expression of proteins was induced with 100 µM $CuSO_4$ in YP-Glucose for 4 h. Boiled extracts were loaded on a 10% SDS-Gel, blotted for 30 min on nitrocellulose using the TURBO Blot system. Blots were incubated with anti-HA (αHA) antibody (3F10-rat at 1:2,000) overnight at 4°C and with anti IGG coupled to fluorophore (680 nm emission peak) for 2 h at room temperature. Strains used were: yFP55, yFP56, yFP80, yFP81,

yFP83, yFP84. **C)** Amino acid sequence of the C-terminal extensions in the different reporter constructs used in B) and C). **D)** Microscope images of different reporters with Nis1s C-terminal domain. Cells were grown in YP-Glucose with 100 µM $CuSO_4$ for 4 h. Image acquisition: FITC: 600 ms for ctrl; 55AA, *Δ17*; 800 ms for *Δ8*, 17AA, SIM. Strains used were: yFP55, yFP56, yFP80, yFP81, yFP83, yFP84. **D)** Microscope images of nocodazole arrested reporter constructs linked to Nis1 C-terminal domain. Cells were grown 3 h in YP-Glucose and then arrested with 15 µg/ml Nocodazole for 2 h. Acquisition: FITC: 600 ms. Strains used were: yFP55, yFP56, yFP80. **Scale: 5 µM.**

First, the different reporter constructs were analyzed by western blotting (**Fig. 10 B**). This analysis confirmed that all reporters were expressed and displayed electrophoretic mobility according to their calculated molecular weight. To analyze the cellular localization of the reporter, fluorescence microscopy was performed (**Fig. 10 C**). Here, the control construct was evenly distributed in the cytoplasm without any accumulation at the bud neck. The control construct also did not display a strong nuclear localization. Only in a few cells, one could find a more prominent nuclear localization, but to a certain degree proteins diffuse freely into the nucleus depending on their size and charge explaining the heightened nuclear localization in some cells (Timney et al., 2016). When the full-length C-terminal domain (55AA) of Nis1 was attached to the reporter, the nuclear localization increased. In most cells a clear nuclear localization became visible, although a large portion of the protein was still localized in the cytoplasm. Deletion of the last 8 amino acids (*Δ8*), up until the SIM, did not change this. Here, nuclear localization was comparable to the reporter with the full-length C-terminal domain. This changed, however, upon deletion of the SIM (*Δ17*). Here, nuclear localization was at background level comparable to the control reporter construct. From these data, it can be concluded that the SIM is involved in the increased nuclear localization.

Furthermore, two reporters were designed that include the SIM, but were truncated. The first reporter carried only the last 17 residues of Nis1 whereas the second reporter carried only the SIM. Surprisingly, both reporters did not have the same nuclear localization as the reporter carrying the full-length C-terminal Nis1 domain. Both were slightly more nuclear than the background level, but not significantly. This suggests that not only the SIM but also the surrounding regions are involved in the nuclear localization of the reporter. The possibility that the C-terminal Nis1 domain harbors a hidden nuclear localization signal (NLS) was tested using online tools (https://nls-mapper.iab.keio.ac.jp;

http://www.moseslab.csb.utoronto.ca/NLStradamus). However, no NLS could be found. Still, the surrounding regions could enhance effect of the SIM or make it more accessible for interaction with SUMO. It is possible that the direct attachment of the SIM to the neongreen reporter, which has a barrel-like structure, hinders accessibility of the SIM.

Interestingly, apart from nuclear localization, the full-length reporter could also be observed at the bud neck. This was especially pronounced in nocodazole arrested cells (**Fig. 10 E**). This specific localization was visible for the full-length construct but not for the control or the *Δ17* construct where the SIM is was deleted. This points towards a role of the SIM in bud neck localization. Upon nocodazole treatment, cells arrest in the M-phase where septins are known to be SUMOylated (Johnson & Blobel, 1999). Localization of the reporter at the bud neck at this stage of the cell cycle indicates a functioning SIM mediating interaction with SUMOylated septins. Interestingly, in the context of full-length Nis1, the bud neck localization is conferred through Nba1 (Meitinger et al., 2014) and the deletion of the SIM will not abolish the localization at the bud neck.

To summarize, it could be shown that the C-terminal domain of Nis1 is able to target a reporter to the nucleus. It can also target the reporter to the bud neck during M-phase. Furthermore, it could be shown that both localizations are SIM-dependent. This now prompts the question of whether they are also SUMO-dependent.

### 2.1.8 Nuclear Localization of Nis1 C-terminal Domain Reporter depends on SUMOylation

To investigate if SUMOylation is involved in the nuclear localization of reporter proteins carrying the Nis1 C-terminal domain, a strain deficient in SUMOylation was employed. Here, the *uba2-ts* strain was used. This strain expressed a mutant version of Uba2, a subunit of SUMO-activating enzyme, and hence displays strongly reduced protein SUMOylation and temperature-sensitive growth properties. The nuclear localization of the full-length reporter was investigated using fluorescence microscopy (**Fig. 11 A**). DAPI staining was used to visualize the nucleus and verify the nuclear localization of the reporter. In the wild type, nuclear localization could be observed as previously (**Fig. 10 D**). This was reduced to background level in *uba2-ts* pointing

towards the role of SUMOylation in nuclear localization of the full-length reporter construct.

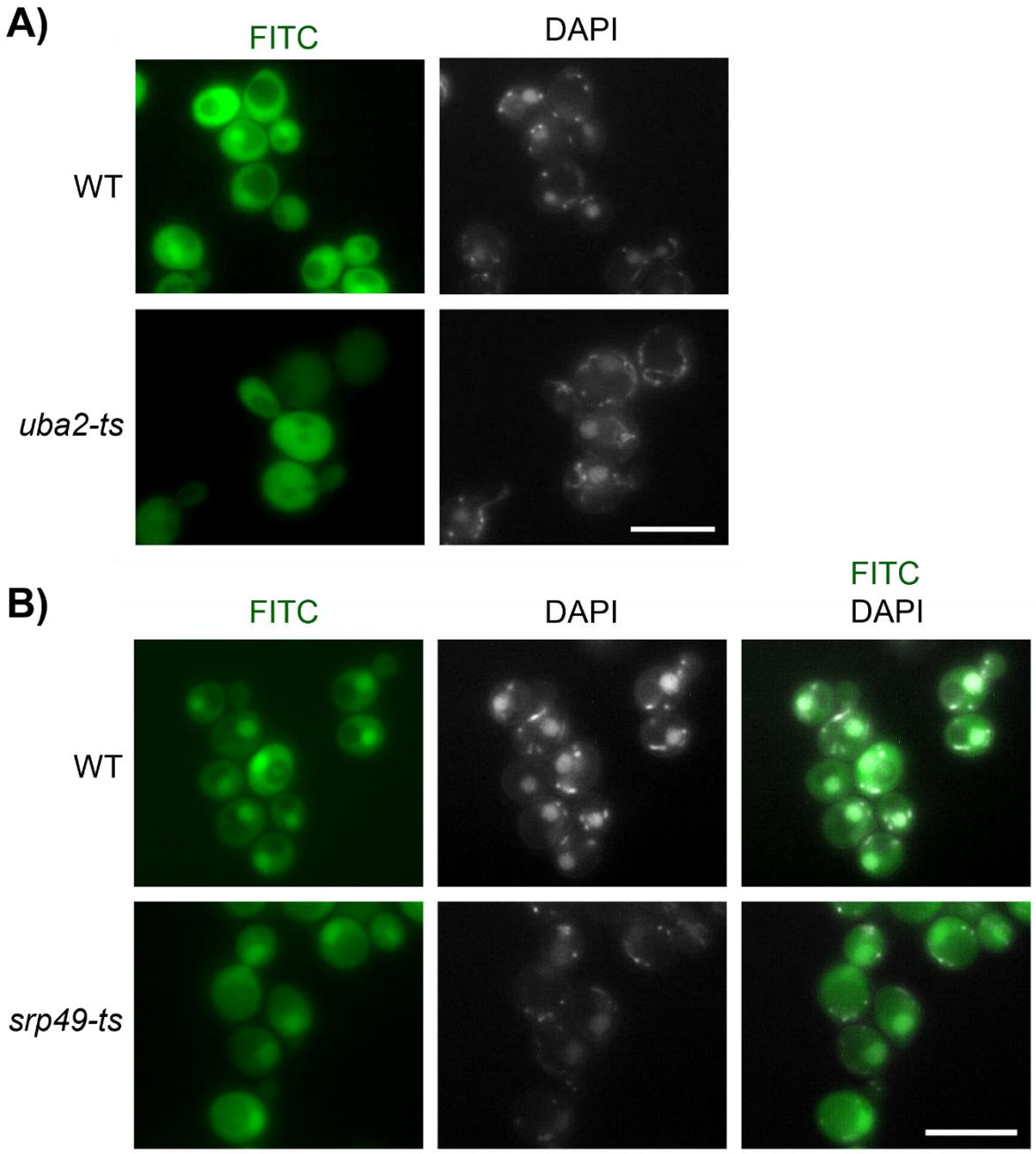


**Figure 11 Nuclear localization of Nis1 C-terminal domain reporter depends on SUMOylation. A)** Microscope images of C-terminal domain reporter 55AA in wild type and *uba2-ts* strains. Cells were grown in YP-Glucose with 100 µM $CuSO_4$ at 30 °C for 4 h followed by an incubation with DAPI for 30 min. Image acquisition: neongreen: 1.6 s; DAPI: 1.8 s. Strains used were: yFP55, yKU25-2a with pFP14. **B)** Microscope images of C-terminal domain reporter 55AA in wild type and *srp49-ts* cells. Cells were grown in YP-Glucose with 100 µM $CuSO_4$ for 4 h followed by an incubation with DAPI for 30 min. Acquisition: FITC: 1.6 s; DAPI: 1.8 s. Strains used were: GSY154 with pFP14; GSY203 with pFP14. **Scale: 10 µM.**

A previous study reported an impairment of the pathway that mediates nuclear localization of proteins with canonical nuclear localization signals (cNLS) in the *uba2-ts* strain (Stade et al., 2002). To exclude that the effect observed in the *uba2-ts* strain is due to the impairment of the cNLS pathway, the *srp49-ts* mutant was tested (**Fig. 11 B**). This temperature-sensitive mutant has a strong and specific defect in the cNLS-dependent import pathway. If the reporter was imported via the cNLS pathway, a strong reduction in nuclear localization would have been expected. The reporter, however, showed similar nuclear localization in *srp49-ts* cells as in the respective wild type. It can be concluded that the reporter carrying the C-terminal Nis1 domain is not imported into the nucleus via the cNLS pathway and therefore must employ an alternative pathway for SIM- and SUMO- dependent nuclear translocation.

### 2.1.9 Uls2 targets Overexpressed Nis1

Lastly, the targeting of nuclear Nis1 was through Uls2 was investigated using an overexpression construct of Nis1. As previously discussed, overexpression of Nis1 allows monitoring of its nuclear fraction, which might be targeted by Uls2. Thus, an overexpression construct of Nis1 was designed (**Fig. 12 A**). The construct was introduced into the wild type and the $P_{GAL1}$*ULS2* strains. The latter strain enabled both shut off as well as alternatively overexpression of Uls2. The protein levels of Nis1 were compared in wild type and $P_{GAL1}$*ULS2* under shut off or overexpression conditions by western blot (**Fig. 12 B**). The overexpressed Nis1 ran differently during SDS-PAGE than the previously investigated Nis1-6HA expressed from its native promoter in the genome, which displayed three distinct bands (**Fig. 5 B**). The overexpression construct, by contrast, resulted only in a Nis1-HA double band. These differences could be due to multiple factors. Firstly, the overexpressed Nis1 had only one HA tag compared to the one expressed from the endogenous locus, which carried a 6HA tag. This increased the detection of low abundant forms, since more antibodies can bind to the protein and amplify the signal. Secondly, the overexpression of Nis1 could imbalance the system and certain modifications may have an insufficient capacity to modify the excess of Nis1. Thirdly, modifications depending on the localization via Nba1 may be limited to a small part of the Nis1 pool, since Nba1 is not co-overexpressed. Finally, in addition to the HA tag the overexpressed protein carries GFP which induces a size shift and contributes to a different running pattern.

Nevertheless, Nis1 levels could be compared under different conditions. In the wild type on galactose, Nis1 protein level was slightly reduced by 12% compared to the wild type on glucose. In the $P_{GAL1}$*ULS2* strain on galactose, the Nis1 protein level was reduced significantly by 37% compared to the wild type on galactose. This indicates that Nis1 is targeted by Uls2. In the $P_{GAL1}$*ULS2* strain under shut off conditions, Nis1-HA levels did not vary significantly from those in the wild type cells. This was surprising since one could have expected an accumulation of Nis1 upon deletion of Uls2. There are multiple possible explanations why stabilization of Nis1 cannot be detected. First, it could be that Nis1 accumulates in the shut off strain, but specifically its SUMOylated forms. Those forms would run higher and not necessarily as a clear band, which might put them under the detection limit. Second, Nis1 forms aggregates which cannot be resolved with the performed lysis. Third, other enzymes compensate for the loss of Uls2. Lastly, a shutdown of 4 hours could be insufficient to achieve a stabilization of Nis1. However, previous experiments performed with overnight incubation of the $P_{GAL1}$*ULS2* strain in YP-Glucose also did not show any stabilization of Nis1 (data not shown). This indicates that the shutdown time is unlikely a contributing factor to the lack of Nis1 stabilization in the Uls2 shut off.

In conclusion, even though stabilization of Nis1 could not be detected upon shutdown of Uls2 expression, the targeting of Nis1 could be shown by overexpression of Uls2. This suggests that nuclear Nis1 is a substrate of Uls2.

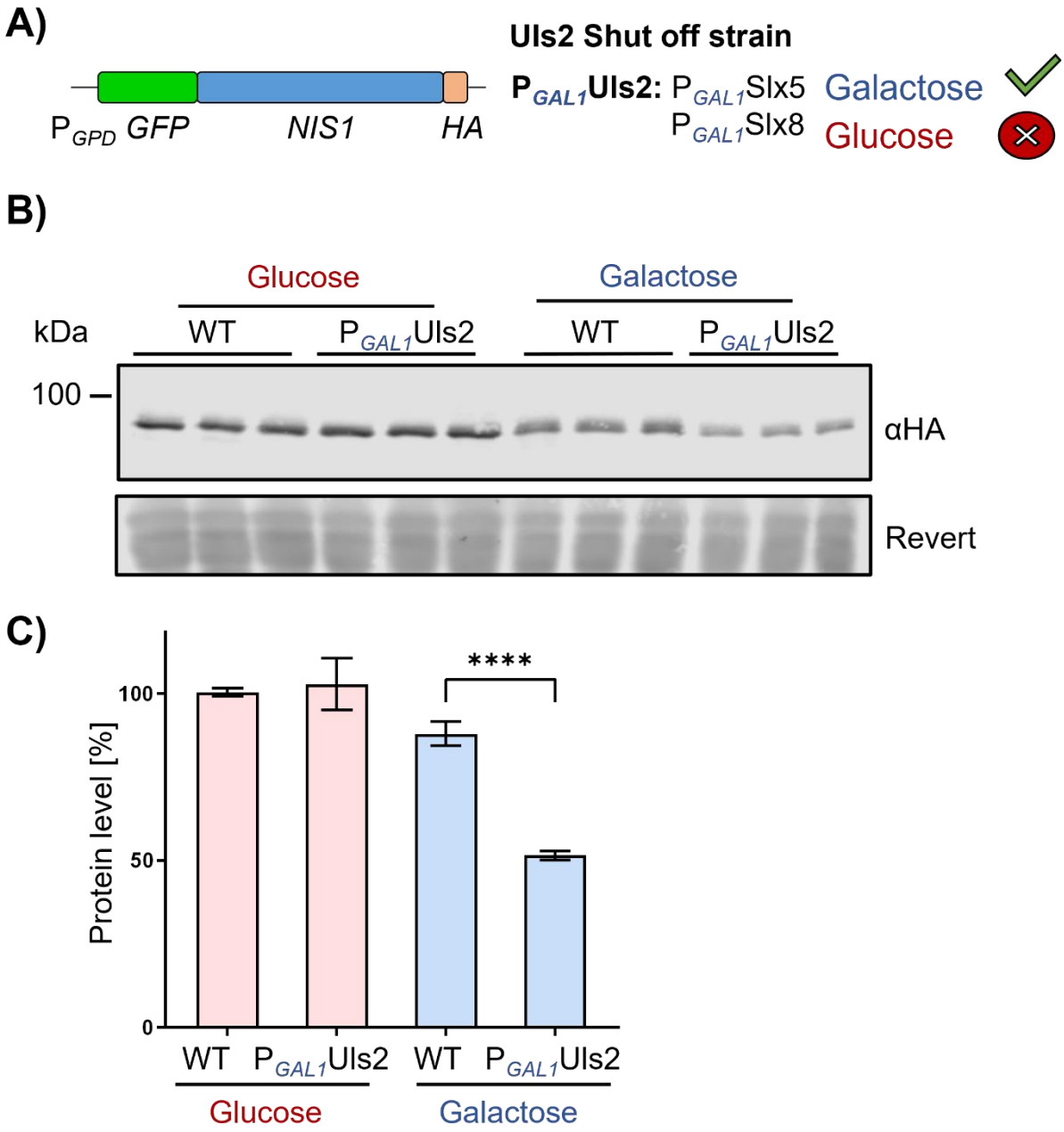


**Figure 12 Uls2 targets overexpressed Nis1. A)** Constructs used in B) and C) **B)** Western blot of P$_{GPD}$*GFP-NIS1-HA* in wild type and P$_{GAL1}$*ULS2* strains. After overnight preculture in YP-Raffinose, cells were grown 4 h in YP-Glucose or YP-Galactose. For sample preparation an alkaline lysis followed by TCA precipitation was performed. The resulting samples were loaded on an 8% SDS-Gel and blotted for 1 h at 400 mA, 100 V at 4 °C on nitrocellulose using wet blot. Blots were incubated with anti-HA (αHA) antibody (3F10-rat at 1:2,000) overnight at 4°C and with anti IGG coupled to fluorophore (800 nm emission peak) for 2 h at room temperature. Strains used were: yFP2, yFP21. **B)** Quantification of P$_{GPD}$*GFP-NIS1-HA* P$_{GAL1}$*ULS2* western blot. Students t-test; n=6; * = p<0.05; ** = p <0.01; *** = p < 0.001; **** = p< 0.0001.

To achieve independent proof for the abovementioned conclusion, Nis1 localization was investigated in $P_{GAL1}$*ULS2* using fluorescence microscopy (**Fig. 13 A**). Here, in the wild type on glucose, Nis1 had a prominent nuclear localization. Additionally, it was localized in the cytoplasm, and in some cases it could be observed at the bud neck. Interestingly, Nis1 displayed different forms of nuclear localization, which were monitored in three categories. The first category was cells with a smooth nucleus (*smooth nucleus*). Here, Nis1 was evenly spread in the nucleus, and no aggregates were visible (**Fig. 13 B**). In the wild type this was the most common phenotype. *Smooth nuclei* were detected in 39% of the cells. The second phenotype was categorized as *spotty nucleus*. Here, the nucleus had evenly distributed Nis1 as well as Nis1 accumulated in small aggregates. For the wild type this occurred in 10% of the cells. The third category included cells with prominent aggregates (*single aggregates*). Here, the nucleus harbored one, sometimes more, aggregates. Unlike the phenotype *spotty nucleus* there was no even staining throughout the nucleus. Single aggregates occurred in less than 1% of the cells in the wild type.

In the $P_{GAL1}$*ULS2* strain under shut off conditions, two phenotypes increased. *Spotty nuclei* increased from 10% to 15% and “single aggregates” increased from <1% to 9.5%. Unlike the western blot, the microscopy analysis revealed a stabilization of Nis1. The reason could be the previously hypothesized aggregates. Microscopic analysis revealed that Nis1 indeed forms aggregates. Additionally, these aggregates accumulated under shut-off conditions. If those aggregates were insoluble, this would explain the discrepancy between microscopy and western blot results under shut off conditions.

Upon overexpression of Uls2, the distribution of the phenotypes changed drastically. Cells with *smooth nuclei* were reduced from 31% in wild type on galactose to 6% in $P_{GAL1}$*ULS2* on galactose. Notably, also the intensity of nuclear fluorescence appeared to be reduced. *Spotty nuclei* were not detected anymore upon overexpression of Uls2. Only the *single aggregates* did not change significantly. The results from the quantitative analysis of fluorescence microscopy images therefore support the western blot results. Nis1 protein level is reduced upon overexpression of $P_{GAL1}$*ULS2*.

In conclusion, microscopic analysis revealed that Nis1 accumulates in aggregates upon shutoff of Uls2. Apparently, these aggregates were not resolved upon cell lysis by boiling in sample buffer. Overexpression of Uls2 showed targeting of Nis1 both by

reduction of microscopically detectable nuclear Nis1 and by reducing overall Nis1 level detectable by western blotting.

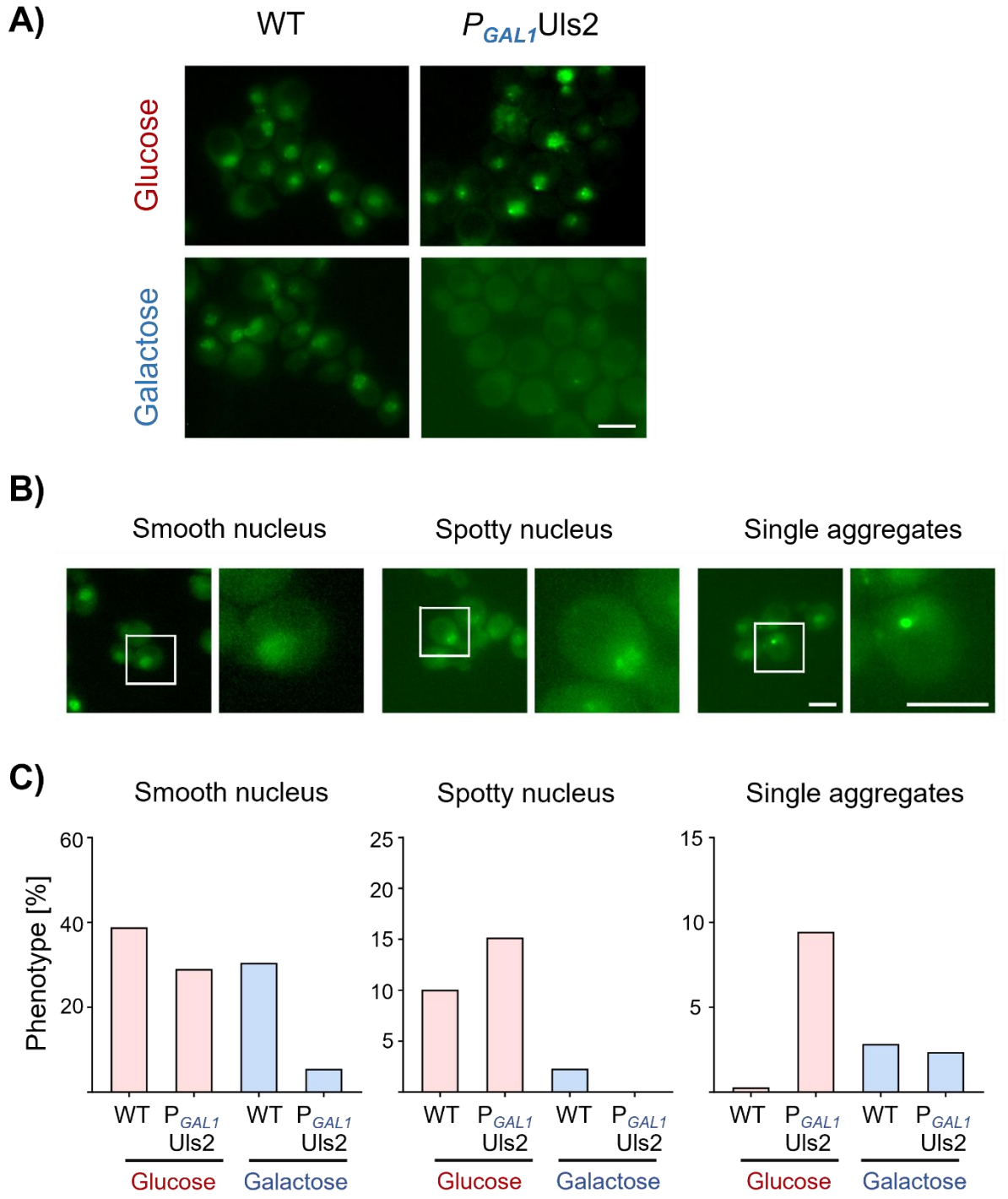


**Figure 13 Uls2 targets overexpressed, nuclear Nis1. A)** Microscope images of $P_{GPD}$*GFP-NIS1* in wild type and $P_{GAL1}$*ULS2.* After overnight preculture in YP-Raffinose, the cells were grown 5 h in YP-Glucose or YP-Galactose. Image acquisition: GFP: 1000 ms. Strains used were: yLA13, yLA17. **B)** Representative images of $P_{GPD}$GFP-Nis1 nuclear phenotypes. Acquisition: GFP: 800 ms. Strain used was: yLA13. **C)** Quantification of different nuclear localization phenotypes seen in fluorescence microscopy of $P_{GPD}$GFP-Nis1 in wild type and $P_{GAL1}$*ULS2* strains. **Scale: 5 µM.**

# 2.2 Fir1

So far, Nis1 has been identified as a substrate of Uls2. Interestingly, targeting through Uls2 occurs when Nis1 is overexpressed and undergoes nuclear localization. To assemble further evidence supporting a possible link between SIM- and SUMO-dependent nuclear targeting and STUbL-mediated degradation, the next goal was to find another target of these mechanisms. Fir1 was chosen as a potential candidate, because it harbors multiple similarities to Nis1. Fir1 carries a SIM and it interacts with SUMO in a yeast-two-hybrid assay (Uzunova et al., 2007). Furthermore, upon deletion of its interactor Spa2 and Cdh1, Fir1 can be observed in the nucleus (Nils Johnsson, University of Ulm, personal communication). Therefore, Fir1 was investigated as a potential substrate of Uls2.

## 2.2.1 Overexpressed Fir1 Displays Strong Aggregate Formation

Based on the observation of Fir1 nuclear localization in *spa2Δ cdh1Δ*, it seemed likely that overexpression of Fir1 might promote is nuclear localization, similar to the results described above for overexpressed Nis1. To investigate this, a strain overexpressing Fir1 was constructed. To our knowledge, there are no previous reports of an Fir1 overexpression strain. Therefore, the effect of Fir1 overexpression was investigated as well as the localization of overexpressed Fir1. The Fir1 overexpression construct was designed parallel to the Nis1 overexpression cassette. A copy of the *FIR1* gene was put under control of the *TDH3* promoter and fused to sequences encoding N-terminal GFP and a C-terminal HA tag. This construct was integrated at the *LEU2* locus leaving the endogenous protein untampered. Wild-type cells harboring the Fir1 overexpression cassette were studied using brightfield and fluorescence microscopy. Brightfield microscopy revealed that the cells clumped together (**Fig. 14 A**). In contrast, wild-type cells laid smoothly next to each other on the microscope slide. Cells rarely overlapped or reached in another layer. Fir1 cells laid in clumps on top of each other protruding in different focus planes. Intense vortexing did not disrupt the clumping of the cells. It appeared as if the cytokinesis of the cells was not fully finished.

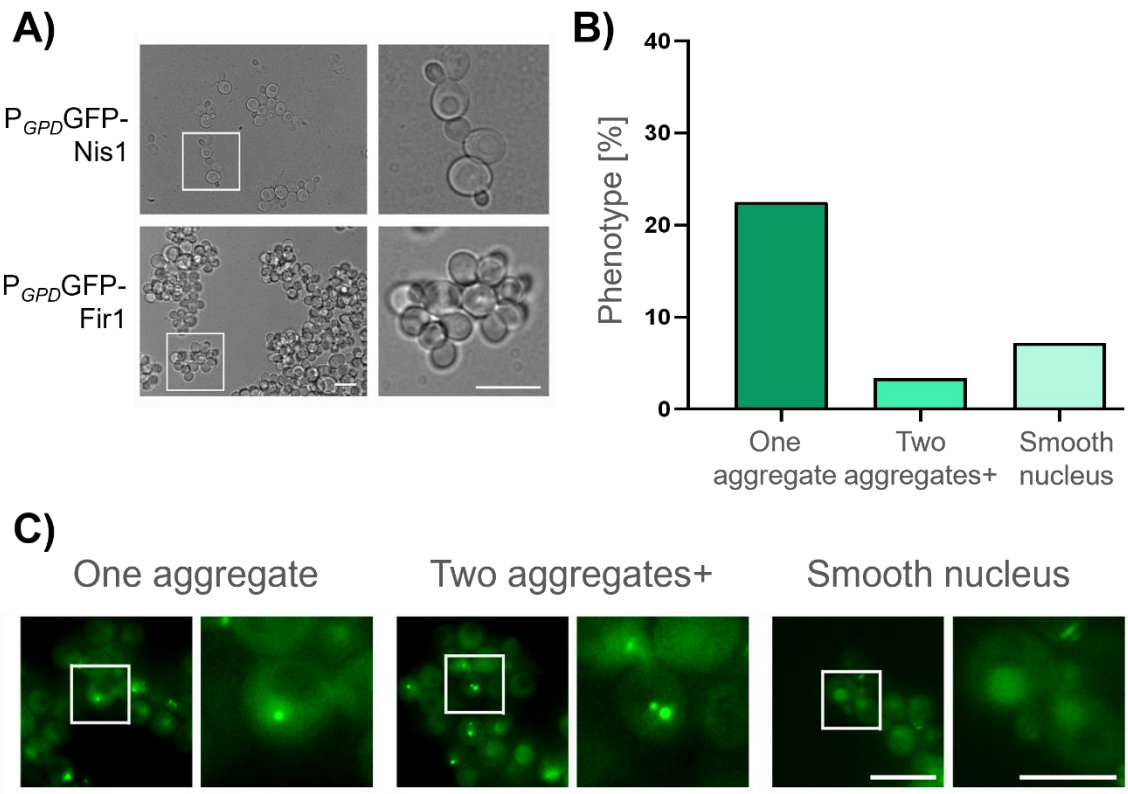


**Figure 14 Overexpressed Fir1 displays strong aggregate formation**. **A)** Microscope images of otherwise wild-type cells expressing a P$_{GPD}$*GFP-FIR1-HA* construct. The two panels at the top display an otherwise wild-type strain expressing P$_{GPD}$GFP-Nis1-HA. In comparison, the bottom panels display cells with the *GFP-FIR1-HA* construct. The panels on the right are cropped areas from the left panels indicated by the white square. Image acquisition: Brightfield: 13 ms. Strains used were: yFP167, yLA13. **Scale: 10 µM**. **B)** Quantification of Fir1 phenotypes. **C**) Overview over nuclear phenotypes of Fir1. Strain used was: yFP167 Acquisition: GFP: 900 ms. **Scale: 5 µM.**

Next, the localization of overexpressed Fir1 was examined using fluorescence microscopy. Endogenous Fir1 has been described to localize at the bud neck during the cell cycle, or it is distributed throughout the cytoplasm (Brace et al., 2019; Müller et al., 2024). Overexpressed Fir1 could also be detected at both locations (**Fig. 14 C**). Additionally, it displayed a nuclear localization. This nuclear localization showed a variety of phenotypes. The phenotypes were divided into different categories. The first category was cells with *one aggregate* which includes cells which have one large aggregate. This aggregate is either nuclear or nucleus associated. This phenotype occurred in around 22% of the cells. The second category was cells with *two aggregates+*. This phenotype is similar to the phenotype *one aggregate* but with two or more aggregates in the cell. In these otherwise wild-type cells this phenotype was rarer with an occurrence rate of ~3%. The third phenotype *smooth nucleus* included

cells, which did not have any aggregates, but instead displayed Fir1 smoothly distributed in the nucleus.

To summarize, overexpression of Fir1 leads to cells not being fully separated. Overexpressed Fir1 localized to the nucleus and can therefore be studied as a potential target of Uls2. Furthermore, it forms prominent aggregates which prompt further investigation.

### 2.2.2 Mutation of Fir1's SIM Abolishes Aggregate Formation

After the discovery of Fir1s aggregate formation, the next step was to further investigate these aggregates. The question arose if these aggregates are targeted by Uls2 and if the formation of the aggregates is SIM-dependent. To investigate the role of the SIM, a mutation (I760K) was introduced into Fir1. This mutation replaces a hydrophobic residue in the SIM with a positively charged lysine. This exchange disrupts the interaction of the hydrophobic stretch in the SIM with the hydrophobic grove in SUMO. The SIM mutant of Fir1 was investigated using fluorescence microscopy and western blots.

Using fluorescence microscopy, the localization of the SIM mutant was studied. The control with GFP-Fir1 in the wild-type strain displayed the previously described phenotypes (**Fig. 14 C**). It was localized at the bud neck, the cytoplasm and in the nucleus. Notably, GFP-Fir1 additionally formed aggregates. Strikingly, the formation of aggregates was completely abolished in the strain with GFP-*fir1*$^{I760K}$ (**Fig. 15 A**), whereas the nuclear localization was not abolished. The Fir1 SIM mutant was smoothly distributed in the nucleus suggesting that the SIM is crucial for aggregate formation but not for nuclear localization. Additionally, the localization at the bud neck was also not disturbed by the SIM mutation. A previous study supports that the general localization at bud neck is not disturbed in the SIM mutant but reported that the timing in the cell cycle changes (Müller et al., 2024).

Western blot analysis revealed a stabilization of *fir1*$^{I760K}$ yielding 128% of wild-type Fir1 (**Fig. 15 D**). Stabilization of mutant Fir1 suggests that the SIM plays a role in Fir1 degradation. Taken together microscope and western blot analysis suggest that the SIM promotes aggregation as well as proteolytic targeting of Fir1. SIM involvement in aggregate formation implies that SUMO is involved as well. This further suggests that the aggregates might be targeted by Uls2.

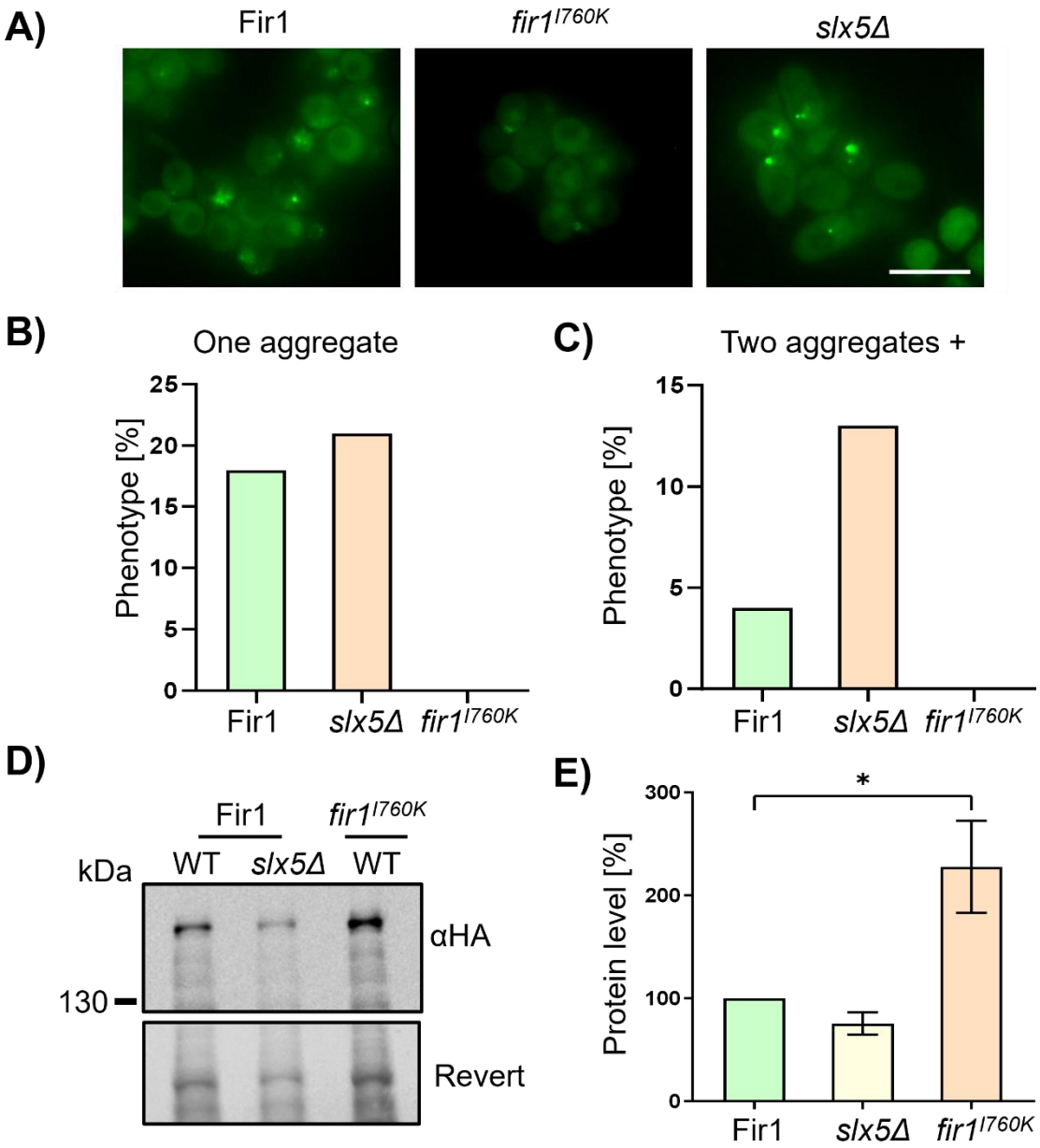


**Figure 15 Mutation of Fir1s SIM abolishes aggregate formation. A)** Microscope images of $P_{GPD}$*GFP-FIR1-HA* and $P_{GPD}$*GFP-fir1*$^{I760K}$*-HA* in wild type and in *slx5Δ* strains. Image acquisition: GFP: 900 ms. Strains used were: yFP167, yFP169, yFP172. Scale: 10 µM **B)** Quantification of the phenotype *One aggregate* in A). **C)** Quantification of the phenotype *Two aggregates+* in A). **D)** Western blot of $P_{GPD}$*GFP-FIR1-HA* and $P_{GPD}$*GFP-fir1*$^{I760K}$*-HA* in wild type and in *slx5Δ* strains. Samples of postalkaline lysis were loaded on an 8% SDS-PAGE, blotted for 1 h at 400 mA, 100 V at 4 °C on nitrocellulose using wet blot. Blots were incubated with Revert before blocking. Blocked membranes were incubated with anti-HA (αHA) antibody (3F10-rat at 1:2,000) overnight at 4°C and with anti IGG coupled to fluorophore (800 nm emission peak) for 2 h at room temperature. Strains used were: yFP167, yFP169, yFP172. **E)** Quantification of western blot in D) n=3; Students T-test; * = p<0.05; ** = p <0.01; *** = p < 0.001; **** = p< 0.0001.

Next, it was investigated whether Fir1 aggregates are targeted by Uls2 by examining the levels and distribution of GFP-Fir1 the *slx5*Δ strain. If Fir1 is targeted by Uls2, absence of the Slx5 subunit of Uls2 should lead to a stabilization of Fir1. First, the aggregates were investigated using fluorescence microscopy (**Fig. 15 A**). Indeed, Fir1 aggregates were increased in *slx5Δ* cells, which harbored around 8% more cells with the phenotype *two aggregates+* than wild-type cells (**Fig. 15 C**). Cells with *one aggregate* were only slightly increased (**Fig. 15 B**). This supports the theory that the Fir1 aggregates are targeted by Uls2. This was further investigated using western blots. It was expected that *slx5*Δ would result in a stabilization of Fir1 and thus higher steady-state levels. Surprisingly, the western blot showed the opposite result (**Fig. 15 D**). In *slx5Δ* cells, Fir1 levels were reduced by 24%. Especially in the context of the microscopy results, this was surprising. Fluorescence microscopy revealed more cells with aggregates which were not reflected in the western blot. Notably, Nis1 western blots showed similar results. Upon shut off of Uls2, stabilization of Nis1 could not be observed even though under overexpression a clear targeting was seen. For Nis1 four reasons were discussed (Chapter 2.1.9). Two possible explanations for the results of the Nis1 could be relevant here as well. First, SUMOylated forms of Fir1 and Nis1 could accumulate in the deletion or shut off strain. Those forms would run higher and not necessarily as a clear band, which might put them under the detection limit. Second, Fir1 and Nis1 form aggregates which cannot be resolved with the performed lysis. For both proteins, aggregates could be observed using microscopy. However, the aggregates were more intense and more common for Fir1 overexpression explaining why the effect for Fir1 on western blot is more striking.

In conclusion, it could be demonstrated that Fir1's SUMO interaction motif is essential for formation of aggregates. Additionally, fluorescence microscopy showed that limiting the cellular levels of Uls2 causes an increase of Fir1 aggregate formation prompting a further investigation of the targeting of Fir1 in the $P_{GAL1}$*ULS2* strain.

## 2.2.3 Uls2 Targets Fir1 Aggregates

So far, stabilization of Fir1 aggregates in *slx5Δ* could be shown suggesting proteolytic targeting by Uls2. Therefore, the next goal was to obtain additional evidence for a direct role of the StUbL Uls2 (alias Slx5-Slx8) in the SIM-dependent proteolytic targeting of Fir1. To study this, the $P_{GAL1}$*ULS2* strain was employed. First, the aggregates of Fir1 were investigated using fluorescence microscopy. $P_{GAL1}$*ULS2* cells were examined under shut off and overexpression conditions and compared to wild-type cells (**Fig. 16 A**). Under shut off conditions, the results were similar to the previously investigated *slx5Δ* strain (**Fig. 15 A**). For the $P_{GAL1}$*ULS2* strain grown in glucose, cells harboring *single aggregates* were increased by 15% (**Fig. 16 B**). Cells with *two aggregates+* were increased from 5% to 12%. Notably, cells with a *smooth nucleus* were not detected under these conditions. Upon overexpression of Uls2 in galactose media, aggregates of Fir1 disappeared in nearly all cells. In contrast, cells with *smooth nuclei* increased from 0% (shut off) to 5% (overexpression). Non-aggregated Fir1 seemed unaffected by Uls2 overexpression. This suggests that Uls2 specifically either targets Fir1 molecules that have a tendency to aggregate or the aggregates directly.

Next, Fir1 protein levels were investigated using western blotting (**Fig. 15 C**). Under conditions of Uls2 shutdown (glucose media), Fir1 levels were slightly increased compared to the wild type (10%), although not significantly. This was not surprising considering the previous results obtained with the *slx5Δ* strain which demonstrated problems with the solubility of the aggregates. More surprising is that there was not the same drop in protein level as in the *slx5Δ* strain. Under galactose media, there was a drop in Fir1 protein level both in WT (to 70%) and in $P_{GAL1}$*ULS2* cells (to 40%) (**Fig. 15 D**). These results support the microscopical data, even though fluorescence microscopy suggested a stronger targeting. This further supports the theory that the aggregates are not efficiently extracted by boiling cells in sample buffer. The effect could be especially strong, if Uls2 mainly targets aggregated Fir1 opposed to free Fir1.

To summarize, Fir1 molecules that are either prone to aggregate or that are part of aggregates are targeted by Uls2 as suggested by the complete disappearance of such aggregates under overexpression conditions. Western blot results support the microscopy data, although the effect is not as striking due to incomplete extraction of aggregates with the method employed here. Still, Fir1 is clearly a substrate of Uls2. Furthermore, formation of the targeted aggregates is SIM-dependent. This raises the

question whether SUMOylation of Fir1 on the one hand mediates Uls2-targeting, and on the other hand promotes aggregate formation.

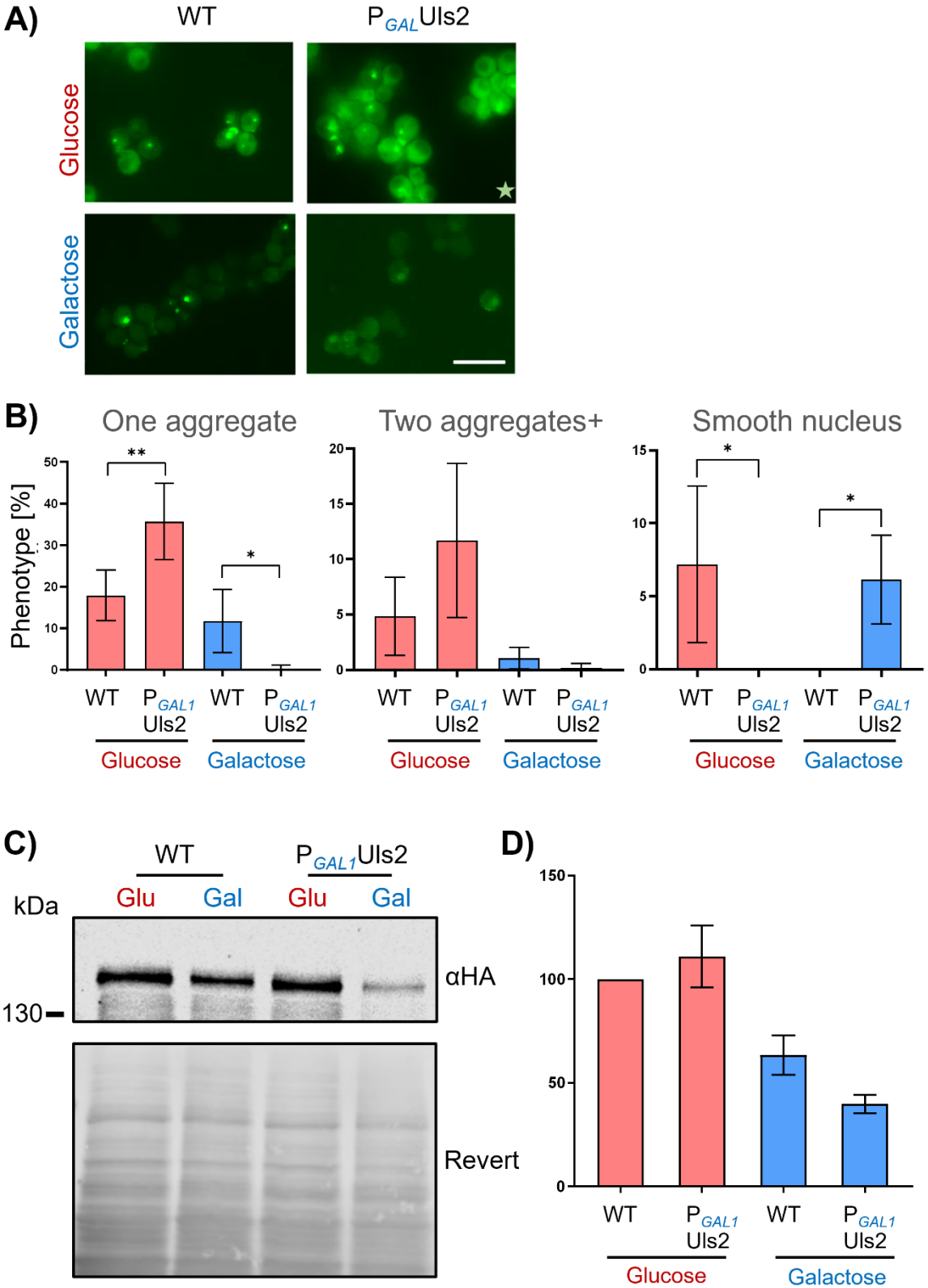


**Figure 16 Uls2 targets Fir1 aggregates. A)** Microscope images of $P_{GPD}$*GFP-FIR1-HA* in $P_{GAL1}$*ULS2* strains. After overnight preculture in YP-Raffinose, the cells were grown 4 h in YP-Glucose or YP-Galactose. Acquisition: GFP: 1 s. Strains used were: yFP167, yFP168 **Scale: 10 µM. B)** Quantification of fluorescence microscopy of

$P_{GPD}$*GFP-FIR1-HA* in $P_{GAL1}$*ULS2*. **C)** Western blot of $P_{GPD}$*GFP-FIR1-HA* in wild type and $P_{GAL1}$*ULS2* strains. After overnight preculture in YP-Raffinose, the cells were grown 5 h in YP-Glucose or YP-Galactose. Post-alkaline lysis samples were loaded on an 8% SDS-Gel, blotted for 1 h at 400 mA, 100 V at 4 °C on nitrocellulose using wet blot. Blots were incubated with Revert before blocking and blocked blots were incubated with anti-HA (αHA) antibody (3F10-rat at 1:2,000) overnight at 4°C and with anti IGG coupled to fluorophore (800 nm emission peak) for 2 h at room temperature. Strains used were: yFP167, yFP168. **D)** Quantification of $P_{GPD}$GFP-Fir1-HA $P_{GAL1}$*ULS2* Western blot. n=5; Students T-test; * = p<0.05; ** = p <0.01; *** = p < 0.001; **** = p< 0.0001.

## 2.2.4 SUMOylation is Involved in Fir1 Aggregate Formation

To investigate if SUMO is involved in Fir1 aggregate formation, two mutant strains were employed: *uba2-ts* and *smt3*$^{KallR}$. The *uba2-ts* strain has a severe defect in SUMOylation and the *smt3*$^{KallR}$ strain is unable to form SUMO chains because all Smt3 lysines are exchanged with arginine residues (Bylebyl et al., 2003; Schwienhorst et al., 2000). With these strains, the involvement of SUMOylation in the aggregate formation and the involvement of SUMO chains in the aggregate formation were investigated, respectively. The aggregate formation in both strains was investigated using fluorescence microscopy (**Fig. 17 A**). In the *uba2-ts* background, no aggregates could be detected. This suggests that SUMOylation is essential for aggregate formation. In few cells, the phenotype *smooth nucleus* could still be detected. Therefore, nuclear localization of Fir1 was not completely abolished. This is not surprising since the *uba2-ts* strain still has some amount of SUMOylation, because otherwise it would be unviable. Considering the low amount of nuclear localization of Fir1 observed in this mutant, however, SUMOylation likely plays a role in nuclear localization of Fir1.

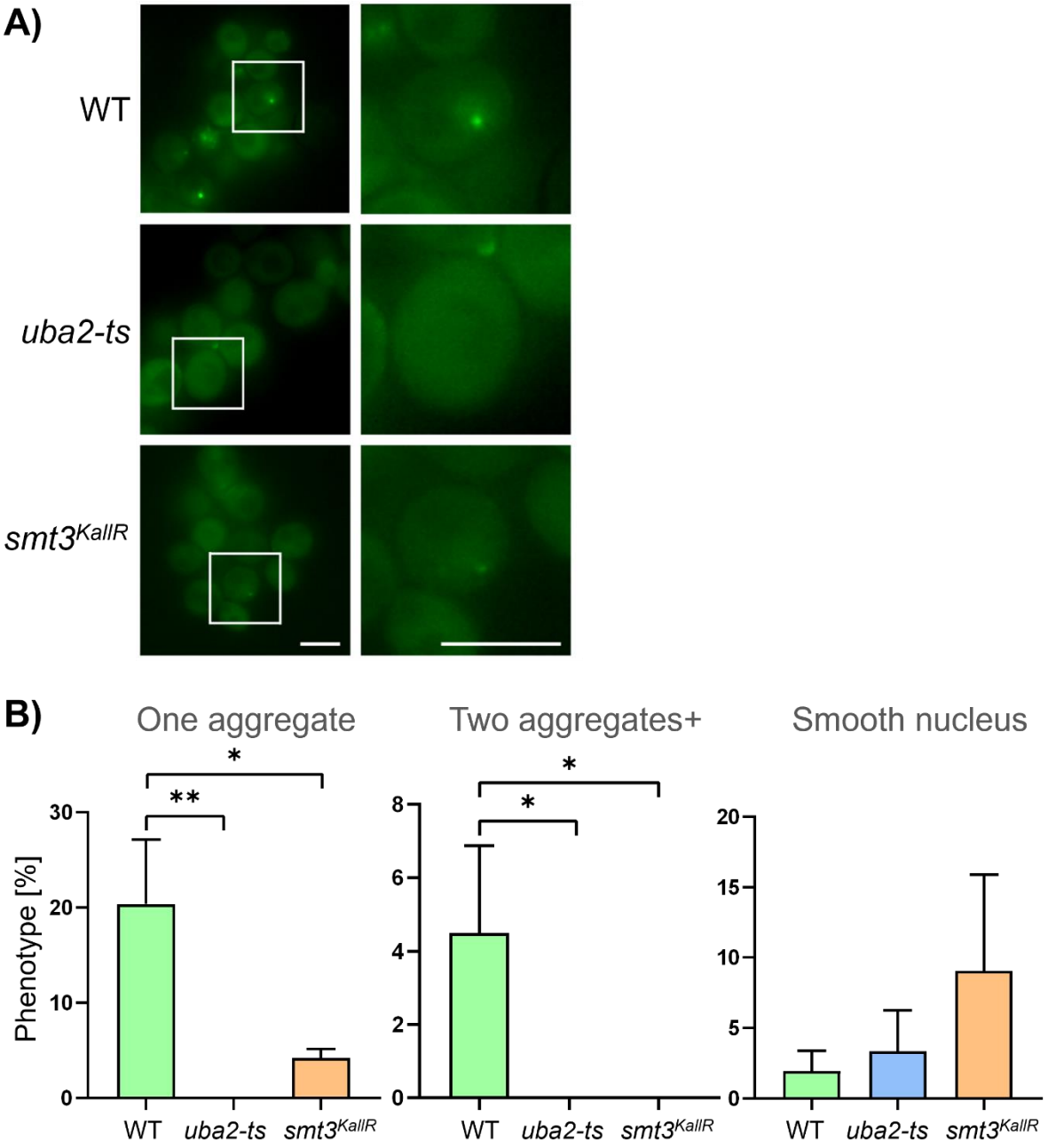


**Figure 17 SUMOylation is involved in Fir1 aggregate formation. A)** Microscope images of $P_{GPD}$*GFP-FIR1-HA* in wild type, *uba2-ts* and *smt3*$^{KallR}$ strains. The strains were grown into exponential phase for 4 h at 30 °C in YP-Glucose medium. Image acquisition: GFP: 1 s, 700 ms, 900 ms. Strains used were: yFP167, yFP237, yFP238. **B)** Quantification of fluorescence microscopy of $P_{GPD}$*GFP-FIR1-HA* in $P_{GAL1}$*ULS2*. Students T-test. * = p<0.05; ** = p <0.01; *** = p < 0.001; **** = p< 0.0001. **Scale: 5 µM.**

Next, it was examined whether SUMO chains are involved in aggregate formation using the *smt3*$^{KallR}$ strain. Even though, in this mutant, aggregate formation was not completely abolished as in the *uba2-ts* mutant, the microscope analysis revealed a stark drop in the formation of aggregates from 20% in wild type to 4% in *smt3*$^{KallR}$ strain (**Fig. 17 B**). Notably, aggregates observed in *smt3*$^{KallR}$ showed an apparently much fainter fluorescence than the aggregates in the wild type (**Fig. 17 A**).

In conclusion, complete absence of aggregates in the *uba2-ts* strain revealed that SUMOylation is essential for aggregate formation. Analysis of *smt3*$^{KallR}$ showed that SUMO chains play a role in aggregate formation but are not absolutely essential. These results, together with the importance of the SIM on aggregate formation prompted the question whether SUMO itself is part of the aggregates.

## 2.2.5 Colocalization of Fir1 Aggregate with mCherry-Smt3

To investigate if SUMO is part of the aggregates, a colocalization assay was employed. Therefore, GFP-tagged Fir was co-expressed with inducible mCherry-tagged Smt3. Localization of these constructs was investigated using fluorescence microscopy with a focus on the aggregates (**Fig. 18 A**). First, the number of GFP-Fir1 aggregates was determined. Then, the number of mCherry-Smt3 aggregates was determined. In 316 wild type cells, 60 GFP-Fir1 aggregates were found and 24 mCherry-Smt3 aggregates (**Fig. 18 B**). Out of the 24 mCherry-Smt3 aggregates, 22 colocalized with GFP-Fir1. This showed that SUMO is indeed part of the Fir1 aggregates.

To summarize, upon overexpression Fir1 forms aggregates in the nucleus. SUMOylation and Fir1's SIM are essential for the formation of those aggregates. Consistent with these conclusions, SUMO is not only essential for the formation but also a part of the aggregates. Lastly, these aggregates are targeted by Uls2. This points towards a SIM-mediated polySUMOylation of Fir1, which results in targeting through Uls2.

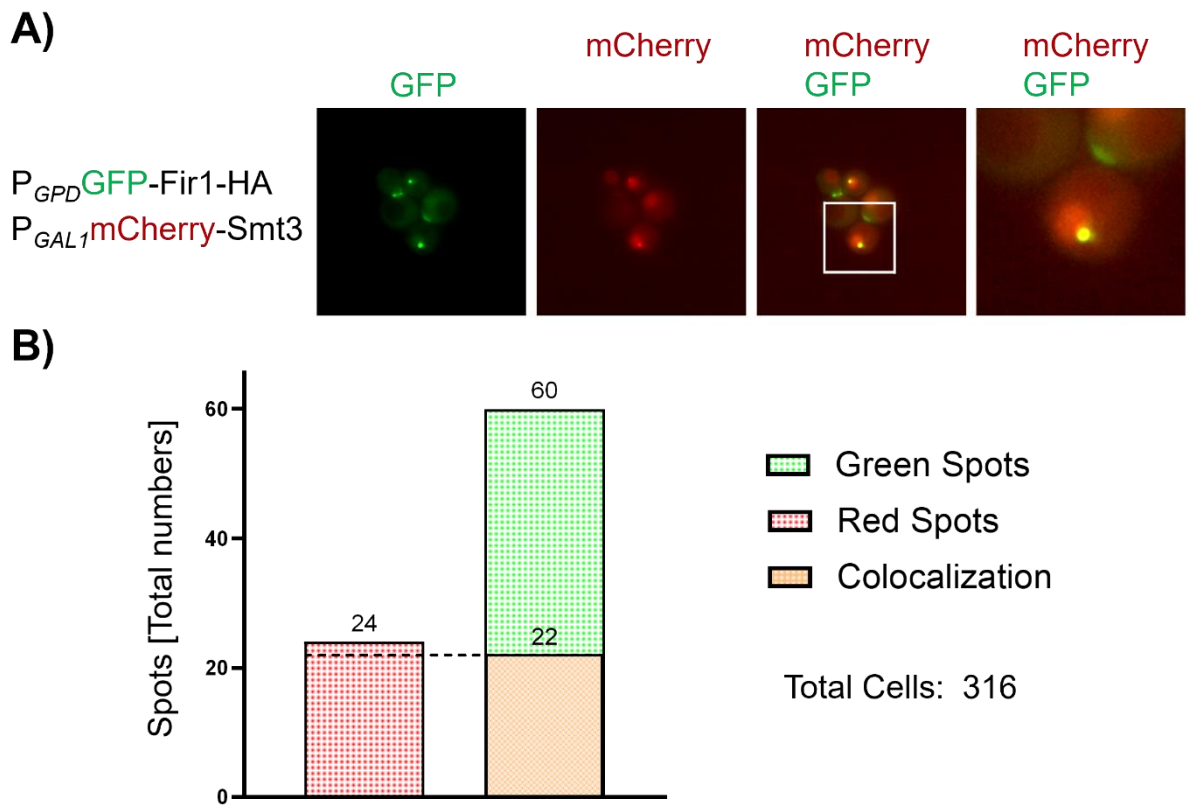


**Figure 18 SUMO is part of Fir1's aggregates**. **A)** Microscope images of $P_{GPD}$*GFP-FIR1-HA* with $P_{GAL1}$mCherry-Smt3 in wild type cells. After overnight preculture in Sgal-URA the cells were grown 5 h in SGal-Ura. Acquisition: GFP: 800 ms; Cy3: 300 ms. Strains used were: yFP167 with pMM86 **Scale: 5 µM**. **B)** Quantification of aggregates found in A).

## 2.2.6 JUNQ Lysis Dissolves Fir1 Aggregates

Lastly, it was attempted to align microscopy data with the western blot results. Previously performed microscope analysis of the $P_{GAL1}$*ULS2* strain under overexpression indicates that Fir1 aggregates are targeted by Uls2. So far, the targeting of Fir1 could also be shown on western blot as well, however the stabilization of Fir1 under shut-off conditions was not observed. As previously discussed this could be due to multiple reasons one of them being the insolubility of the aggregates in a lysis by boiling in sample buffer. This is supported by the observed accumulation of aggregates in *slx5Δ* and $P_{GAL1}$*ULS2*.

Therefore, it was investigated which lysis method was most suitable for the extraction of Fir1 aggregates. Various methods such as native glass bead lysis, alkaline lysis with TCA precipitation or boiled lysis were not sufficient (data not shown). Lastly, a lysis method used a lysis method used to dissolve aggregates of misfolded proteins found in so-called juxtanuclear quality control compartment (JUNQ)

aggregates was used (Rolli et al., 2024). In this procedure, the yeast cells were resuspended in 8 M urea buffer and vortexed with glass beads. SDS was added to a final concentration of 4% and the samples were incubated for 5 min at 65 °C. The sample was centrifuged and the supernatant used for SDS-PAGE and western blot analyses. Using this method, a 50% increase of Fir1 protein levels was observed in the *slx5Δ* strain compared to the wild type (**Fig. 19 A, B**). These data are in line with the expected result and consistent with the microscopic data. The observed increased steady-state levels of Fir1 in *slx5Δ* cells indicates that Fir1 is targeted by Uls2. This matches the microscope analyses which showed a clear stabilization of the aggregates and thus Fir1.

In summary, western blotting of samples prepared with a lysis specialized for JUNQs was able to reveal a stabilization of Fir1 in *slx5Δ*. This aligns with the previously obtained microscope data that clearly shows a stabilization of Fir1 in aggregates in both the *slx5Δ* strain as well as in $P_{GAL1}$*ULS2*.

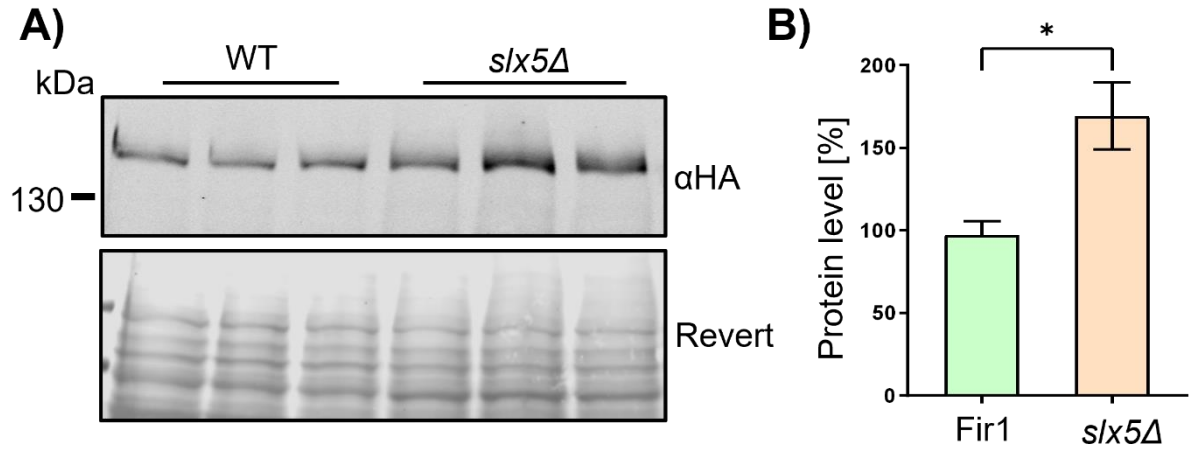


**Figure 19 JUNQ Lysis dissolves Fir1 aggregates. A)** Western blot of $P_{GPD}$*GFP-FIR1-HA* in wild type and *slx5Δ* strains. Samples of JUNQ lysis were loaded on an 8% SDS-PAGE, blotted for 1 h at 400 mA, 100 V at 4 °C on nitrocellulose using wet blot. Blots were incubated with anti-HA (αHA) antibody (3F10-rat at 1:2,000) overnight at 4 °C and with anti IGG coupled to fluorophore (800 nm emission peak) for 2 h at room temperature.. Strains used were: yFP167, yFP169, yFP172. **B)** Quantification of western blot in F) Students T-test; n = 3; * = p<0.05; ** = p <0.01; *** = p < 0.001; **** = p< 0.0001.

## 2.3 Hypothesis

So far, two proteins – Nis1 and Fir1 – could be identified as substrates of the SUMO-targeted ubiquitin ligase Uls2. Interestingly, both proteins are targeted under overexpression conditions. Based on this observation, a working hypothesis was formulated (**Fig. 20**). Since both proteins are targeted under non-endogenous conditions, it was hypothesized that Uls2 might serve as part of a quality control mechanism Uls2 mediating the degradation of defective or unmatched proteins. Upon absence of a partner protein, simulated by overexpression, or upon stress, a hidden SIM or SUMOylation motif gets exposed. This exposure leads to the SUMOylation of the protein and relocalization into the nucleus, where it is targeted by Uls2. Uls2 recognizes the polySUMO tag of the protein and mediates the ubiquitylation of the SUMO chain. Subsequently, the protein is degraded by the proteasome.

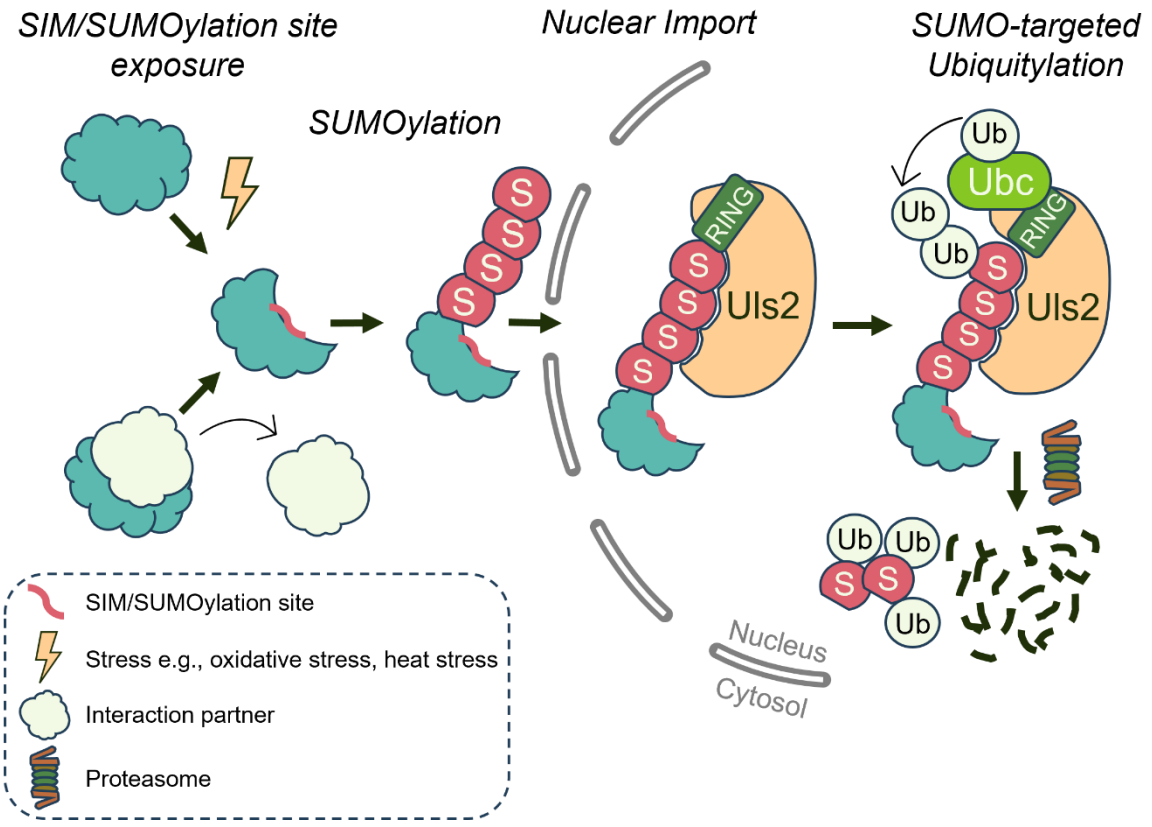


**Figure 20 Working hypothesis. Uls2 serves as part of a quality control mechanism for SIM and SUMOylation site-containing proteins.** Upon absence of a partner protein or folding stress, an internal SIM or SUMOylation site is exposed. This site promotes SUMOylation of the protein and subsequently its relocalization to the nucleus. There the SUMO-chain is recognized by Uls2. Uls2 ubiquitylates the SUMO-chain, which leads to the degradation of the protein.

# 2.4 Proteomic Approach

## 2.4.1 Establishing Conditions for Proteomics Approach

So far, two substrates of Uls2 – Nis1 and Fir1 – have been identified. Both were targeted upon overexpression. The next goal was to identify substrates of Uls2 under endogenous conditions. Therefore, a whole cell proteomics approach was chosen. To identify endogenous substrates that are targeted by Uls2, protein levels in Uls2-deficient cells were compared with and without stress. Proteomics allow the identification of multiple proteins that might expose a SIM or a SUMOylation site upon stress and are subsequently targeted by Uls2.

For the proteomics approach, a wild-type and a Uls2 deficient strain should be compared with and without stress. As a Uls2 deficient strain, either the $P_{GAL1}$*ULS2* strain or the *slx5Δ* strain could be used. The $P_{GAL1}$*ULS2* strain has the advantage that the targeting as well as the stabilization of a protein can be detected in the same background. However, more controls such as the wild type on galactose with and without stress, would be necessary. Additionally, the carbon source switch from glucose to galactose influences other proteins. Therefore, to minimize proteome changes unrelated to the direct targeting by Uls2, the *slx5Δ* strain was chosen in combination with glucose media.

To determine what kind of stress might be suitable for the proteomics approach, preliminary western blots were performed. Here, heat stress and oxidative stress were tested, because both were reported to increase SUMOylation (Niskanen et al., 2015; Zhou et al., 2004). Wild type cells were treated with 200 µM $H_2O_2$ or incubated at 42 °C for 45 minutes (**Fig. 21 A**). Cells were harvested and boiled in Laemmli buffer. The SUMOylation pattern of the treatments was compared on western blot by employing Smt3 antibody. Without stress, the SUMOylated proteins were distributed across each lane. This was expected, since many proteins of different sizes are SUMOylated. Heat stress and oxidative stress increased SUMOylation by 130% and 120%, respectively (**Fig. 21 B**). In unstressed, healthy cells, the stacking gel was comparatively empty and high-molecular weight (HMW)-SUMO conjugates did not accumulate. Under $H_2O_2$-induced oxidative stress, HMW-SUMO conjugates accumulated in the stacking gel, in addition to a strong overall increase in the amounts of SUMOylated proteins. Since Uls2 is known to especially target polySUMOylated

proteins (Uzunova et al., 2007), oxidative stress was chosen as a condition for the proteomics approach.

For the proteomics approach, it was decided to study four conditions: wild type versus *slx5Δ* untreated and wild type versus *slx5Δ* treated with 200 µM $H_2O_2$ for 45 min (**Fig. 21 C**). The cultures were harvested and stored at -80 °C. For the mass spectrometry, quadruplicates of the four samples were performed. Whole cell extracts were prepared using glass bead lysis in 8 M urea buffer with 4% SDS and protein concentrations were measured using the nanodrop. Of each extract, 2 ng were used. The LysC and Trypsin digest and stage tip preparation was performed at the proteomics facility together with Luisa Schmidt from AG Krüger. Mass spectrometry measurements and analysis of raw data were performed by Luisa Schmidt.

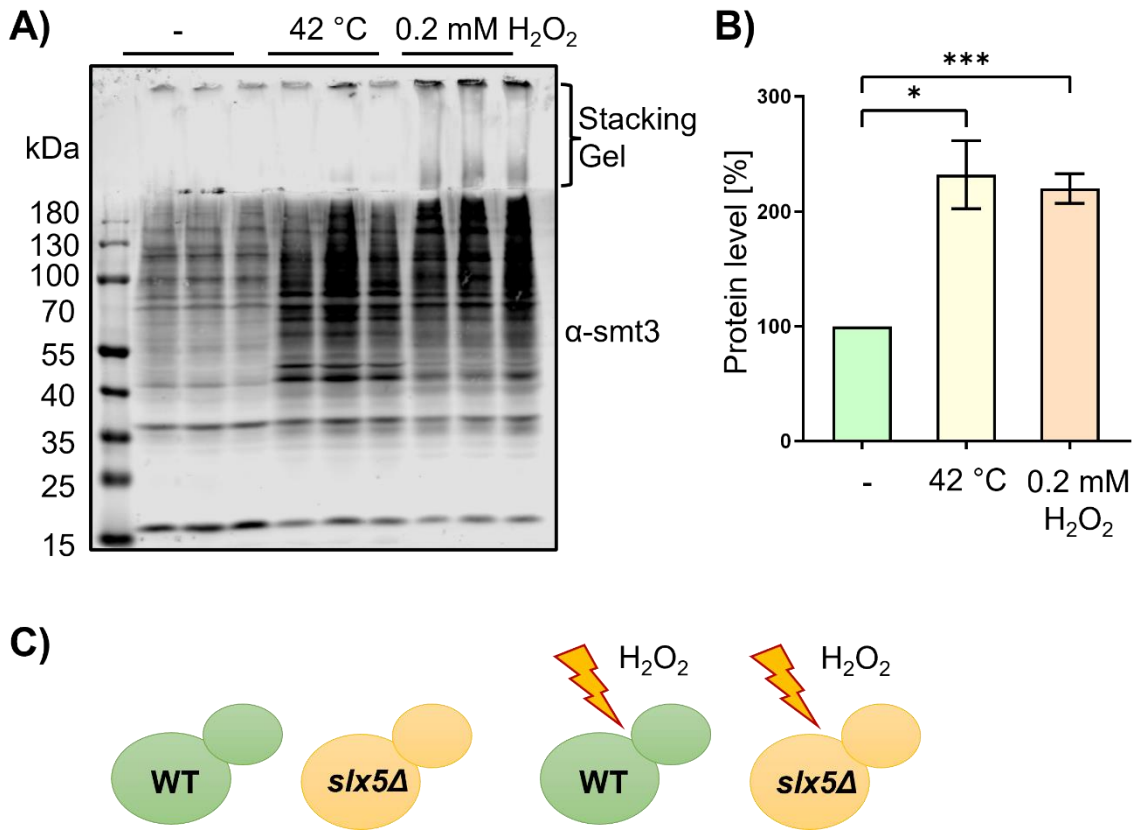


**Figure 21 Establishing conditions for proteomics approach**. **A)** Western blot of wild type with different stress conditions. Cultures were grown 4 h in YP-Glucose and then subjected to stress for 45 min. Boiled lysis samples were loaded on a 10% SDS-Gel, blotted for 1 h at 400 mA, 100 V at 4 °C on nitrocellulose using wet blot. Blots were incubated anti-Smt3 (αsmt3-rb at 1:20,000) overnight at 4 °C and with αrb-680 for 2 h at room temperature. Strains used were: JD47-13C **B)** Quantification of western blot in A). Students T-test; n=3; * = p<0.05; ** = p <0.01; *** = p < 0.001; **** = p< 0.0001 **C)** Samples used for whole cell proteomics. The samples included four

conditions wild type and *slx5Δ* strains untreated and wild type and *slx5Δ* strains treated for 45 min with 200 µM $H_2O_2$.

## 2.4.2 Proteomics Reveal Stark Differences in Protein Levels between Wild Type and the slx5∆ strain

The proteomics study provided a comprehensive assessment of the *slx5Δ* proteome compared to the wild type. Out of 5934 yeast proteins, 2903 proteins were found in this study (*Saccharomyces* Genome Database, accessed 25.11.25). Out of those 2903 proteins 694 were significantly changed between the different sample groups and 344 were increased in *slx5Δ* (**Fig. 22 B**). Here, the focus was on two groups of proteins. The first group is comprised of proteins whose levels were increased in *slx5Δ* independent of treatment. This group reveals potential targets of Uls2. In the second group, proteins were compiled, levels of which were only increased in *slx5Δ* treated with $H_2O_2$. This group includes proteins which became potential targets of Uls2-mediated quality control upon oxidative stress. These groups were identified by using hierarchical clustering (hCluster) (**Fig. 22 A**).

The hierarchical cluster (hCluster) groups proteins based on their log2 transformed intensities. Included in the hCluster are proteins levels of which are significantly changed between the groups based on an ANOVA analysis. The hCluster groups proteins based on their similarity in expression pattern and the corresponding heat map displays if proteins are increased (red) or decreased (blue) in the different strains and conditions. The hCluster analysis groups the proteins in nine clusters (c1 – c9). The largest cluster is cluster 4 (c4). C4 includes 280 proteins whose levels increase upon *SLX5* deletion, but independent of treatment. This shows the strong effect the deletion of *SLX5* has on the yeast proteome. These 280 proteins are potential targets of Uls2. Alternatively, they may also have reached higher levels due to other reasons such as stress induced by *SLX5* deletion. The proteins in cluster 4 were investigated by GO Term analysis in regards of their function and their activity (**Fig. 22 C**). Proteins increased in *slx5Δ* include enzymes of carbohydrate catabolic processes and protein catabolic processes. Proteins with catalytic and transferase activities are particularly increased. Conversely, proteins involved in cytoplasmic translation and ribosome biogenesis, as well as proteins which are involved in RNA and DNA binding are decreased in *slx5Δ* compared to the wild type.

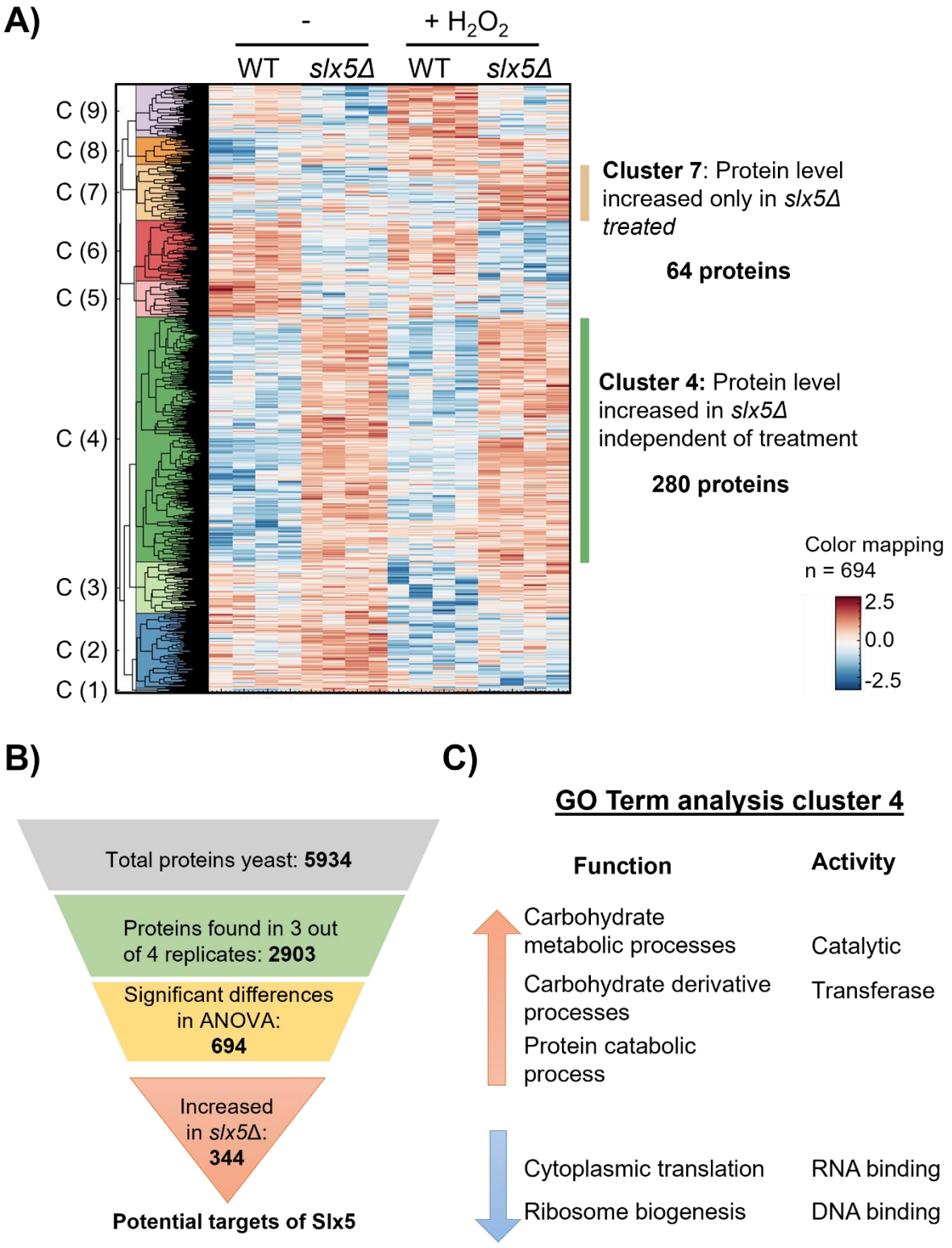


**Figure 22 Mass spectrometry analysis reveals stark difference in protein expression in *slx5Δ* compared to WT. A)** hCluster of proteins found in mass spectrometry significant in ANOVA and found in 3 out of 4 replicates. **B)** Overview of number of proteins in *S. cerevisiae* and number of proteins found in mass spectrometry approach. **C)** GO Term analysis of cluster 4 representing proteins increased in *slx5Δ*. GO-term analysis was performed with https://go.princeton.edu/. The 5934 total yeast proteins are all verified Open Reading frames (ORFs) including uncharacterized ORFs.

Another interesting group is cluster 7, which includes proteins that are only increased in *slx5Δ* treated with $H_2O_2$. This cluster harbors 64 proteins that are potential targets of Uls2-mediated quality control and therefore of special interest in the light of the starting working hypothesis (**see Fig. 20**).

The hCluster provides a great overview of how protein levels vary between the different treatment groups. It emphasizes the effect of *SLX5* deletion on the protein landscape. For a given protein, the observed changes might either be due to direct targeting by Uls2 or caused by other indirect effects Slx5 or its absence has on the cell.

## 2.4.3 Selection of Proteins

To identify substrates of Uls2-mediated quality control using the data from the proteome analysis, proteins were selected based on defined criteria (**Fig. 23 A**). First, all proteins from the hCluster, so all proteins significantly changed between groups were investigated. Second, the hCluster was screened for proteins which showed increased protein levels in *slx5Δ* treated with $H_2O_2$ and decreased protein levels in wild type treated with $H_2O_2$. This criterium assumes that in the wild type upon stress, the proteins are targeted by Uls2 and therefore the protein level decreases. Upon deletion of *SLX5* the proteins are not targeted anymore and protein levels increase. 40 proteins were identified using these criteria. These proteins were distributed over three clusters: c3, c4 and c7. The last criterium was that the proteins should have a SIM or a SUMOylation site, which could be exposed upon stress. This resulted in a list of 25 proteins (**Fig. 23 B**). The list includes the candidates, their mean average from hCluster analysis, the SIM or SUMOylation site, as well as reported SUMOylation and ubiquitylation. SIMs and SUMOylation sites were found using an R-code “SIM-finder” provided by Lennard Maximilian Döring. For SUMOylation and ubiquitylation the yeast genome database SGD was used.

Next to this stringent approach, another list of proteins was assembled without employing concrete criteria. Here, internal lab reports and especially strong stabilization in volcano blots were the reason those proteins were selected. Multiple candidates from the first list (**Fig. 23 B**) were investigated as well as all candidates from the second list (**Fig. 24 A**).

**A)**

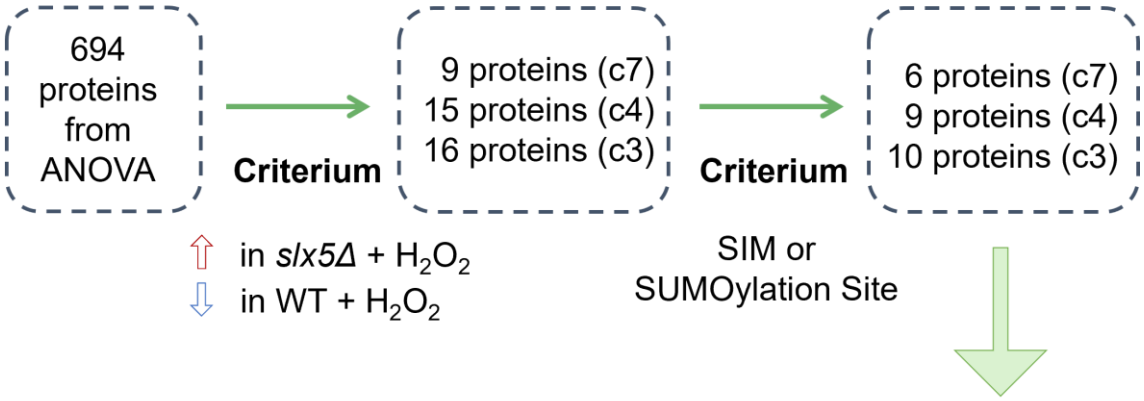


**B)**

| Cluster | Gene Name | Average values from hCluster* | Potential SIM | SUMOylation Site | Reported Ubiquitylation/ SUMOylation |
|---|---|---|---|---|---|
| c7 | SNX41 | -0 -1 -1 1,4 | VIYISSE | VKKD | Ubi |
| | TOR1 | -0 -0 -1 1,1 | no | LKDD, LKTE, IKSE, LKND | Ubi |
| | CUE3 | 0,1 -0 -1 1,1 | EELSIL | LKED | Ubi |
| | MSF1 | -0 -0 -1 1,3 | ESVKLV | no | no |
| | YPK2 | -0 0,1 -1 1,3 | no | LKID, LKID, LKPE, VKSE | Ubi |
| | THI7 | -0 -0 -1 1,3 | no | LKGE, VKHD | Ubi |
| c4 | PRX1 | -1 0,6 -1 1,1 | no | LKPE | SUMO |
| | SST2 | -1 0,7 -1 1 | no | LKVD | no |
| | STT4 | -0 0,6 -1 1 | LLAVSED | 5 SUMO sites | Ubi |
| | SPT16 | -0 0,6 -1 0,8 | LVINLEE | VKND, LKKE | Ubi |
| | MDL2 | -0 0,3 -1 1,1 | SSVCIV | no | no |
| | JEM1 | -0 0,7 -1 0,7 | LVYIDS | LKVD | no |
| | AIM41 | -0 0,2 -1 1,1 | no | LKGD | no |
| | MIR1 | -0 0,3 -1 1,1 | no | LKEE | no |
| | RPT6 | -1 0,7 -1 1 | DELRLL | IKDE | Ubi |
| c3 | ERG26 | 0,2 0,1 -1 0,9 | DSVLII | no | Ubi |
| | YPR1 | -0 0,2 -1 1,1 | no | LKTD | Ubi |
| | DCS1 | -0 0,4 -1 1 | DELRLL | IKQD | Ubi |
| | MET3 | 0 0,7 -2 0,8 | VVLFLED | IKPD | no |
| | PPN1 | 0,2 0,3 -1 0,7 | ESLQLL | no | Ubi |
| | SRB2 | 0,3 0,2 -1 0,7 | no | IKGD | no |
| | SLA2 | -0 0,5 -1 0,9 | LVSVSDPDE | LKLD | Ubi |
| | CMK1 | -0 0,4 -1 0,8 | DELDIL | LKPE, LKSD, LKSE | no |
| | HMG2 | -0 0,5 -1 0,9 | EDSVLLIIDS | IKPD, LKSD | Ubi |
| | VPS13 | -1 0,6 -1 1 | LISDDD; VVADDD; SELQLVL | 6 SUMO sites (e.g. IKND) | Ubi |

*WT, *slx5Δ*, WT +$H_2O_2$, *slx5Δ* +$H_2O_2$

**Figure 23 Identifying substrates of Uls2-mediated quality control. A)** Workflow used to narrow down potential targets of Uls2-mediated quality control. **B)** List of proteins identified in A).

**A)**

| Cluster | Gene Name | Reasons of interest | Potential SIM, SUMOylation Site | Reported Ubiquitylation/ SUMOylation |
|---|---|---|---|---|
| c7 | Pam16 | Found only in *slx5Δ* with stress | ILNIEE, LKWE | |
| | Cue3 | Found in suppressor screen $P_{GAL1}$Slx5, *smt3*$^{KallR}$ | | |
| c4 | Hsp82 | SUMOylated, Chaperone | | SUMOylated |
| | Ssa3 | SUMOylated | | SUMOylated (Bhagwat et al. 2021) |
| | Gph1 | SUMOylated & Ubiquitylated, in Volcano Blot WT vs *slx5Δ* | MKIE | SUMOylated & Ubiquitylated |
| | Sod2 | SUMOylated, in Volcano Blot WT vs *slx5Δ* | LKWD | SUMOylated |
| | Tps1 | Complete Trehalose-Synthase pathway stabilized | | |
| No | YBR053C | Found in Messner et al. 2023 | | |

**B)**

| | WT | | | | *slx5Δ* | | | | WT + $H_2O_2$ | | | | *slx5Δ* + $H_2O_2$ | | | |
|---|---|---|---|---|---|---|---|---|---|---|---|---|---|---|---|---|
| Pam16 | -0,30 | -0,80 | -1,08 | -0,92 | 0,16 | -1,29 | -0,35 | -0,53 | -0,47 | -0,23 | -0,16 | -0,51 | 1,77 | 1,67 | 1,43 | 1,62 |
| Cue3 | 1,53 | 0,19 | -0,49 | -0,99 | -0,66 | 0,36 | -0,10 | 0,01 | -0,86 | -1,10 | -0,53 | -1,65 | 0,32 | 1,36 | 0,42 | 2,18 |
| Hsp82 | -1,01 | -0,81 | -1,88 | -1,23 | 0,80 | 1,24 | 0,96 | 0,85 | -1,03 | -0,64 | 0,01 | -0,57 | 1,35 | 0,28 | 1,26 | 0,43 |
| Ssa3 | -0,56 | -1,07 | -1,39 | -0,97 | 0,64 | 1,26 | 1,31 | 0,71 | -0,89 | -1,18 | -0,80 | -0,87 | 1,33 | 0,69 | 1,08 | 0,69 |
| Gph1 | -1,06 | -1,00 | -1,37 | -0,96 | 1,00 | 1,14 | 1,02 | 0,80 | -0,75 | -1,01 | -0,97 | -0,80 | 0,89 | 1,04 | 1,04 | 0,99 |
| Sod2 | -1,62 | -1,51 | -1,71 | -1,75 | 0,71 | 0,48 | 0,35 | 1,05 | 0,16 | 0,61 | -0,33 | 0,63 | 0,46 | 0,77 | 0,83 | 0,86 |
| Tps1 | -0,30 | -2,05 | -0,79 | -0,98 | 0,68 | 1,50 | 1,01 | 0,03 | -1,88 | 0,17 | -0,02 | 0,00 | 0,80 | 1,44 | 0,27 | 0,11 |

**Figure 24 Hand-picked substrates of Uls2. A)** List of hand-picked proteins investigated as targets of Uls2. **B)** Summary of hCluster values for proteins in list A).

## 2.4.4 Monitoring Protein Levels of Selected Proteins

Multiple proteins were chosen from the assembled lists for further investigation. To examine their targeting by Uls2, protein levels were investigated by western blotting. Here, multiple approaches were used. If available, an antibody against the protein itself was used (e.g. Hsp90, Prx1, Rpt6). The proteins found using stringent criteria (**Fig. 23 B**) were endogenously C-terminally tagged using a PCR-based approach (Knop et al., 1999). Handpicked candidates (**Fig. 24 A**), instead, were cloned into an integrative cassette. In this cassette the genes of interest were under the control of the copper-inducible $P_{CUP1}$ promoter and fused in frame to a sequence encoding a 2HA-tag. The cassettes were integrated into the 3'-non-coding area of the *LEU2* locus.

There were various reasons to employ the different systems. First, using the available antibodies was the easiest approach enabling the monitoring of the untampered proteins. Though, for screening many proteins, the availability of such specific antibodies is the limiting factor. Therefore, this approach was only chosen if antibodies were available to the lab. PCR-based tagging of the endogenous protein only tampers with the C-terminus of the protein and the terminator region of the gene. It is a well-established method to investigate proteins encoded by the endogenous gene driven by its native promoter. However, if a protein is low in abundance, this approach might go along with problems in detection. Lastly, the integration cassette is a good way to investigate a protein outside of any transcriptional control it might be under. Here, the gene is under the copper-inducible promoter $P_{CUP1}$ followed by a 2HA-tag and the terminator $T_{CYC1}$. Using this construct, one can determine with certainty whether the protein itself is targeted or stabilized. This method excludes transcriptional regulation as a cause for observed changes in protein levels. Additionally, one can regulate the amount of protein produced by omission or addition of copper.

## 2.4.5 Different Candidates Display Distinct Protein Levels

As a first substrate of Uls2, Hsp82 was investigated. Hsp82 is a member of the Hsp90 family. In yeast, there are two Hsp90 chaperones: Hsp82 and Hsc82. Both are not distinguishable by antibody but by mass spectrometry (Girstmair et al., 2019). In this thesis, Hsp82 was found in the mass spectrometry analysis to be increased in *slx5Δ,* independent of treatment (**Fig. 25 B**). Hsc82 levels did not vary between wild type and *slx5Δ*. Here, the protein level of both Hsp90 chaperones together was investigated using western blot and detection with an antibody against Hsp90

chaperones. The Hsp90 protein level was investigated in wild-type and $P_{GAL1}$*ULS2* cells under shut-off and overexpression conditions (**Fig. 25 A**). Upon the shut-off of Uls2, the Hsp90 level decreased. This was unexpected, but a similar effect was observed for Fir1 and Nis1 previously. For Fir1, employing a different cell lysis optimized for aggregates resolved the issue. Hsp90 might form aggregates itself or might be recruited to aggregated proteins, which could not be resolved here. Under overexpression conditions, Hsp90 protein level dropped to 32% in wild type and to 9% in $P_{GAL1}$*ULS2* (**Fig. 25 D**). Thus, while the medium switch already had an effect, the effect of the overexpression of Uls2 was even stronger. The overexpression of Uls2 reduces Hsp90 protein level significantly. The western blot suggests that Hsp90 is targeted by Uls2. Together with the proteomics data, it can be concluded that it is especially Hsp82 which is targeted and not Hsc82.

The next protein investigated was the product of the gene *YBR053C*. So far, the protein does not have an official name in the *S. cerevisiae* genome database (SGD) but has been annotated as the homolog of human regucalcin. For clarity, the protein will therefore be referred to as regucalcin. Regucalcin was handpicked as a candidate, because it was previously reported in another proteomics study, where it showed the strongest stabilization in *slx5Δ* (Messner et al., 2023). The *YBR053C* gene was cloned into the *LEU2* integration cassette and integrated into wild type and $P_{GAL1}$*ULS2*. The protein level of regucalcin was investigated on western blot (**Fig. 25 B**). Upon the shut-off of Uls2, regucalcin was stabilized indicating targeting through Uls2 (**Fig. 25 D**). Surprisingly, regucalcin was also stabilized upon overexpression of Uls2. This was highly unexpected. Stabilization under both shut off and overexpression does not suggest targeting through Uls2 but instead points to another connection between Uls2 and regucalcin, which remains to be elucidated.

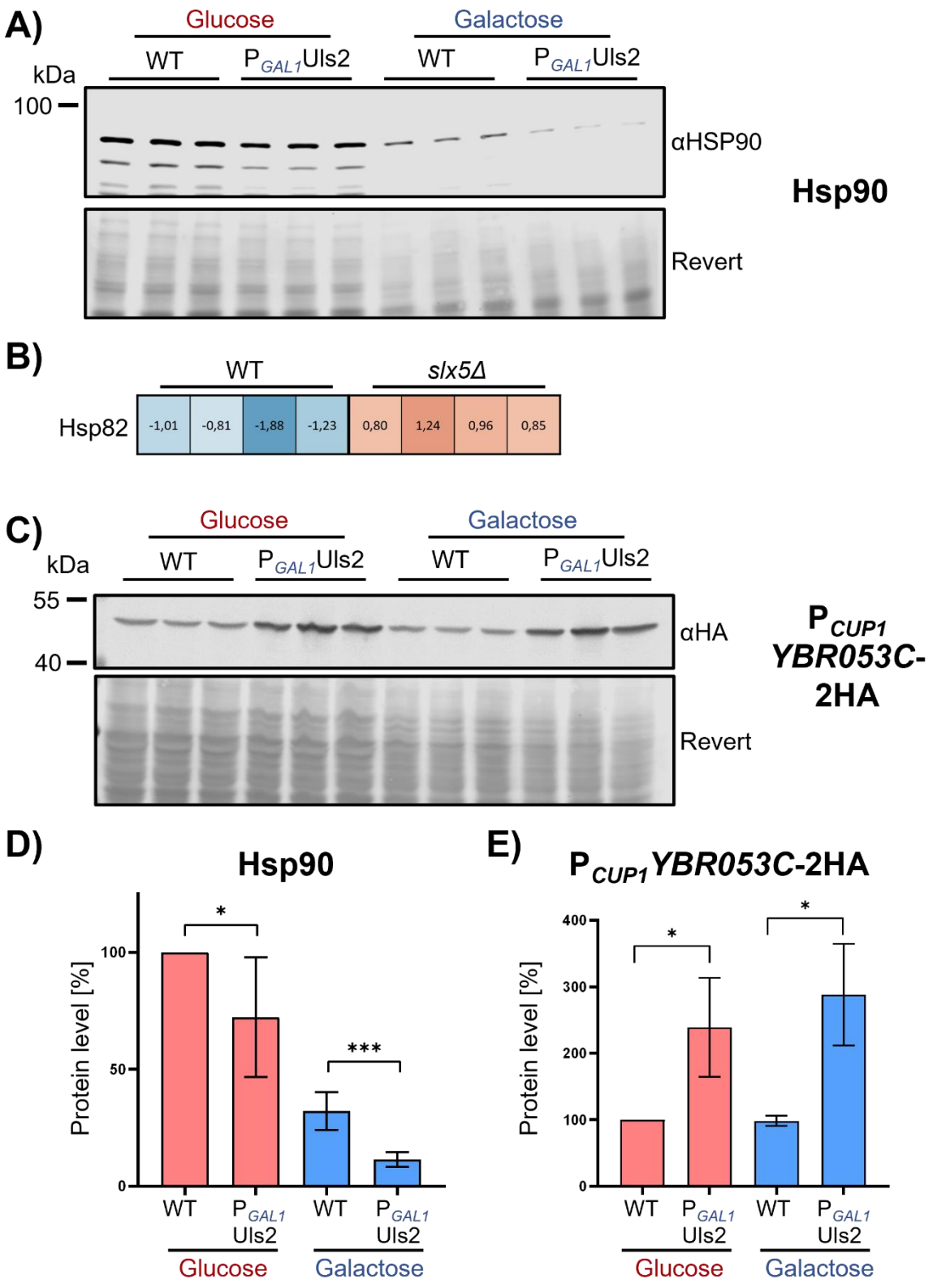


**Figure 25 Different candidates display distinct protein levels. A)** Western blot of Hsp90 in wild type and P$_{GAL1}$*ULS2* strains. After overnight preculture in YP-Raffinose, the cells were grown 4 h in YP-Glucose or YP-Galactose. Boiled lysis was loaded on an 8% SDS-Gel, blotted for 1 h at 400 mA, 100 V at 4 °C on nitrocellulose using wet blot. Blots were incubated with Revert before blocking. Blocked blots were incubated with anti-Hsp90 (αHsp90-rabbit at 1:5,000) overnight at 4°C and with anti IGG coupled to fluorophore (800 nm emission peak) for 2 h at room temperature. Strains used were:

yFP211, yFP223. **B)** hCluster values of Hsp82. **C)** Western blot of *YBR053C* (regucalcin) in wild type and $P_{GAL1}$*ULS2* strains. After overnight preculture in YP-Raffinose, the cells were grown 4 h in YP-Glucose or YP-Galactose. Boiled lysis was loaded on a 12% SDS-Gel, blotted for 1 h at 400 mA, 100 V at 4 °C on nitrocellulose using wet blot. Blots were incubated with Revert before blocking. Blocked blots were incubated with anti-HA (αHA) antibody (3F10-rat at 1:2,000) overnight at 4°C and with anti IGG coupled to fluorophore (800 nm emission peak) for 2 h at room temperature. Strains used were: yFP217, yFP224. **D)** Quantification of Hsp90 western blot. n=6. **E)** Quantification of YBR053C/regucalcin western blot. n=3; Students t-test; * = p<0.05; ** = p <0.01; *** = p < 0.001; **** = p< 0.0001.

Next, the protein Pam16 was investigated. Pam16 was only detected in the *slx5Δ* treated with $H_2O_2$ sample. In the hCluster, it was grouped into cluster 7. Therefore, Pam16 was investigated as a target of Uls2 under stress. To examine this, Pam16 was cloned into the *LEU2* integration cassette. The cassette was integrated into the wild-type and the *slx5Δ* strains. Both were subjected to oxidative stress as previously in the proteomics study. The results were investigated using western blots (**Fig. 26 A**). Here, without stress the protein level of Pam16 decreased by 20% in the *slx5Δ* strain. Upon exposure to oxidative stress, the level in wild type cells dropped by 20% as well. Upon oxidative stress in the *slx5Δ* background the Pam16 protein level increased to 115%. Compared to the protein level in the wild type with oxidative stress, this is a significant increase. The western blot only partially reflected the results from mass spectrometry. Here, Pam16 was significantly increased in *slx5Δ* under stress, whereas the protein level in the other samples was roughly the same (**Fig. 26 D**). The western blot showed a high protein level in the wild type without stress which is unexpected. Still, the difference in protein level between wild type and *slx5Δ* under stress could point to a targeting of Pam16 under stress conditions. Further investigation of this targeting will be necessary. Of interest would be the Pam16 protein level in the $P_{GAL1}$*ULS2* strain as well as under different stress conditions.

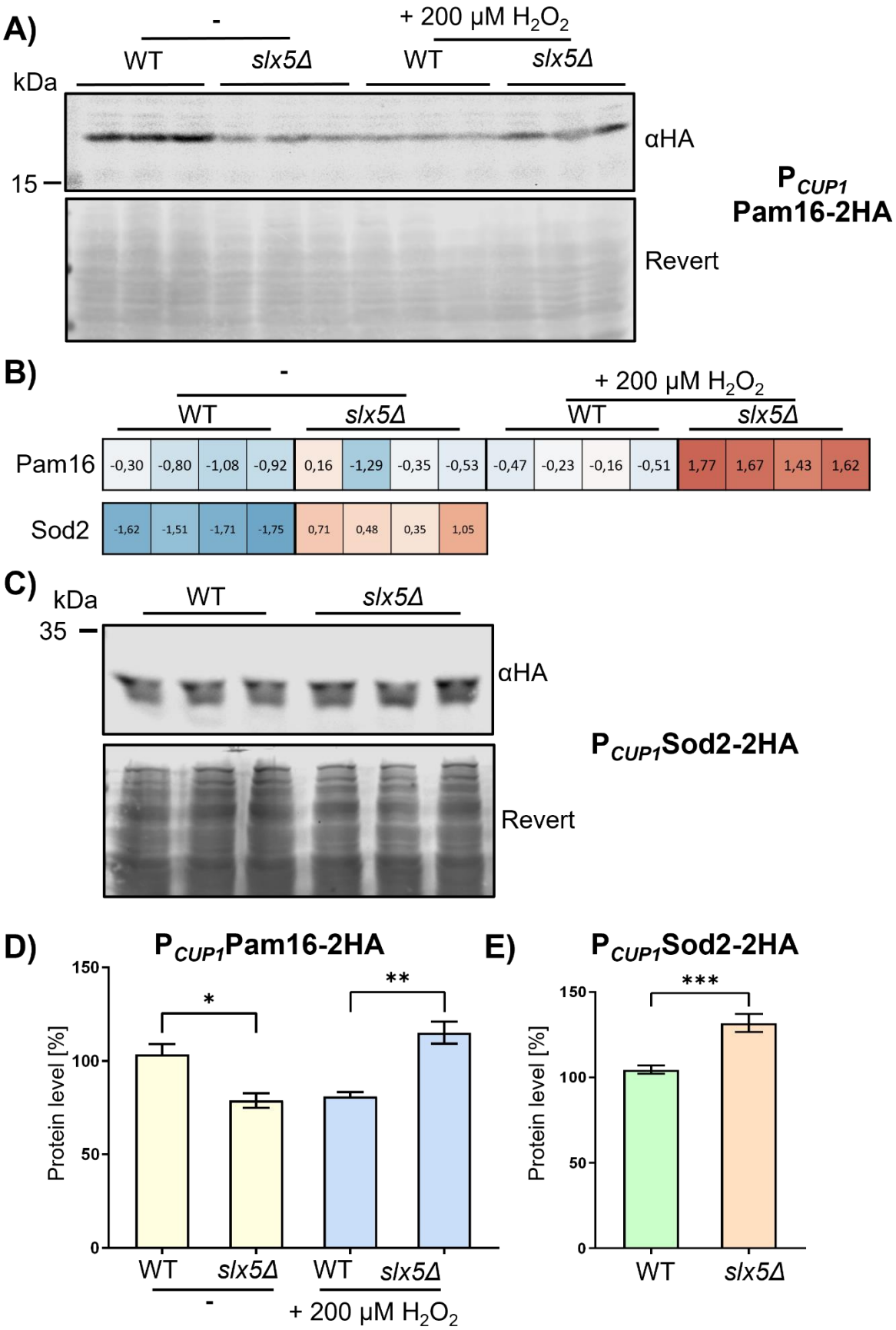


**Figure 26 Different candidates display distinct protein levels A)** Western blot of Pam16 in wild type and *slx5Δ* strains treated with 200 µM $H_2O_2$. Day cultures were grown 4 h in YP-Glucose followed by stress treatment performed for 45 min at 30 °C.

Boiled lysis was loaded on a 12% SDS-Gel, blotted for 1 h at 400 mA, 100 V at 4 °C on nitrocellulose using wet blot. Blots were incubated with Revert before blocking. Blocked membranes were incubated with anti-HA (αHA) antibody (3F10-rat at 1:2,000) overnight at 4°C and with anti IGG coupled to fluorophore (800 nm emission peak) for 2 h at room temperature. Strains used were: yFP215, yFP216. **B)** Relevant hCluster values from Pam16 and Sod2 **C)** Western blot of Sod2 in wild type and *slx5Δ* strains treated with 200 µM $H_2O_2$. Day cultures were grown 4 h in YP-Glucose followed by stress treatments performed for 45 min at 30 °C. Boiled lysis was loaded on a 12% SDS-Gel, blotted for 1 h at 400 mA, 100 V at 4 °C on nitrocellulose using wet blot. Blots were incubated with Revert before blocking. Blocked membranes were incubated with anti-HA (αHA) antibody (3F10-rat at 1:2,000) overnight at 4°C and with anti IGG coupled to fluorophore (680 nm emission peak) for 2 h at room temperature. Strains used were: yFP211, yFP212. **D)** Quantification of Pam16 western blot. n=3. **E)** Quantification of Sod2 western blot. n = 9, Students t-test; * = p<0.05; ** = p <0.01; *** = p < 0.001; **** = p< 0.0001.

Another protein that was investigated is the superoxide dismutase 2 (Sod2). Sod2 was found in cluster 4 and has been reported to be SUMOylated (Bhagwat et al., 2021). Therefore, Sod2 was investigated in the wild type and *slx5Δ* background without stress. Here, the expression cassette was integrated at the *LEU2* locus. Sod2 expression was induced with copper and boiled extracts were investigated by western blotting (**Fig. 26 C**) An increase of Sod2-2HA levels by 25% in the *slx5Δ* background could be detected in comparison to the wild type. Stabilization of Sod2 was weak, but reproducible and therefore statistically significant (**Fig. 26 E**). The western blot results reflect those of the mass spectrometry (**Fig. 26 B**). Together, they suggest that Sod2 is targeted by Uls2, independent of stress. Further analysis using the $P_{GAL1}$*ULS2* strain could enhance the results.

To summarize, multiple proteins that were found in the mass spectrometry study were analyzed in the *slx5Δ* or the $P_{GAL1}$*ULS2* strain. For proteins such as Hsp90, regucalcin or Sod2 the results from the mass spectrometry study could be confirmed. The results for Pam16 could be partially confirmed. Together, the results suggest that Hsp90, Sod2 and Pam16 are targets of Uls2. Hsp90 and Sod2 both seem to be targeted under non-stress conditions whereas Pam16 seems to be a target only under stress conditions. Pam16 should be further investigated regarding Uls2-mediated quality control. For regucalcin the results from the mass spectrometry could be reproduced but expression levels in the $P_{GAL1}$*ULS2* strain were puzzling, as regucalcin was not targeted more efficiently upon *ULS2* overexpression. For other proteins such as Tps1 or Dcs1 (Data not shown) the proteomics data could not be confirmed by western blot.

# 3 Discussion

## 3.1 Evidence for a Role of the STUbL Uls2 in Protein Quality Control

The results of this thesis support our working hypothesis that Uls2 (Slx5-Slx8) serves as part of a quality control mechanism for proteins with SIMs and SUMOylation sites (**Fig. 27**). We could show that two proteins – Fir1 and Nis1 – are targeted to the nucleus upon overexpression, reside in aggregates, and are targeted by Uls2. The targeting through Uls2 could be shown using western blotting and microscopy. For Fir1, it could be demonstrated that nuclear localization as well as aggregate formation are SUMOylation- and SIM-dependent. This implies that Fir1s abundance is regulated through SUMOylation. The observation that Fir1 targeting was particularly prominent upon its overexpression, led us to consider that the targeting pathway through SUMOylation and STUbLs might serve as a quality control mechanism that could for example mediate degradation of proteins lacking their partner polypeptides (**Fig. 27**).

Both Nis1 and Fir1 are targeted under overexpression conditions and have an inhibitory function in the cell cycle. Nis1 is involved in inhibiting the reuse of an old bud site, and Fir1 is involved in inhibiting cytokinesis if certain processes are not yet completed (Brace et al., 2019; Meitinger et al., 2014). For Fir1, we could observe the effect its overexpression has on cell division. Cells become clustered and cytokinesis is not finished properly. Uls2-mediated quality control could serve as a mechanism to fine tune Fir1 levels by eliminating every molecule that is not interacting with its appropriate partners to avoid any unwanted side effects.

Uls2 has previously been described to be involved in quality control of the Mot1 protein. Here, a mutated version of Mot1 (Mot1-301) was targeted to greater extent than the wild-type Mot1, leading to the assumption that Uls2 serves as a quality control mechanism for Mot1 (Wang & Prelich, 2009). Interestingly, unlike Mot1, Nis1 and Fir1 are not inherently nuclear proteins. Both are only nuclear upon overexpression or absence of their respective partners (Perez & Thorner, 2019) (Nils Johnsson, University of Ulm, personal communication). It appears as if Nis1 and Fir1 are solely shuttled to the nucleus to be targeted by Uls2. This might seem surprising at first glance, but the shuttling of cytosolic proteins into the nucleus as part of quality control

has been reported before in the context of intranuclear quality control departments (INQs) (See chapter 1.1). Here, upon stress misfolded proteins can be transported into the nucleus through chaperone-assisted nuclear import. In the nucleus the misfolded proteins are sequestered by the aggregase Btn2 into INQs (Miller et al., 2015). Another study supported this and argued that the relocalization of misfolded proteins serves as a mechanism to ensure an equal distribution across the quality control systems, so that cytosolic protein quality control systems are not overloaded (Malinovska et al., 2012). The relocalization to the nucleus has also been described for mitochondrial proteins. Here, the nuclear localization is triggered by an import deficiency. In the nucleus, the proteins are then targeted by the proteasome as part of nuclear-associated mito-protein degradation (Shakya et al., 2021). Interestingly, it has been reported that mitochondrial import deficiency and impaired proteostasis lead to SUMOylation of diverse mitochondrial proteins (Paasch et al., 2018), some of which were also detected in our proteomic approach, such as Tim9 or Nde1.

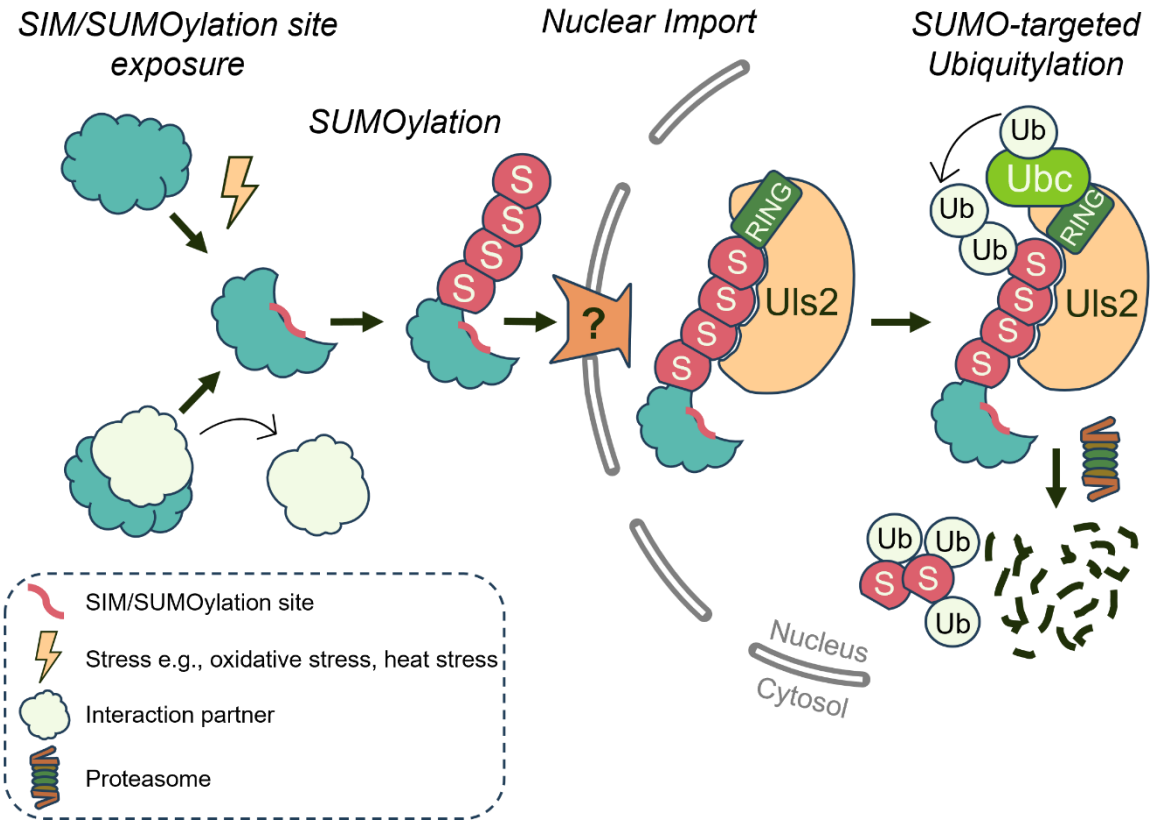


**Figure 27 Working hypothesis. Uls2 serves as part of a quality control mechanism for SIM- and SUMOylation site-containing proteins.** Upon absence of a partner protein or folding stress, an internal SIM or SUMOylation site is exposed. This site promotes SUMOylation of the protein and subsequently its relocalization to the nucleus. There, the SUMO chain is recognized by Uls2. Uls2 ubiquitylates the SUMO chain, which leads to the degradation of the protein.

To further strengthen our model, the mechanism of nuclear localization as well as Fir1's SUMOylation should be investigated in more detail in future studies. Microscopy data from Fir1 suggests that SUMOylation is required for nuclear localization. However, it is not yet established that Fir1 itself is SUMOylated to facilitate the relocalization, or if Fir1 interacts with other SUMOylated proteins through its SIM. Notably, however, it could be demonstrated that a Fir1 SIM mutant (*fir1*$^{I760K}$) is still able to localize to the nucleus. Strikingly, the formation of aggregates was abolished by this mutation. This favors the interpretation that Fir1 itself is SUMOylated and not just piggyback transported to the nucleus by interacting with SUMOylated proteins via its SIM. Further investigation of this matter should focus on dissecting Fir1's SUMOylation in the cytosol and its subsequent nuclear localization.

Nuclear importers involved in this process should be determined using nuclear import mutants. Then, it should be demonstrated that Fir1 is SUMOylated. This can be done by using either SUMO or Fir1 pulldowns. So far, SUMOylation of Fir1 has not been sufficiently established, although Fir1 has been found SUMOylated at residue K715 in a proteomic approach that investigated SUMOylation during meiosis (Bhagwat et al., 2021). To investigate if Fir1 SUMOylation is required for nuclear localization, it should be dissected if SUMOylation of Fir1 takes place in the cytosol. This could be achieved by performing SUMO pulldowns of Fir1 in the import mutants, here SUMOylated Fir1 can only be detected if Fir1 is SUMOylated prior to its import. Another approach would be to generate a Fir1 mutant, which cannot be SUMOylated by replacing all lysine residues with arginine. However, since Fir1 is a large protein and contains 67 lysine residues, this approach is not feasible and might result in an unfunctional protein.

In conclusion, the results of this thesis and current literature support our model that Uls2 serves as part of a quality control system for proteins with hidden SIMs or SUMOylation sites. This model deepens our understanding of quality control of cytosolic proteins involving their nuclear relocalization. Details of the mechanism of nuclear import of such SUMOylated or SIM-containing proteins remain to be elucidated.

## 3.2 Formation of Aggregates in Uls2 Targets

Interestingly, Nis1 as well as Fir1 accumulated in aggregates, which seemed to be unresolvable using the standard boiling lysis. Hsp90 has been reported to aggregate in stress granules in fission yeast upon arsenite treatment, under non-stress conditions evidence of aggregation is still missing (Tomimoto et al., 2024). In this thesis Hsp90 displayed a similar pattern on western blot as Fir1 and Nis1. All three proteins showed a decrease in protein level upon Uls2 overexpression, but no or only slight changes of the levels under shut off conditions leading to Uls2 depletion. The decreased level of these proteins indicated that they are targeted efficiently if sufficient amounts of Uls2 are around. However, stabilization of the same proteins was expected upon Uls2 depletion. A possible explanation for this, at first glance puzzling, result can be derived from the analysis of cellular distributions of these proteins. The microscopy results for Nis1 and Fir1 revealed an accumulation of both proteins in nuclear aggregates in the absence of Uls2. A possible explanation for this seemingly discrepant finding is that the aggregates are probably insoluble by boiling in Laemmli buffer. Supporting this notion, for Fir1, a lysis which was described in a paper working on JUNQs (Rolli et al., 2024), improved the lysis of the aggregates. For Nis1 and Hsp90 this procedure remains to be tested and would be the logical next step to further strengthen the point that both proteins are substrates of Uls2, and, in its absence, accumulate in aggregates that are insoluble under standard extraction conditions.

The formation of aggregates of multiple targets of Uls2 prompts the question whether aggregation of the proteins is part of the Uls2 targeting mechanism and assists in targeting SIM-containing proteins for degradation. For Fir1, we could show that the formation of aggregates is SUMOylation- as well as SIM-dependent. One could imagine that SUMOylated Fir1 interacts with the SIM of another Fir1 and thus forms small aggregates. These aggregates ensure that SUMOylated Fir1 does not disturb other processes, and they enable Uls2 to target Fir1. Uls2 interacts with the SUMOylated Fir1 using its SIMs and ubiquitylates the SUMO chains leading to the degradation of Fir1. The idea that STUbLs target aggregates has been proposed before in the context of stress granules in mammalian cells. Here, it was demonstrated that upon proteotoxic stress, stress granules are formed, which are targeted by the STUbL Rnf4. If this STUbL pathway is impaired, stress granules accumulate (Keiten-Schmitz et al., 2020).

To determine if the aggregates are an active step in the targeting pathway, one could investigate Fir1 targeting in an aggregation deficient mutant such as the SIM mutant *fir1*$^{I760K}$. If SIM-mediated aggregation is critical for recognition, Uls2 should target Fir1 less efficiently. Since an improved lysis method for Fir1 was established, the SIM mutant of Fir1 should be compared to the wild-type Fir1 to analyze the role of the SIM on Uls2 targeting using this procedure. Furthermore, this could be investigated using artificial reporter constructs that carry a SUMO chain as well as an accessible flexible SIM. For reporters carrying a SUMO chain it was already shown that they localize to the nucleus and are targeted by Uls2 (Lennard Doering, PhD thesis, 2021). In the context of a possible benefit of aggregation, it would be interesting to investigate whether attachment of a SIM to the reporter could induce its aggregation and enhance targeting through Uls2.

So far, it could be shown that the aggregates accumulate in a Uls2 shut-off strain and disappear upon overexpression of Uls2. This suggests that Uls2 targets the aggregates. However, direct evidence of Uls2 targeting the aggregates is still missing. This could be addressed by monitoring live yeast cells, here, cells pregrown in YP-glucose could be plated on thin agar pads containing galactose. Then, aggregates in cells could be chosen and monitored over time. When the aggregates disappear upon induction of Uls2 one can conclude that Uls2 targets them. Another method could include preculturing cells in YP-glucose under Uls2 shut-off conditions and monitoring the amounts of aggregates. Then the medium will be switched to YP-galactose to induce the overexpression of ULS2. The number of aggregates should then be drastically decreased thus proving the targeting of the aggregates through Uls2.

To summarize, based upon the findings of this thesis, the role of aggregation in Uls2 targeting is a promising direction that could be further investigated using the suggested methods.

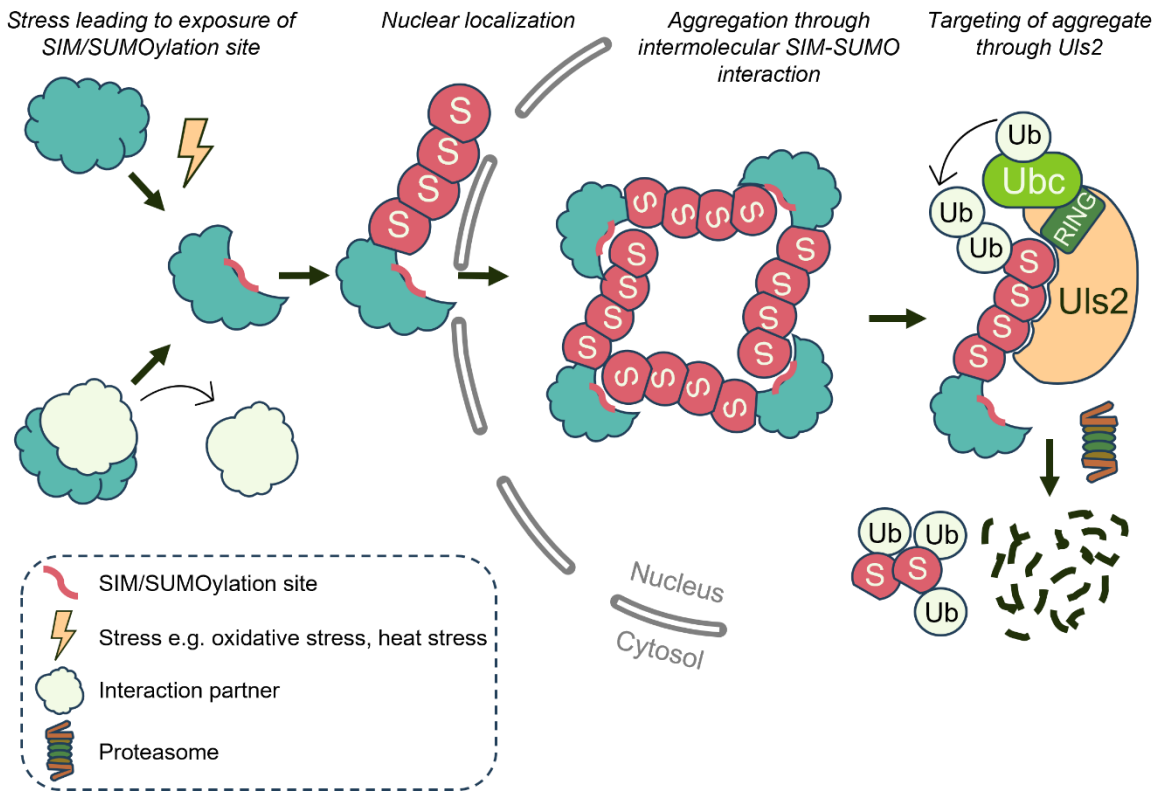


**Figure 28 Working hypothesis. SUMOylated substrates interact intermolecularly via SIMs and form aggregates enhancing Uls2 targeting**. Upon absence of a partner protein or folding stress, an internal SIM or SUMOylation site is exposed. This site promotes SUMOylation of the protein and subsequently its relocalization to the nucleus. There, intermolecular SUMO-SIM interactions mediate aggregation of the protein. Uls2 recognizes the aggregate through interaction of its SIMs with SUMO chains. Uls2 ubiquitylates the SUMO chain, which leads to the degradation of the protein.

# 3.3 Proteomic Approach

## 3.3.1 Evaluating Proteins Found in Proteomic Approach

With the aim to scrutinize the working hypothesis of this thesis, a whole cell proteome approach was performed to identify targets of Uls2. The analyses of potential substrates did not only focus on candidates that would fit our working hypothesis but generally comprised all potentially interesting targets of Uls2. Therefore, two lists of candidates were assembled. First, a list of 25 proteins was generated that were chosen through stringent selection criteria including the presence of SIMs or SUMOylation sites. This list aims to identify proteins that support the working hypothesis. So far, the large number of candidates on this list need to undergo further scrutinization and future research will determine which ones of them support the working hypothesis.

Additionally, a list of eight handpicked candidates was assembled. This list includes proteins that were selected based on extreme values in the proteome approach, such as Pam16 or because they were of special interest due to previous lab internal reports, such as Cue3. Three of the selected candidates, namely the mitochondrial proteins Sod2 and Pam16, and the chaperone Hsp82, showed promising results in western blot analyses proving that the proteomic approach was a useful tool for finding targets of Uls2.

At first, the targeting of mitochondrial proteins such as Sod2 and Pam16 seemed surprising since SUMOylation and Uls2 targeting occur mainly in the nucleus (Chen et al., 2024; Cook et al., 2009). However, it was previously reported that mitochondrial proteins can undergo localization to the nucleus upon import failure (Shakya et al., 2021). Additionally, it was shown that mitochondrial proteins can become targets of SUMOylation when their import into mitochondria is impaired (Paasch et al., 2018). Interestingly, several SUMOylated mitochondrial proteins found by Paasch et al. were also found in the present study. Examples include proteins such as Arg56, Cox8, Hem14, and Nde1, which were all found in cluster 4 that comprised proteins increased in *slx5Δ* independently of stress treatment. Furthermore, two candidates from cluster 7, which includes proteins with increased protein levels in stressed *slx5Δ* cells, Rsm28 and Tim9 were also identified as SUMOylated mitochondrial proteins (Paasch et al., 2018). This indicates that SUMOylation upon impaired mitochondrial import could result in the targeting of mitochondrial proteins through Uls2. This aligns well with the working hypothesis of this thesis. In the case of mitochondrial proteins, failed localization, instead of stress or missing interaction partners, could trigger SUMOylation and subsequently nuclear localization and targeting through Uls2. This would further strengthen the hypothesis that Uls2 is part of a broader quality control mechanism. As previously discussed, the purpose of the import into the nucleus could be to ensure that the cytosolic quality control systems are not overloaded (Borgert et al., 2022).

In this thesis, Sod2 and Pam16 were investigated as representatives of mitochondrial proteins. In the proteome analysis, they were attributed to cluster 4 and cluster 7, which were comprised of proteins showing increased levels in the *slx5Δ* strain either independent or dependent on oxidative stress, respectively. However, to prove both proteins are targets of Uls2, their levels should be further investigated in the $P_{GAL1}$*ULS2* strain.

Of special interest is the protein Pam16. It was found to be stabilized only under conditions of oxidative stress in the *slx5Δ* strain, thus fitting perfectly into the working hypothesis. Additionally, Pam16 contains a SIM-like sequence (ILNIEE 61-66). Usually, the SIM-like sequence is partially hidden in an α-helix, as demonstrated by crystallization of the Pam18-Pam16 complex (Mokranjac et al., 2006). For future research, mutation of the SIM-like sequence could reveal if the SIM is involved in targeting of Pam16 by Uls2. Furthermore, Pam16 has one lysine (K109) that lies in a SUMOylation site and that should be considered a potential site of SUMOylation. So far, SUMOylation of Pam16 has not been reported and needs to be examined. This could be investigated by employing SUMO pulldowns. Since Pam16 protein level increases upon oxidative stress, the SUMO pulldown should be performed using the *slx5Δ* strain under these conditions. Oxidative stress should promote SUMOylation of Pam16. The absence of Slx5, at the same time, should result in a stabilization of SUMOylated Pam16. Furthermore, the localization of Pam16 should be investigated. Here, based upon our hypothesis, it would be expected that Pam16 relocalizes to the nucleus upon mitochondrial import stress.

Another promising target of Uls2 identified by proteomics was the chaperone Hsp82. Here, the targeting of Hsp82 could be shown in the $P_{GAL1}$*ULS2* strain. Future research should focus on investigating the localization of Hsp82 under different conditions and in the *slx5Δ* strain. Furthermore, it should be dissected if the targeting through Uls2 is only detectable for Hsp82 or also for its isoform Hsc82. The proteome analysis showed only the stabilization of Hsp82, but western blot analysis could not distinguish them due to their high sequence similarity (Girstmair et al., 2019). Tagging Hsp82 and Hsc82 with a unique protein tag could be employed to dissect the targeting of the two isoforms.

However, not all proteins found in the proteomic approach could be confirmed as direct substrates of Uls2 by western blotting. For the *YBR053C* gene product, increased levels were observed in the $P_{GAL1}$*ULS2* strain under both shut-off and overexpression conditions suggesting that the *YBR053C* gene product is not targeted by Uls2. So far, the interplay between Uls2 and *YBR053C* remains to be elucidated. Due to the lack of literature on *YBR053C,* further speculations on their interplay would be unfounded.

Although, for some proteins, such as Sod2 or Pam16, the results from mass spectrometry could be verified using western blotting, this was not the case for every

protein tested. For some proteins, such as Tps1, the stabilization of the protein observed in the proteomics approach could not be verified by western blotting (data not shown). Here, multiple explanations could be possible. An interesting explanation based on previous results obtained in this thesis could be the aggregation of proteins such as Tps1, which could have hindered the detection by western blotting and thus obscured the stabilizing effect. Another explanation could be that those proteins are not targeted by Uls2 but instead are transcriptionally upregulated in Uls2 mutants. Western blot analyses of levels of tagged Tps1 employed cells expressing the *TPS1* gene under control of the *CUP1* promoter. Therefore, the transcriptional regulation of the endogenous *TPS1* gene is not in place. The different results from the proteomics and western blot approaches therefore suggest that changes in levels of some of the proteins initially identified in the proteomics approach are not due to direct targeting by Uls2 but more likely influenced by effects of the *SLX5* deletion on transcription. Indeed, Tps1 is transcriptionally regulated by the protein Gts1 (Xu et al., 2004; Yaguchi & Tsurugi, 2003). Interestingly, Gts1 was also found in the proteomics approach. Unlike Tps1, which was found in cluster 4, Gts1 was attributed to cluster 2. In cluster 2, the protein levels increased in *slx5Δ* without oxidative stress and decreased in wild type with oxidative stress whereas the other two treatment groups displayed a protein level in the middle between the first two groups. For Gts1, the lowest protein level was detected in wild type with oxidative stress, followed by wild type untreated, then *slx5Δ* with stress and lastly *slx5Δ* untreated. Based on the hCluster values, both Tps1 and Gps1 increased in *slx5Δ,* with and without stress, indicating that the increase of Tps1 levels could be attributed to the increase in Gts1. This would indicate that Gts1 could be the direct target of Slx5, which could be addressed in future experiments. In conclusion, for the interpretations of the proteomic data, it should be considered that proteins such as Tps1 might not be targeted directly by Uls2 but instead are influenced transcriptionally by targeting of their transcriptional regulator.

To summarize, this study could identify Hsp82 as a substrate of Uls2 and reproduce the results from the proteomic approach for Pam16 and Sod2 making them promising candidates for further investigation. Additionally, potential candidates can be found in the assembled lists in this study. Furthermore, it should be considered to inspect those proteins identified in the proteomic approach of this study which overlap with the proteins identified in Paasch et al. (2018), as the combined findings characterize these as promising candidates as substrates of SUMOylation and Uls2.

### 3.3.2 Efficiency of the Proteomic Approach

The proteomic approach used in this study proved to be useful to obtain an overall image of the effect a *SLX5* deletion has on the proteome and it produced a list of potential candidates that undergo targeting through Uls2. However, the proteomic approach also had some limitations, such as the coverage of proteins found. In this proteomic approach, 2903 proteins were found, which is roughly 50% of the total number of proteins in *S. cerevisiae* of the reportedly 5934 verified proteins including some proteins of unknown function (*Saccharomyces cerevisiae* genome database, accessed 28.11.2025).

The number of proteins found in proteomic studies is highly dependent on the preparation of the samples. For this study, whole cell extracts were submitted for mass spectrometry. This has the advantage that the preparation is easy to perform and cost efficient when submitting samples from multiple conditions. Using the same approach of using whole cell extracts, other studies obtain a similar number of proteins (Messner et al., 2023; Mosley et al., 2009; Soares Rodrigues et al., 2023). For example, a proteomic study on 3000 *S. cerevisiae* deletion strains obtained on average 2552 proteins when doing a similar lysis using urea buffer and glass bead lysis (Messner et al., 2023). The reason for this is that many low abundant proteins get overshadowed by highly abundant proteins and thus cannot be found in the proteome analysis (Boschetti & Righetti, 2023). If one wants to further focus on detecting low abundant proteins, the samples could be separated by SDS-PAGE and then fractionated into different gel pieces as performed by Gao and colleagues who combined gel fractionation with optimized mass spectrometry to obtain a near-complete yeast proteome (Gao et al., 2021). Gao et al. show that the detection of low abundant proteins could be increased immensely, but this would result in high costs. Nevertheless, for future studies one could employ parts of these methods and fractionate *slx5Δ* samples by SDS-PAGE with focus on the stacking gel, which often contains HMW-SUMO conjugates. Those would be of special interest in light of this thesis and could provide more substrates of Uls2.

In summary, the proteomics approach was successful in identifying potential Uls2 substrates with the caveat that many low abundant proteins will have escaped the detection.

## 3.4 Posttranslational Modification of Nis1

This study showed that Nis1 is heavily posttranslationally modified both by phosphorylation and ubiquitylation. The performed dephosphorylation assay indicated that the middle band of Nis1 represents phosphorylated Nis1. Phosphorylation of Nis1 is supported by previous proteomic studies that have found Nis1 to be phosphorylated on a total of 15 residues. Out of these 15 residues, 12 have been found in more than one study (Albuquerque et al., 2008; Holt et al., 2009; Lanz et al., 2021; Leutert et al., 2023; MacGilvray et al., 2020; Swaney et al., 2013; Zhou et al., 2021). These proteomic studies cover a range of conditions for phosphorylation from general phosphorylation sites in *S. cerevisiae* (Albuquerque et al., 2008; Lanz et al., 2021) to phosphorylation in response to multiple stress factors (Leutert et al., 2023) or stress-induced phosphorylation by DTT (MacGilvray et al., 2020). One study specifically investigated the substrates of the **c**yclin-**d**ependent **k**inase 1 (Cdk1) and showed that Nis1 is a target of Cdk1 (Holt et al., 2009). In light of this study, one could investigate if Cdk1 is involved in phosphorylated Nis1 detected in the middle band, which could help to elucidate the regulation of Nis1 through phosphorylation.

In the context of SUMOylation, the serine residue S388 could be of special interest. This residue was reported to be phosphorylated in two studies (Lanz et al., 2021; Leutert et al., 2023). Serine 388 is just three residues in front of Nis1's SIM, and phosphorylation of this residue adds an additional negative charge to the SIM. This could point towards a phosphoSIM, a SIM where phosphorylation increases the hydrophobic charge and further strengthens the SIM (Lascorz et al., 2022). Increasing strength of the SIM could play a role in the cell cycle-dependent regulation of Nis1. In support of the possibility of a phosphoSIM, is the reporter construct with the C-terminal domain of Nis1. The reporter demonstrated that the C-terminal domain was sufficient to target the reporter to the nucleus, but deletion of the SIM reverted the nuclear localization to background level. Interestingly, attachment of only Nis1's SIM targeted a reporter to the nucleus but could not reproduce the nuclear localization caused by the full C-terminal domain. It could be speculated that other features of the sequence or just the distance to the reporter might be important. Here, it might be the missing phosphorylation of serine 388 that enhances the nuclear localization through the SIM to full extent.

Interestingly, Nis1 has also been found in a proteomic study investigating the crosstalk between phosphorylation and ubiquitylation. Here, Nis1 is co-modified with

ubiquitin and a phosphor group (Swaney et al., 2013). Although, no specific residue is reported for Nis1 ubiquitylation. In this thesis, the ubiquitylation of Nis1 could be shown by employing an ubiquitin shift assay as well as ubiquitin pulldowns. The results of Swaney et al. could suggest that the ubiquitylation of Nis1 is regulated by phosphorylation. In this thesis, it was hypothesized that the ubiquitylation of Nis1 is driven by SUMOylation and subsequent targeting through the STUbL Uls2. This is supported by western blotting and microscopy results that show the targeting through Uls2. A preliminary ubiquitin pulldown in a *slx5Δ* background also supports the Uls2 dependency of Nis1s ubiquitylation.

Together these results support the intriguing idea that Nis1 could be regulated in a complex manner by phosphorylation resulting in a phosphoSIM leading to increased SUMOylation and subsequent ubiquitylation. Here, evidence linking phosphorylation of Nis1 to its SUMOylation is missing. This is especially important, considering that so far there is only indirect evidence of Nis1 SUMOylation but no direct evidence proving Nis1 itself is SUMOylated. Still, targeting by Uls2, as shown in this study, as well as accumulation of HMW-SUMO conjugates, as shown in other studies strongly suggest that Nis1 is SUMOylated (Uzunova et al., 2007). Another possibility would be that Nis1 phosphorylation and SUMOylation could act independently of each other promoting the ubiquitylation of Nis1. Here, phosphorylation or SUMOylation could provide the correct timing of ubiquitylation of Nis1 and its subsequent degradation.

Further research should focus on the interplay of Nis1 posttranslational modifications by further dissecting their dependencies. A useful tool would be a mutant of the kinase Cdk1, which has been shown to phosphorylate Nis1 and investigating Nis1s ubiquitylation in this mutant (Holt et al., 2009). To investigate the possibility of a phosphoSIM for Nis1, a phosphorylation-deficient S388A mutant could be employed. This would eliminate the possibility of phosphoSIM. In this mutant the HMW-SUMO conjugates upon *nis1*$^{S388A}$ overexpression could be investigated to determine if SUMOylation of Nis1 is decreased. The S388A mutation could also be introduced into the Nis1 C-terminal domain reporter to investigate the impact on nuclear localization. Furthermore, the *6HIS*-ubiquitin pulldown of different Nis1 mutants and SUMO mutants could be performed to dissect the requirement of the SIM and the SUMOylation machinery for the ubiquitylation further. Additionally, the cell cycle dependency of the posttranslational modifications should be further investigated. Here, cell cycle arrests could be combined with mass spectrometry to dissect the timing in the cell cycle of

phosphorylation, ubiquitylation and SUMOylation of Nis1. This could also provide the final evidence of Nis1s SUMOylation.

To summarize, this study provides a valuable insight into the complex posttranslational modifications of Nis1 by showing its phosphorylation as well as its ubiquitylation. Further investigation of the PTMs of Nis1 and their interaction could elucidate its regulation.

## 3.5 Fir1 Clump Phenotype

To our knowledge, this thesis is the first study that describes a Fir1 overexpression strain in detail. Here, we employ a constitutively expressed Fir1 which results in altered cell morphology. It was observed that cytokinesis in overexpressed Fir1 cells is not completed, instead cells remain together and form clumps. An explanation for this phenotype could be the role of Fir1 in cell division. Reportedly, Fir1 serves as a checkpoint protein in the ECO pathway by inhibiting Cbk1 activity and thereby septum destruction (Brace et al., 2019). At the same time, Fir1 anchors Skt5 in the split septin ring leading to an increased amount of enzymes for construction of the secondary septin (Müller et al., 2024). Overexpression of Fir1 could lead to an uncontrolled amount of Fir1, which inhibits septum destruction and supports construction of the secondary septum. Thereby, it leads to unseparated cells which appear as clumps. The phenotype described in this thesis supports the previously published studies claiming Fir1’s role as a checkpoint protein in the ECO pathway.

# 4 Materials and Methods

## 4.1 Materials

### 4.1.1 Equipment

**Table 1** Equipment used in this study

| Equipment | Source |
|---|---|
| Blue LED Illuminator | Nippon Genetics |
| Bunsen burner | neoLAB |
| Centrifuge 5415 D | Eppendorf |
| Centrifuge 5424 | Eppendorf |
| Centrifuge 5430 R | Eppendorf |
| Centrifuge 5810 R | Eppendorf |
| Centrifuge Allegra X-22R | Beckman-Coulter |
| Centrifuge Avanti J-20 XP | Beckman-Coulter |
| ChemDoc | Bio Rad |
| Developer for X-ray films Curix 60 | Agfa |
| FastGene FAS-DIGI PRO | Nippon Genetics |
| Fluorescence microscope Axioplan 2 | Zeiss |
| Gel casting system (Agarose gels) | Peqlab |
| Gel casting system (SDS-PAGE) | Mini-Protean Bio Rad |
| Heat block | Thermo scientific |
| Incubators innova 4230 | New Brunswick Scientific |
| Macro Pipette controller | Brand |
| Magnetic rack | Invitrogen |
| Magnetic stirrer | H + P |
| Microliter pipets | Eppendorf |
| Microwave oven | - |
| Nitrocellulose membrane, 0.2 µM | Amersham |
| Odyssey Imager | LI-COR |
| pH meter | Mettler Toledo |
| Pipettes (Set) | Gilson |

| | |
|---|---|
| Power supply | BioRad |
| Pump | KNF Lab |
| Rocking platform | VWR |
| Rotating wheel | University workshop, GLW |
| Semi-dry Western blot system | Bio-Rad |
| Spectrophotometer | Pharmacia Biotech |
| Stirrer with Heating Block | AKM LAB |
| Tetrade Microscope | Zeiss |
| Thermocycler (T3) | Biometra |
| Turbo Blot system | BioRad |
| Vibrax Shaker | Ika |
| Vortex | Ika |

## 4.1.2 Chemicals

**Table 2** Chemicals used in this study

| **Chemicals** | **Manufacturer** |
|---|---|
| GeneRuler 1 kb DNA ladder | Thermo Fisher |
| GeneRuler 50 bp DNA Ladder | New England Biolabs |
| Acrylamid/bisacrylamid | Carl Roth |
| Adenine | Carl Roth |
| Agar | Formedium |
| Agarose | Sigma-Aldrich |
| Ammonium persulfate | Sigma-Aldrich |
| Ampicillin | AppliChem |
| Bacto peptone | Thermo fisher |
| Boric Acid | Carl Roth |
| Bromphenolblue | Serva |
| Carrier-DNA | Selfmade |
| cOmplete protease inhibitor, EDTA-free | Sigma-Aldrich |
| Copper sulfate | Sigma-Aldrich |
| Developer | Agfa |

| | |
|---|---|
| Disodium hydrogen phosphate | VWR |
| dNTPs | New England Biolabs |
| DTT | AppliChem |
| EDTA | Carl Roth |
| Ethanol | VWR |
| Fixer | Agfa |
| Galactose | VWR |
| Geneticin (G418) | VWR |
| Glass Beads (425-600 µm) | Sigma-Aldrich |
| Glacial acetic acid | VWR |
| Glucose | Carl Roth |
| Glycerol | VWR |
| Glycine | VWR |
| Immersion oil | Merck |
| Isopropanol | VWR |
| L-Arginine | Carl Roth |
| L-Histidine | Merck |
| Lithium acetate | Sigma-Aldrich |
| L-Isoleucine | Carl Roth |
| Liquid nitrogen | Lab filling system |
| L-Leucine | AppliChem |
| L-Lysine | Carl Roth |
| L-Methionine | Merck |
| L-Phenylalanine | Carl Roth |
| L-Threonine | AppliChem |
| L-Tryptophan | VWR |
| Methanol | VWR |
| MG132 | Sigma-Aldrich |
| Midori Green | Nippon Genetics |
| Skim milk powder | Carl Roth |
| N-ethylmaleimide | Sigma-Aldrich |
| Nocodazole | Sigma-Aldrich |
| Nourseothricin | Jena Bioscience |
| NucleoSpin Gel and PCR Clean Up | Macherey-Nagel |

| | |
|---|---|
| Omega Bio-Tek E.Z.N.A. Plasmid Kit | Omega Bio-Tek |
| PageRuler Prestained protein ladder | Thermo Fisher |
| PageRuler Plus Prestained protein ladder | Thermo Fisher |
| PEG 3015-3685 g/mol | Sigma-Aldrich |
| PureCube Co-NTA MagBeads | Cube Biotech |
| Potassium dihydrogen phosphate | VWR |
| Raffinose | Serva |
| REVERT Total protein Stain | LI-COR |
| Sodium chloride | VWR |
| Sodium dihydrogen phosphate | Merck |
| Sodium dodecyl sulfate | Serva |
| Sodium hydroxide | Merck |
| Super RX-N X-ray film | Fujifilm |
| SuperSignal West Femto | Thermo Fisher |
| SYBR Safe | Serva |
| TCA (Trichloroacetic acid) | Carl Roth |
| TCE (2,2,2-Trichlorethanol) | Sigma-Aldrich |
| TEMED | AppliChem |
| Tris | Carl Roth |
| Tryptone | Formedium |
| Uracil | Sigma-Aldrich |
| Urea | Carl Roth |
| Yeast extract | Formedium |
| Yeast nitrogen base | Formedium |
| Zinc sulfate | Merck |
| β-mercaptoethanol | Sigma-Aldrich |

### 4.1.3 Software and Websites

**Table 3** Software and websites used in this study

| **Software** | **Purpose** |
|---|---|
| AlphaFoldServer | Prediction of protein structures |
| AxioVision 4.7, Zeiss | Acquisition of Microscope images |

| | |
|---|---|
| Benchling | Plasmid construction |
| ChatGPT | Language optimization |
| ChimeraX | Presentation of protein structures |
| eLab Journal | Documentation software |
| EndNote 2021 | Citation software |
| ImageJ / Fiji | Microscope images |
| Image Lab, Bio Rad | Acquisition of TCE images |
| ImageStudio 5 | Western Blot detection |
| GraphPad Prism | Graphs |
| Microsoft office | Presentation of data |
| NEB Ligation calculator | Calculation of ligation ratios |
| NLS-mapper | NLS prediction |
| NLStradamus | NLS prediction |
| OMERO | Storage of microscope images, Visualization |
| OMERO.insight | Upload of Microscope images |
| Perplexity | Paper research |
| SIM finder | Detection of SIM like sequences |

### 4.1.4 Enzymes

**Table 4** Enzymes

| **Enzyme** | **Origin** |
|---|---|
| B7 Polymerase | Biozym |
| Dream Taq Polymerase | Thermo Fisher |
| FastAlkaline Phosphatase | Thermo Fisher |
| In-Fusion HD Cloning Kit | Takara |
| λ-phosphatase | New England Biolabs |
| LysC | Provided by AG Krüger |
| Restriction enzymes | Thermo Fisher and New England Biolabs |
| RNAse A | Omega Bio-Tek |
| S7 Fusion DNApolymerase | Mobdiag |
| T4 DNA Ligase | New England Biolabs or Thermo Fisher |
| Trypsin | Provided by AG Krüger |
| Zymolyase 20T | Carl Roth |

### 4.1.5 Antibodies

Antibodies were diluted in 4% milk in PBS. The diluted antibodies were stored at -20 °C and thawed in a water bath before use. POD antibodies were not reused.

**Table 5** Antibodies

| Target | Host | Dilution | Supplier |
|---|---|---|---|
| **Primary Antibodies** | | | |
| αHA (3F10) | Rat, monoclonal | 1:2.000 | Sigma-Aldrich |
| αHSP90 (5833) | Rabbit, polyclonal | 1:5.000 | |
| αPGK1 (22C5D8) | mouse, monoclonal | 1:5.000 | Thermo Fisher |
| αSMT3 | Rabbit, polyclonal | 1:20.000 | Laboratory collection |
| αTPI1 | Rabbit, polyclonal | 1:20.000 | Laboratory collection |
| αUb (P4D1) | Mouse, monoclonal | 1:1.000 | Santa Cruz Biotechnology |
| **Secondary Antibodies** | | | |
| αmouse Alexa Fluor 680 | goat, polyclonal | 1:5.000 | Thermo Fisher |
| αmouse Alexa Fluor+ 800 | goat, polyclonal | 1:5.000 | Abcam |
| αmouse POD | goat, polyclonal | 1:5.000 | Sigma-Aldrich |
| αrabbit Alexa Fluor + | goat, polyclonal | 1:5.000 | Thermo Fisher |
| αrabbit POD | donkey, polyclonal | 1:5.000 | VWR |
| αrat Alexa Fluor 680 | goat, polyclonal | 1:5.000 | Santa Cruz |
| αrat DyLight 800 | rabbit, polyclonal | 1:5.000 | Biotechnology |
| αrat- POD | goat, polyclonal | 1:5.000 | Thermo Fisher |

### 4.1.6 Yeast Strains

**Table 6** Laboratory yeast strains used in this study

| Strain Name & Stock Number | Relevant Genotype | Source |
|---|---|---|
| kMY38 (13) | *trp5-27,* Matα | Laboratory collection |
| kMY39 (14) | *trp5-27,* Mata | Laboratory collection |
| JD47-13C (188) | *ADE2 leu2-3,112 lys2-801 his3Δ200 trp1Δ63 ura3-52*, Mata | Laboratory collection |
| GSY154 (1331) | wild-type to GSY203t; URA3 *leu2 trp1 his3 ade2*, Matα | K. Stade |
| GSY203 (1333) | *srp1-49 (ts)*; URA3 *leu2 trp1 his3 ade2* | K. Stade |
| yKU5 (2073) | *NIS1-6HA*::*klTRP1*, Mata | Laboratory collection |
| yKU25-2A (2083) | *uba2-ts* (from the sul screen), Mata | Laboratory collection |
| yKU87 (2169) | *slx5Δ*::*TRP1*, Mata | Laboratory collection |
| yKU148 (2172) | *slx5Δ*::*TRP1*, Matalpha | Laboratory collection |
| ySP2 (3993) | *slx5Δ*::*TRP1 slx8Δ*::*kanMX4*, Mata | Laboratory collection |
| ySP104-1 (4628) | *8HIS-smt3*$^{KallR-I96R}$::*kanMX4*, Mata | Laboratory collection |
| ySP103-1 (4627) | *smt3*$^{KallR}$::*kanMX4*, Mata | Laboratory collection |
| yLA13 (4997) | $P_{GPD}$*GFP-NIS1::LEU2*, Mata | Laboratory collection |
| yLA17 (5001) | $P_{GPD}$*GFP-NIS1::LEU2* $P_{GAL1}$ *SLX5::kanMX4* $P_{GAL1}$ *SLX8::HIS3*, Mata | Laboratory collection |

**Table 7** Yeast strains produced in this study

| Strain name & stock number | Relevant Genotype |
|---|---|
| yFP2 (4421) | *NIS1-6HA::klTRP1* (Mata) |
| yFP14 (4433) | $P_{GAL1}$*SLX5::KanMX* $P_{GAL1}$*SLX8::HIS3* (Matα) |

| | |
|---|---|
| yFP21 (4532) | *NIS1-6HA::klTRP1* $P_{GAL1}$*SLX5::KanMX* $P_{GAL1}$*SLX8::HIS3* (Mata) |
| yFP23 (4562) | *8HIS-SMT3::kanMX* (Mata) |
| yFP24 (4563) | *8HIS-SMT3::kanMX NIS1-6HA::klTRP1* (Mata) |
| yFP28 (4567) | *nba1∆::kanMX NIS1-6HA::TRP1* (Mata) |
| yFP45 (4610) | *NIS1*-Neongreen::klTRP1 (Mata) |
| yFP47 (4612) | *NIS1*-Neongreen::klTRP1 *nba1∆::kanMX* (Mata) |
| yFP55 (4727) | $P_{CUP1}$*FLAG-neongreen-8HIS::LEU2* (Mata) |
| yFP56 (4728) | $P_{CUP1}$*FLAG-neongreen-NIS1-CT (358-407)-8HIS::LEU2* (Mata) |
| yFP80 (4824) | $P_{CUP1}$*FLAG-neongreen-nis1∆8-CT (358-399)-8HIS::LEU2* (Mata) |
| yFP81 (4825) | $P_{CUP1}$*FLAG-neongreen-nis1∆17-CT (358-390)-8HIS::LEU2* (Mata) |
| yFP83 (4827) | $P_{CUP1}$*FLAG-neongreen-nis1SIMonly* (391-399)*-8HIS::LEU2* (Mata) |
| yFP84 (4828) | $P_{CUP1}$*FLAG-neongreen-nis1 17AA-cterminus(390-307)-8HIS::LEU2* (Mata) |
| yFP105 (4987) | *NIS1-6HA::nat* (Mata) |
| yFP167 (5249) | $P_{GPD}$*yeGFP-FIR1-HA::LEU2* (Mata) |
| yFP168 (5250) | $P_{GAL1}$*SLX5::KanMX* $P_{GAL1}$*SLX8::HIS3* $P_{GPD}$yeGFP-FIR1-HA::LEU2 (Mata) |
| yFP169 (5251) | *slx5Δ::klTRP1* $P_{GPD}$*yeGFP-FIR1*-HA::LEU2 (Matα) |
| yFP172 (5254) | $P_{GPD}$*yeGFP-fir1-I360K-HA::LEU2* (Mata) |
| yFP173 (5255) | $P_{GAL1}$*SLX5::KanMX* $P_{GAL1}$*SLX8::HIS3* $P_{GPD}$*yeGFP-fir1*$^{I360K}$*HA::LEU2* (Mata) |
| yFP174 (5256) | *slx5Δ::klTRP1* $P_{GPD}$*yeGFP-fir1*$^{I360K}$*-HA::LEU2* (Matα) |
| yFP211 (5445) | $P_{CUP1}$*-SOD2-2HA::LEU2* (Mata) |
| yFP212 (5446) | *slx5Δ::klTRP1* $P_{CUP1}$*-SOD2-2HA::LEU2* (Matα) |
| yFP215 (5449) | $P_{CUP1}$-Pam16-2HA::LEU (Mata) |
| yFP216 (5450) | *slx5Δ::klTRP1* $P_{CUP1}$*Pam16-2HA::LEU2* (Matα) |
| yFP217 (5451) | $P_{CUP1}$*YBR053C-2HA::LEU2* (Mata) |

| | |
|---|---|
| yFP223 (5457) | $P_{GAL1}$*SLX5::KanMX* $P_{GAL1}$*SLX8::HIS3* $P_{CUP1}$*-SOD2-2HA::LEU2* (Mata) |
| yFP224 (5458) | $P_{GAL1}$*SLX5::KanMX* $P_{GAL1}$*SLX8::HIS3* $P_{CUP1}$-YBR053C-2HA::LEU (Mata) |
| yFP237 (5471) | *smt3*$^{KallR}$*::KanMX* $P_{GPD}$*yeGFP-FIR1-HA::LEU2* (Mata) |
| yFP238 (5472) | *uba2-ts* $P_{GPD}$*yeGFP-FIR1-HA::LEU2* (Mata) |

## 4.1.7 Plasmids

**Table 8** Plasmids cloned during this study

| **Strain Name & Stock Number** | **Insert** | **Cloning Details** |
|---|---|---|
| pFP3 (4690) | $P_{SMT3}$*-8HIS-SMT3-* $T_{SMT3}$(part1) $T_{ADH1}$ kanMX4 $T_{SMT3}$(part2) | **Backbone**: pSP60, **Insert**: PCR onto Genomic extract with F5509 & FP5510 |
| pFP5 (4744) | *NIS1(243-407) neongreen* $T_{CDC12}$::klTRP $T_{NIS1}$(474 bp) | **Backbone:** pYM3-mNG (SacI & SacII) **Insert**: PCR1: FP5333 & FP5334 Nis1 (SalI & HindIII) PCR2: FP5335 & FP5336 $T_{NIS1}$ (SacI & SacII) |
| pFP7 (4746) | $P_{NBA1}$ kanMX4 $T_{NBA1}$ | **Backbone:** pUC21 **Insert**: PCR onto Genomic extract from Euroscarf *nba1Δ* *Primers: FP5462 & 5463* |
| pFP8 (4747) | *NIS1(243-407) neongreen* $T_{CDC12}$::*nat* $T_{NIS1}$(474 bp) | **Backbone**: pFP5 **Insert**: nat cassette from pYM17 SalI & SacI |
| pFP10 (4749) | *NIS1(243-407) 6HA::klTRP1* $T_{NIS1}$ (474 bp) | **Backbone:** pYM3 **Insert**: FP5333 & 5536 (HindIII & SacII) onto genomic extract of *NIS1-* |

| | | |
|---|---|---|
| | | *6HA::TRP1* strain tagged through Knop et al., 1999 |
| pFP11 (4750) | *NIS1(243-407) 6HA::nat*-$T_{NIS1}$(474 bp) | **Backbone:** pFP10<br>**Insert**: nat cassette from pYM17 SalI & SacI |
| pFP13 (4764) | $P_{CUP1}$ *FLAG neongreen 8HIS* $T_{CYC1}$::*LEU2* | **Backbone:** pFP14, Digest with BglII & NcoI, CloneJet Blunting reaction, Religation |
| pFP14 (4765) | $P_{CUP1}$ *FLAG-Neongreen-NIS1-CT 55AA(358-407)-8HIS* $T_{CYC1}$::*LEU2* | **Backbone**: pLD20 (HindIII & XmaI)<br>**Inserts:**<br>PCR 1: FP5663& FP5664 (HindIII & BglII) onto neongreen<br>PCR 2: FP5665 & FP5666 (BglII & XmaI) onto Nis1 |
| pFP15 (4766) | $P_{CUP1}$ *FLAG-Neongreen-NIS1-cterminusΔ17-(358-390)-8HIS* $T_{CYC1}$::*LEU2* | **Backbone:** pFP14, Digest with BglII & NcoI<br>**Insert**: PCR FP5665 &FP5771 |
| pFP24 (4848) | $P_{CUP1}$ FLAG-Neongreen-NIS1-cterminus17AA (390-407) 8HIS $T_{CYC1}$::LEU2 | **Backbone:** pFP14, Digest with BglII & NcoI<br>**Insert**: PCR FP5854 &FP5666 |
| pFP25 (4849) | $P_{CUP1}$ FLAG-Neongreen-NIS1-cterminus-Δ8 (358-399)-8HIS $T_{CYC1}$::LEU2 | **Backbone:** pFP14, Digest with BglII & NcoI<br>**Insert**: PCR FP5665 &FP5855 |
| pFP26 (4850) | $P_{CUP1}$ FLAG-Neongreen-NIS1-cterminus-SIM (358-399)-8HIS $T_{CYC1}$::LEU2 | **Backbone:** pFP14, Digest with BglII & NcoI<br>**Insert**: Oligoduplex FP5852 & FP5853 |
| pFP43 (5156) | $P_{GPD}$-yeGFP-Fir1-HA-$T_{CYC1}$ | **Backbone**: pFP14<br>**Insert**: Assembly PCR with PCR 1) FP6312 & FP6313 onto pYM-N17 |

| | | |
|---|---|---|
| | | PCR 2) FP6318 & FP6319 onto Gen. Extr.<br>**Restriction Sites:** BamHI/BglII & XmaI |
| pFP45 (5158) | $P_{GPD}$ -yeGFP-*fir1I360K*-HA-$T_{CYC1}$ | **Base vector**: pFP43<br>**Insert**: Assembly PCR with PCR 1) FP6318 & FP6322 Gen. Extr.<br>PCR 2) FP6321 & FP6319 onto Gen. Extr.<br>**Restriction Sites:** KpnI & XmaI |
| pFP54 (5225) | $P_{CUP1}$*SOD2-2HA::LEU2* | **Backbone:** pLA10, Digest with HindIII & KpnI<br>**Insert**: PCR FP6422 & FP6423 onto genomic extract |
| pFP56 (5227) | $P_{CUP1}$ *PAM16-2HA::LEU2* | **Backbone:** pLA10, Digest with AgeI & KpnI<br>**Insert**: PCR FP6426 & FP6427 onto genomic extract |
| pFP57 (5228) | $P_{CUP1}$*YBR053C-2HA::LEU2* | **Backbone:** pLA10, Digest with HindIII & KpnI<br>**Insert**: PCR FP6428 & FP6429 onto genomic extract |

**Table 9** Plasmids from the laboratory collection

| **Strain Name & Stock Number** | **Relevant Genotype** | **Source** |
|---|---|---|
| pKU103 (1847) | $P_{GAL1}$HIS6-Ub-$T_{CYC1}$::URA3 (CEN) | Laboratory collection |
| pLA6 (4899) | $P_{GPD}$*yeGFP-NIS1::LEU2* | Laboratory collection |
| pMM86(2451) | $P_{GAL1}$*mCherry-SMT3*:: URA3 | Laboratory collection |
| pRB240 (379) | $P_{CUP1}$mycUB (in YEPLAC195) | Laboratory collection |
| yEPLAC195 (203) | *URA3* 2 µM | Laboratory collection |

## 4.1.8 Primers

Primers were obtained from Integrated DNA technology (IDT). Dry primers were resuspended in Milipore water to a final concentration of 100 µM.

**Table 10** Primers

| Name | Sequence 5' -> 3' | Purpose |
|---|---|---|
| M13FOR | TGTAAAACGACGGCCAGT | Sequencing primer |
| M13REV | CAGGAAACAGCTATGACCATG | Sequencing primer |
| $P_{CUP1}$FOR (JD5185) | CTCCTTGTCTTGTATCAATTGC | Sequencing primer |
| $T_{CYC1}$REV | TCGTTTCTGTCTTTTTC | Sequencing primer |
| JD5156 | GATGCTGTCGCCGAAGAAGTTAAG | Sequencing primer |
| KU973 | ATACCCGACAGTCAAGACGATAGTATACTTAGTAGCGACCCCTTTCGTACGCTGCAGGTCGAC | S2-primer (Knop et al. 1999); NIS1 |
| KU974 | TCTAAGGCTATGCAATGGCTATGCAATCCAGGGGGGGTTACCTACATCGATGAATTCGAGCTCG | S3 primer, Knop et al., 1999); NIS1 |
| FP5455 | CCCGACAGTCAAGACGATAGTATACTTAGTAGCGAC CCCTTTAGTAAAGGAGAAGAACTT | Longtine, pFA6a-GFP-TRP1, for |
| FP5456 | TAAGGCTATGCAATGGCTATGCAATCCAGGGGGGGT TACCTACCTATTTCTTAGCATTTT | Longtine, pFA6a-GFP-TRP1, rev |
| FP5457 | GTAGGTAACCCCCCCTGGATTGCAT | *NIS1*-DS, for |
| FP5458 | TCTAGAGGATCCCCGGGTACCGTACTGGTCATACAA AGCTCTTAA | *NIS1*-DS, rev |
| FP5462 | CGCGCGGCCGCCCATCCCCTGTTTCTTGGTTACTAC | Euroscarf, *nba1Δ*, for |

| | | |
|---|---|---|
| FP5463 | GCGGCGGCCGCGGAGACGGACTTGCTGCTATC TGGG | Euroscarf, *nba1Δ*, rev |
| FP5509 | CAGTGAATTCGAGCTCGGATGGTCACGTTTTTG CCGCCGAA | $P_{SMT3}$, for |
| FP5510 | TAAGAGTCCTAATACGTAGCACCACCAATCTG | *SMT3*, rev |
| FP5533 | CGCAAGCTTAGTCGTCCACCGTATCTAAGGAAC | *NIS1*-CT, for |
| FP5534 | ACCCTTAGAAACCATGTCGACAAAGGGGTCGCT ACTAAGTATACT | *NIS1*-CT, rev |
| FP5535 | TTCTGGCCTCGAGGCGAGCTCGTAGGTAACCCC CCCTGGATTGCA | *NIS1*-DS, for |
| FP5536 | CGCCCGCGGTCTTAATCTCAGATGTGGATGCAG | *NIS1*-DS, rev |
| FP5663 | GCGAAGCTTATGGACTACAAAGACGATGACGAC AAGATGGTTTCTAAGGGTGAAGAAGAC | HindIII-FLAG-NG, for |
| FP5664 | CGCAGATCTCTTGTACAATTCGTCCATACCCATAA CGTC | NG-BglII, rev |
| FP5665 | CGCAGATCTAGCTCTGTCTGCTCTTCTAACGCCA GCGACTTAG | BglII-Nis1-CT, for |
| FP5666 | ATACCCGGGCTAGTGGTGATGGTGATGATGGTG GTGCCATGGAAAGGGGTCGCTACTAAG | *NIS1*-CT-NcoI-*8HIS*-XmaI, rev |
| FP5771 | CGCCCATGGAGGATTGCTTTTGGT | *nis1Δ17*, rev |
| FP5852 | GATCTATAATTATACCCGACAGTCAAGACGATC | Oligoduplex *NIS1* SIM, for |
| FP5853 | CATGGATCGTCTTGACTGTCGGGTATAATTATA | Oligoduplex *NIS1* SIM, rev |
| FP5854 | CGCAGATCTATAATTATACCCGACAGTCAA | 17 AA von *NIS1* CT, for |
| FP5855 | CGCCCATGGATCGTCTTGACTGTCGGGTA | *nis1Δ8*, rev |
| FP6312 | AGATTGCGCTGGGATAGATCTGAAGCTTTTTTTC CGATTATGCAGTTTATCATTATCAAT | *FIR1* S1 für PgpdyeGFP |
| FP6313 | TGTACTGCACACTTTGCTCTTGACAGGTGTAACA GGGAGGCTTTTGTACAATTCATCCAT | *FIR1* S4 für $P_{GPD}$yeGFP |
| FP6314 | GATCGACTGTAATGATTTTGA | *FIR1*Verification Primer |
| FP6315 | AGCCTCCCTGTTACACCTGTC | *FIR1*, for |

| | | |
|---|---|---|
| FP6316 | AGACCCGGGTCAAGCGTAATCTGGAACATCGTA GGGGTATTTTAGTTTGCGATGAGATGG | *FIR1*, rev |
| FP6318 | AGCCTCCCTGTTACACCTGTC | *FIR1*Start |
| FP6319 | AGACCCGGGTCAAGCGTAATCTGGAACATCGTA GG GGTATTTTAGTTTGCGATGAGATGG | *FIR1*-HA XmaI, rev |
| FP6321 | ATACCCGGGTTATTTTAGTTTGCGATGAGATGG | *FIR1*-XmaI, rev |
| FP6322 | AAAATGGTTGAGGTTAAGCTTTTAGATGAGGATG AA | *fir1*$^{I360K}$, for |
| FP6422 | AGAAAGCTTATGTTCGCGAAAACAGCA | *SOD2* for |
| FP6423 | ATAGGTACCTGATCTTGCCAGCATCGAATCT | *SOD2* rev |
| FP6426 | AGAACCGGTATGGCTCACAGGGCTTTCATA | *PAM16* for |
| FP6427 | AGAGGTACCTCTGATTGCTGCTTGCACTATT | *PAM16* rev |
| FP6428 | AGAAAGCTTATGAGTAGTGTTGGCGATTTT | *YBR053C* for |
| FP6429 | ATAGGTACCTGTGGAGAGGTTGTCGCTTTGT | *YBR053C* rev |

# 4.2 Methods

## 4.2.1 Growth Media

Yeast cultures were grown in **Y**east **P**eptone medium (YP), or if constant selection was required, in **S**ynthetic **D**efined medium (SD). As a carbon source glucose, galactose or raffinose were used at a concentration of 2%. Under standard conditions yeast was grown in YP-Glucose medium. Otherwise, the used medium is indicated in the figure legend. *E. coli* cultures were incubated in LB medium and if selection was required LB with 1 µg/ml ampicillin. For plates, 20 g/l agar was added.

**Table 11** Composition of Synthetic defined medium

| Component | Amount |
|---|---|
| Carbon source | 20 g/l |
| Yeast nitrogen base | 6.7 g/l |
| Isoleucine, Leucine, Phenylalanine | 60 mg/l |
| Threonine | 50 mg/l |
| Lysine, Tryptophan, Uracil | 40 mg/l |
| Adenine, Arginine | 20 mg/l |
| Histidine, Methionine | 10 mg/l |

**Table 12** Composition of YP-medium

| Component | Amount |
|---|---|
| Bacto peptone | 20 g/l |
| Yeast extract | 10 g/l |
| Carbon source | 20 g/l |

**Table 13** Composition of LB-medium

| Component | Amount |
|---|---|
| NaCl | 10 g/l |
| Trypton | 10 g/l |
| Yeast extract | 5 g/l |

### 4.2.2 Extraction of Yeast Genomic DNA

Genomic extracts of yeast strains were used as a template for PCR. To extract genomic DNA from yeast, cells were first grown into log phase and then treated with zymolyase to produce spheroplasts. After spheroplasting, the protocol continues using the Wizard Genomic DNA purification Kit from Promega.

At first the desired strain was precultured overnight in 3 ml YP-Glucose and then diluted to an $OD_{600}$ of 0.3 in 10 ml YP-Glucose. The cells were grown into log-phase ($0.5<OD_{600}<1.0$). Then, the culture was centrifuged using a 15 ml falcon tube at 3,000 g using the Allegra X-22R. The supernatant was discarded, and the cells were resuspended in 15 ml 0.1 M Tris-HCl with 10 mM DTT (pH 9.4) followed by 25 min incubation at 30 °C. Then, the culture was centrifuged again for 5 min at 3,000 g and the supernatant was discarded. Next, the cells were resuspended in 10 ml 1.2 M sorbitol with 20 mM potassium phosphate, 0.5 mM MgCl (pH 7.4) and 375 U/ml zymolyase 20 T were freshly added. The cells were incubated for 20 min at 30 °C. After this incubation, the culture was examined under the brightfield microscope for formation of spheroplasts. When most of the cells had formed spheroplasts, the culture was harvested by centrifuging 5 min at 3,000 g. The pelleted yeast was then transferred to a microcentrifuge tube using the nuclei lysis solution from the Wizard Genomic DNA purification kit from Promega. The following steps were then performed according to the user manual of the Wizard kit.

### 4.2.3 Polymerase Chain Reaction

**P**olymerase **C**hain **R**eactions (PCRs) were performed for different purposes such as cloning or strain verification. The protocol was adapted for each individual PCR depending on the purpose. When the PCR product was generated for cloning, the S7 Fusion polymerase from Mobidiag or the B7 polymerase from Biozym were used. To verify generated yeast strains or *E. coli* colonies, the DreamTaq polymerase from Thermo Fisher was used. For yeast colony PCRs (cPCR), cells were streaked out and grown overnight at 30 °C. From the fresh streak out a sesame seed amount of cells was resuspended in 1 µl MPW and boiled for 5 min. For an *E. coli* colony PCR, a colony was picked and resuspended in 1 µl MPW and was immediately used as a template. The PCR mix was prepared as displayed in Table 14 and the PCR program was set as reported in Table 15.

**Table 14** PCR Mix

| | **S7 Polymerase** | **B7 Polymerase** | **DreamTaq** |
|---|---|---|---|
| 5x or 10x Buffer | 10 µl | 10 µl | 2 µl |
| 20 mM dNTPS | 1 µl | - | 0.4 µl |
| Primer for (100 µM) | 0.5 µl | 0.2 µl | 0.2 µl |
| Primer rev (100 µM) | 0.5 µl | 0.2 µl | 0.2 µl |
| Polymerase | 0.5 µl | 0.5 µl | 0.2 µl |
| Genomic extract/ Plasmid | 1 µl / 0.25 µl | 1 µl / 0.25 µl | 1 µl MPW + cells |
| MPW | Up to 50 µl | Up to 50 µl | Up to 20 µl |

**Table 15** PCR cycler program

| | **S7 Polymerase** | | **B7 Polymerase** | | **cPCR** | |
|---|---|---|---|---|---|---|
| Initial denaturation | 98 °C | 30 s | 95 °C | 60 s | 95 °C | 3 min |
| Denaturation | 98 °C | 10 s | 98 °C | 15 s | 95 °C | 30 s |
| Annealing | $T_m$-5 °C | 30 s | $T_m$-5 °C | 15 s | $T_m$-5 °C | 30 s |
| Extension | 72 °C | 30 s/kb | 72 °C | 30 s/kb | 72 °C | 60 s/kb |
| Cooling | 4 °C | ∞ | 4 °C | ∞ | 4 °C | ∞ |

## 4.2.4 Gel Electrophoresis

To verify PCRs or restrictions digests, DNA fragments were separated by size using agarose gels. Gels contained between 0.6% and 2 % agarose in TAE buffer dependent on the size of the DNA fragment. Lower agarose concentrations (0.6%) were used for restriction digests of plasmids and higher percentages (1%-2%) for PCR fragments. The agarose was heated in the microwave until it was completely dissolved in TAE buffer. The hot agarose solution was poured into a casting stand, and a DNA stain was added. As a DNA stain either SYBR safe from Invitrogen (3 µl) or Midori green from Nippon Genetics(2 µl) was added to the liquid agarose. After the gel solidified, the samples were loaded, the gel was submerged in TAE buffer, and the DNA was

separated at 120 V for 15 to 30 minutes. To estimate the size of the DNA fragments 7.5 µl of a size standard were loaded. Here, either the 1 kb GeneRuler or 100 bp GeneRuler from Thermo Fisher were used. The gel was examined using the FastGene FAS-DIGI Pro from Nippon genetics. If the DNA was required for further processes such as cloning, the DNA was cut with a scalpel from the gel using a blue light reader.

### 4.2.5 Restriction Digests

Restriction digests were used to prepare DNA for cloning and to obtain DNA cassettes for yeast transformation. Digests were performed at 37 °C using 1 µl of the desired restriction enzyme and the buffer provided by the manufacturer. For digestion of plasmids 1 µl FastAP (Thermo Fisher) was added to avoid religation. The digests were either heat inactivated according to the manufacturers protocol or cleaned up using the Machery-Nagel PCR clean up and Gel Extraction Kit.

### 4.2.6 Ligation

Ligations were performed using the Thermo Fisher T4-Ligase or the NEB T4-Ligase using the respective buffers provided by the manufacturer. For two-part ligations a backbone-to-insert ratio of 1:3 was used and for three-part ligations backbone-to-insert ratio of 1:5:5. The ratios were calculated using the NEB ligation calculator and DNA concentrations were measured using the NanoDrop from Thermo Fisher. A ligation control omitting the insert was always included. The ligation either was performed for 1-2 h at room temperature or overnight at 4 °C.

**Table 16** Ligation Mix

| **Component** | **Amount** |
|---|---|
| Backbone | 100-150 ng |
| Insert | *Calculated based on size of insert and backbone* |
| T4-Buffer | 2 µl |
| T4-Ligase | 1 µl |
| MPW | Up to 20 µl |

### 4.2.7 *E. coli* Transformation

For cloning and maintenance of plasmids, the DNA was transformed into *E. coli*. 100 µl of chemically competent XL1 Blue cells were thawed on ice. For retransformation of plasmids, 0.5 µl plasmid were added and for cloning 10 µl of the ligation mix were added. The mixture was incubated for 10 min on ice. Then, the cells were heat shocked for 45 s at 42 °C followed by a short incubation on ice, where 1 ml LB-Amp was added. Then the cells were incubated for 25 min at 37 °C. Lastly, the cells were pelleted and the supernatant discarded, whereas the pellet was resuspended in 100 µl MPW and plated on LB-Amp plates. The plates were incubated overnight at 37 °C or over the weekend at room temperature.

### 4.2.8 Plasmid Isolation

To isolate plasmids from *E. coli*, the cells were grown in ml LB medium containing 1 µg/ml ampicillin over night at 37 °C. The isolation was performed using the E.Z.N.A.® Plasmid Mini Kit I from Omega according to the manufacturers' protocol.

### 4.2.9 DNA Sequencing

To sequence plasmids, the LightRun sequencing service from Eurofins Genomics was used. The plasmids were sent in microcentrifuge tubes according to Table 17.

**Table 17** Sequencing mix

| Component | Amount |
|---|---|
| Plasmid | 250-500 ng |
| Primer (100 µM) | 1 µl |
| MPW | up to 10 µl |

### 4.2.10 Yeast transformation

Yeast strains were transformed using the lithium acetate method (Gietz & Schiestl, 2007). Strains were grown overnight at 30 °C in YP-glucose. Day cultures were inoculated at $OD_{600}$ 0.25 in YP-glucose and grown into log-phase. Cells were harvested at 1,900 rpm for 5 min. Then, the cells were resuspended in MPW, transferred into a microcentrifuge tube and washed twice with MPW. The transformation mix was

prepared according to Table 18. The cells were resuspended in 100 µl MPW and added to the transformation mix. After 25 min at 30 °C and 20 min at 42 °C the cells were streaked out on selective agar plates. When a cassette with antibiotic resistance was transformed, the mix was added to 5 ml YP-glucose and incubated at 25 °C overnight. After the overnight incubation, the culture was pelleted and streaked out on YP-glucose plates containing the antibiotic.

**Table 18** Transformation mix

| Component | Amount |
|---|---|
| 50% PEG 3350 | 240 µl |
| 1 M Lithium acetate | 35 µl |
| Ct-DNA | 2.5 µl |
| 2µ plasmid / CEN plasmid/ digested integration cassette/ PCR | 1 µl / 1 µl / 10 µl / 50 µl |

### 4.2.11 Crossing, Sporulation and Tetrad Dissection of *S. cerevisiae*

To obtain new combinations of existing yeast strains, two yeast strains were crossed, the resulting diploids were forced to sporulate, and tetrad dissections were performed. First, two strains with the mating types Mata and Matα, and with different auxotrophic markers, were streaked out against each other on YP-glucose plates and grown at 30 °C for one day. Then, the plate was stamped onto selective plates using an autoclaved velvet cloth. Importantly, the selective plate was deficient in two different amino acids whose production was specific for each one of the strains to select for diploids. The plate was incubated at 30 °C for 1-2 days. Next, single colonies were picked and streaked out on a selective plate. After 1-2 days at 30 °C, the diploid cells were used to inoculate 2 ml of sporulation medium containing amino acids as well as 0.005% zinc sulfate and 1% potassium acetate. The cells were then incubated in a glass tube at 25 °C for 5 days. The lack of nutrients causes the diploid cells to sporulate and form tetrads (Neiman, 2011). After the incubation period, the cells were examined for tetrads using a bright field microscope. When enough diploids sporulated and formed tetrads, 100 µl of cells were treated with zymolyase for ten minutes at room temperature. Since zymolyase is highly efficient, a pipette tip was dipped into the lid of

the tube and then resuspended in the microcentrifuge tube with the cells. Zymolyase digests the sporulation sack and after 10 min incubation at room temperature, 25 µl of the digest were pipetted onto a YP-glucose plate with tetrad agar. The tetrads were dissected using a microscope with a micromanipulator. After dissection, the plate was incubated for 3 days at 30 °C. Then the colonies of the tetrads were picked, streaked out on YP-glucose plates and incubated for 1 day at 30 °C. Lastly, the YP-glucose plate was stamped onto different plates either deficient in an auxotrophic marker or with addition of an selective antibiotic that was present in one of the strains. The growth on those plates was investigated after 2 days at 30 °C, to analyze the genotype of the new spore clones. Next, a mating type test was performed to determine the mating type of the new spore clones. As mating type testers, the strains KMY38 (Matα) and KMY39 (Mata) were used.

### 4.2.12 Preparation of Glycerol Stocks

To preserve newly generated yeast strains, they were frozen in glycerol stocks. Glycerol stocks were stored at -80 °C in a final concentration of 15% glycerol. For yeast stocks, cells were streaked out on YP-Glucose plates freshly, or if required on selective SD plates and grown for 1-2 days at 30 °C. Then the yeast was scraped from the plate using a sterile toothpick and resuspended in 1 ml 15% glycerol. For *E. coli* stocks, 3 ml LB-Amp were inoculated overnight at 37 °C. Of the overnight culture 800 µl were added to 200 µl 75% glycerol.

### 4.2.13 Yeast Cell Treatments

Cultivation of liquid yeast cultures was routinely done for every experiment where yeast cells in the logarithmic phase were required. This was the case for most experiments that generated direct data output. For most experiments, cells were precultured in 3 ml medium in glass tubes overnight at 30 °C. Then the optical density was measured at 600 nm ($OD_{600}$), and cells were inoculated at $OD_{600}$ 0.25 in glass tubes or flasks. Day cultures were grown into log phase, which was reached after 3 h to 7 h of incubation depending on the strain and the medium.

To induce or shut off genes under the *GAL1* promoter, cells were precultured in medium containing raffinose. Raffinose neither induces nor shuts off the *GAL1* promoter (Peng et al., 2015). Thereby raffinose ensures a swift regulation of the

promoter when replaced with glucose or galactose. After the preculture, cells were incubated in galactose-containing medium to induce the expression of the desired gene and in parallel in glucose-containing medium to shut off the transcription of the gene. For galactose inductions all strains were harvested at the same time which was 4 to 5 h after inoculation of the culture. To induce the transcription of genes under the *CUP1* promoter, copper sulfate ($CuSO_4$) was added to the main culture. Copper induction was performed by adding sterile filtered 100 mM $CuSO_4$ in $H_2O$ to a final concentration of 100 µM. Cells were harvested or examined under the microscope 4 hours after induction with copper.

For heat-sensitive strains, the preculture as well as all plates were incubated at 25 °C. The main culture was then shifted to permissive temperature, either 30 °C or 37 °C. To examine strains after heat stress, the main culture was grown for 4 h at 30 °C and then shifted to 42 °C for 45 min followed by immediate harvesting. In a similar manner, treatment with oxidative stress was performed. The main culture grew for 4 h, if necessary with addition of $CuSO_4$. Then, 100 mM $H_2O_2$ was added to the culture to a final concentration of 200 µM.

For cell cycle arrests, the main culture was grown for 2-3 h at 30 °C. Afterwards, the cell cycle arresting chemical was added followed by further incubation for 2 h. Hydroxyurea arrests were performed using 100 µM hydroxyurea while nocodazoles arrests were performed with 15 µg/ml nocodazole.

### 4.2.14 Yeast Lysis Methods

Different yeast lysis methods were performed depending on the application or the size of the protein. For the individual experiments, the performed lysis is indicated in the figure legends. As a standard lysis the samples were boiled in Laemmli buffer, this lysis is also referred to as boiled lysis (Laemmli, 1970). The postalkaline lysis was performed to enhance the extraction of large proteins (Kushnirov, 2000). The glass bead lysis was usually chosen, if the extraction under native conditions was required, whereas the JUNQ lysis was chosen to optimize the extraction of aggregates (Rolli et al., 2024). As a loading buffer Laemmli buffer was used (Table 19).

**Table 19** Composition of Laemmli Buffer

| Component | Amount for 50 ml |
|---|---|
| 0.3125 M Tris-HCl (pH 6.8) | 15.625 ml of 1M stock |
| 10% SDS | 5 g |
| 50% Glycerol | 25 ml |
| Bromophenol blue | Until a dark blue color is reached |
| MPW | To 50 ml |
| [10% β-mercaptoethanol] | Added individually |

#### 4.2.14.1 Boiled Lysis

For the boiled lysis, yeast cells were resuspended in 1x Laemmli buffer (Table 19) at a concentration of 50 µl/$OD_{600}$. The samples were boiled for 5 min at 95 °C and stored at -20 °C.

#### 4.2.14.2 Postalkaline Lysis

For the postalkaline lysis, yeast cells corresponding to 5 $OD_{600}$ of yeast were harvested. The cells were resuspended in 200 µl MPW and 200 µl 0.2 M NaOH were added. Next, the mixture was incubated for 5 min at room temperature. Then the cells were centrifuged for 8 s, and the supernatant was removed. Lastly, the cells were resuspended in 100 µl 1x Laemmli buffer and boiled 5 min at 95 °C. This treatment was mostly used for proteins over 100 kDa (Kushnirov, 2000).

#### 4.2.14.3 Glass Bead Lysis

The native glass bead lysis was performed in a microcentrifuge tube. Cells were resuspended in 15 µl/$OD_{600}$ native lysis buffer (Table 20). The cells were incubated 10 minutes on ice and 50% w/v glass beads were added. Then the microcentrifuge tube was put into the vibrax and vigorously shaken 5 min. Next, the tubes were transferred to a precooled centrifuge set at 30,000 rcf for 15 min. After the centrifugation, the supernatants were transferred into a fresh tube and then subjected to the desired treatment. To stop any reaction, 5x Laemmli sample buffer was added to a final concentration of 1x Laemmli. After addition of the Laemmli buffer the samples were boiled for 5 min at 95 °C and subsequently stored at -20 °C.

#### 4.2.14.4 JUNQ Lysis

The JUNQ lysis was performed according to the lysis performed by Rolli et al., who employed this lysis to investigate JUNQs (Rolli et al., 2024). Here, cells were harvested and then resuspended in 15 µl/$OD_{600}$ urea buffer (Table 20). The cells were lysed by adding 50% w/v glass beads followed by 5 min vigorously shaking in the vibrax. Then, 20% SDS was added to a final concentration of 4%. The samples were incubated at 65 °C for 5 minutes followed by 10 minutes centrifugation at 30,000 rcf. Supernatants were transferred into fresh tubes and 5x Laemmli was added to a final concentration of 1x.

**Table 20** Composition of different lysis buffers

| Native lysis buffer | Urea buffer | Mass Spec. urea buffer |
|---|---|---|
| 150 mM NaCl | 8 M Urea | 8 M Urea |
| 50 mM Tris-HCl, pH7.4 | 100 mM $NaH_2PO_4$ | 100 mM NaH2PO4 |
| 10% Glycerol | 10 mM Tris | 10 mM Tris |
| [1x cOmplete protease inhibitor] | | 4% SDS |

### 4.2.15 λ -Phosphatase Treatment

To examine the phosphorylation of proteins, a dephosphorylation assay was performed. First, the desired cells were cultured as described in chapter 4.2.13 and then a glass bead lysis using native lysis buffer was performed as described in chapter 4.2.14.3. The supernatant of the glass bead lysis was transferred into a fresh tube on ice. Then the supernatant was split into three 40 µl samples. The first sample was immediately supplied with 1x Laemmli buffer and boiled for 5 min at 95 °C. Then the control sample and the λ-phosphatase sample were prepared on ice. 40 µl of the supernatant were transferred into a fresh tube. For both samples 5 µl PMP buffer (from the manufacturer of the λ-phosphatase) and 5 µl $MnCl_2$ were added. To the phosphatase sample, 1.5 µl of λ-phosphatase (NEB) were added which were omitted from the control sample. Then both samples were incubated for 45 min at 30 °C, during which the λ-phosphatase removed phosphorylation from the proteins. After the incubation, 10 µl 5x Laemmli were added to the samples. After 5 min at 95 °C the samples were stored at -20 °C.

### 4.2.16 HIS-Pulldown

To demonstrate the ubiquitylation and SUMOylation of proteins, HIS-ubiquitin and HIS-SUMO pulldowns were employed. Prior to the HIS pulldown, samples containing between 120 and 200 $OD_{600}$ were lysed in 8 M urea buffer pH 8.0 (Table 20) using the glass bead lysis described in chapter 4.2.14.3. Due to the large samples volume, samples were split into multiple microcentrifuge tubes to ensure an efficient lysis. During the centrifugation step, the beads were equilibrated by washing with 5 ml 8 M urea buffer twice. After the centrifugation step, supernatants were pooled in a fresh 5 ml tube containing 50 µl equilibrated magnetic Cobalt-NTA beads (Cube Biotech). The magnetic beads were then incubated with the supernatant overnight on a spinning wheel at room temperature. During the overnight incubation, the HIS-tagged protein bound to the cobalt on the magnetic beads and with it any covalently attached proteins. In the morning, the unbound fraction was discarded, and the beads were washed twice by addition of 5 ml 8 M urea buffer pH 6.0. In the last washing step, the beads were resuspended in 1.5 ml buffer, which were then transferred to a 1.5 ml low binding tube. The washing buffer was removed, and the beads were resuspended in elution buffer (urea buffer with 500 mM imidazole, pH 7.4). The beads were incubated on a rotating wheel for 2 h. The elution was collected in a separate tube and the beads were boiled in 120 µl 1.5x Laemmli buffer. Additional, samples of 100 µl were taken after the glass bead lysis (‘input’) and of the supernatant after the overnight binding (‘unbound’). After elution, 25 µl 5x Laemmli buffer were added to all samples. The samples were boiled 5 min at 95 °C and 50 µl were loaded onto an SDS-PAGE.

### 4.2.17 SDS-PAGE and Western Blot

To evaluate the abundance of proteins, samples were analyzed by SDS-PAGE and western blot. Originally, this method was developed by U. K. Laemmli (Laemmli, 1970). In this thesis, SDS-Gels were poured at different acrylamide concentrations ranging from 6% to 12% depending on the application and were prepared according to the manual provided at https://www.cytographica.com/lab/acryl2.html using 30% rotiphorese bisacrylamid. Additionally, 0.5% TCE was added to the resolving gel mix for protein detection before western blotting (Ladner et al., 2004). SDS-Gels were poured using 1.5 mm plates. The gels were run using two buffers: one for the inside of the chamber and one for the outside of the chamber. Here, Laemmli running buffer

(Table 21) and Laemmli running buffer with 0.1 M NaOAc were used, respectively. As protein standard the Prestained PageRuler (26616) or the Prestained PageRuler Plus (Thermo Fisher 26619) was used. The settings for the SDS Gels depended on the percentage. 10% and 12% SDS Gels were run at 120 V, 150 mA for ~1.40 h whereas 6% and 8% gels were run at 90 V, 150 mA for ~2 h. The time was adapted according to the application. To examine the loading of the samples, an image of the gel under UV light was taken using the BioRad documentation system with the ethidium bromide settings and 7-15 s exposure. Here, the TCE that intercalates with tryptophane was excited by the UV light and provides a total protein stain of gel indicating the loading (Ladner et al., 2004).

To transfer the proteins from an SDS-Gel onto a membrane, western blotting was employed. Depending on the size of the proteins, either a wet blot system from BioRad or the Turbo Blot system from BioRad was used. For larger proteins, the wet blot together with a boric acid buffer was the preferred system (Table 21). Here, the gels were blotted for 1 h at 400 mA with voltage set to 100 V at 4 °C. Alternatively, the gels were blotted overnight for 13 h at 100 mA with the voltage set to 20 V. For smaller proteins under 50 kDa the Turbo Blot system was used, here the ‘Standard Mini Gel 1.5 mm’ program was chosen. After blotting the membranes were either directly blocked with 4% milk in PBS or first stained using the REVERT stain from Licor. For the REVERT stain the membrane was incubated on a shaker with 5 ml REVERT solution for 5 min at room temperature. Then the membrane was washed twice for 30 s with wash solution (30% MeOH and 6.7% acetic acid). Lastly, the membrane was scanned using the Odyssey scanner from using the 700 nm channel at the lowest settings (L0.5). Then the membrane was blocked using 4% milk in PBS for 30 min to 60 minutes at room temperature. The membrane was incubated with the primary antibody overnight at 4 °C. After incubation with the primary antibody, the membrane was washed 4x for 5 min with PBS and then incubated with the secondary antibody for 2 h at room temperature. This was followed by 4x 5 min washing with PBS and scanning using the Odyssey scanner from Licor.

**Table 21** Composition of different buffers

| Laemmli running buffer (LRB) | Transfer buffer | Boric acid buffer | Phosphate buffered saline (PBS) | Tris acetate EDTA buffer (TAE) |
|---|---|---|---|---|
| 25 mM Tris (pH 8.3) | 25 mM Tris | 50 mM Boric acid | 1.8 mM $KH_2PO_4$ | 40 mM Tris |
| 192 mM glycine | 192 mM glycine | 10% Methanol | 10 mM $Na_2PO_4$ | 20 mM Sodium acetate |
| 0.1% SDS | 20% Methanol | | 2.7 mM KCl | 1 mM EDTA |
| For outer chamber: [0.1 M sodium acetate] | | | 137 mM NaCl | |

## 4.2.18 Microscopy

To examine the localization and abundance of proteins *in vivo*, fluorescence microscopy was performed. To perform live cell imaging, cells were precultured as described above (Chapter 4.1.21). If DAPI staining needed to be performed, DAPI solution was added to 1 ml culture to a final concentration of 1 µg/ml and the cells were incubated for 30 min at 30 °C in a heating block. To concentrate the cells for microscopy, 1 ml of culture was pelleted in a microcentrifuge tube and 900 µl of supernatant were discarded. Cells were resuspended in the remaining 100 µl. To immobilize the cells, agarose pads were poured using 1% agarose in TAE buffer. The pads were poured using the SDS-PAGE equipment and 1 mm spacer plates. Pads were freshly cut using a scalpel and transferred onto a microscope slide. Then 2 µl of the cell suspension were pipetted onto the agarose pad. The cells were covered with a cover slip and microscoped immediately. For fluorescence microscopy, the Zeiss Axioplan 2 was used. Either the Zeiss Plan-Neofluar 100x/ 1.30 oil or the Zeiss Apochromat 100/ 1.4 oil objective was employed. Immersion oil was used with both objectives. Two softwares were used to obtain and view microscopw images. AxioVision Rel 4.7 (Zeiss) was used for the acquisition and OMERO for image storage and generation of figures. OMERO is hosted by the image facility of the university of Cologne.

**Table 22** Microscope filters

| Channel | Excitation [nm] | Emission [nm] |
|---|---|---|
| **Brightfield** | 550 | 550 |
| **DAPI** | 359 | 461 |
| **Cy3** | 550 | 570 |
| **FITC** | 490 | 525 |
| **GFP** | 470 | 509 |

### 4.2.19 Mass Spectrometry

Mass spectrometry was performed to gain insight in the proteome of the slx5Δ strain in stressed and unstressed cells. Here, whole cell proteomics were performed where whole cell extracts were submitted to mass spectrometry. The cultures for mass spectrometry were grown as described in 4.1.21. The quadruplicates were grown on individual days and processed together. To extract proteins from the cells, a glass bead lysis was performed using the hydroxyurea buffer for mass spectrometry (Table 20). After pelleting the cell debris, the supernatant containing extracted proteins was transferred to a fresh microcentrifuge tube. The protein content was measured using Nanodrop One from Thermo Fisher. Here, the absorbance at 280 nm was measured. Then samples were prepared containing 2 ng of proteins.

Samples prepared as described above were then handled under the guidance from Luisa Schmidt from the Krüger group (Proteomics facility, CECAD, University of Cologne). The sample preparation was performed as the standard SP3 protocol (Hughes et al., 2019) and the stage tip preparation according to De Napoli et al., 2025. Mass spectrometric and bioinformatic analyses were performed by Luisa Schmidt as described in De Napoli et al., 2025 (De Napoli et al., 2025). A detailed description of the procedure was provided by Luisa Schmidt and can be found in the supplements (**Suppl. 1**).

# 5 Abbreviations

| | |
|---|---|
| *Aim44* | Altered inheritance rate of mitochondria 44 |
| *Aos1* | Activation of Smt3 1 |
| *Atg8* | Autophagy related 8 |
| *Btn2* | Batten disease |
| *Cbk1* | Cell wall biosynthesis kinase |
| *Cdc24* | Cell division cycle 24 |
| *Cdc42* | Cell division cycle 42 |
| *Cdh1* | Cdc20 homolog 1 |
| *CUP1* | Copper |
| *DNA* | Desoxyribonucleic acid |
| *dNTP* | Deoxynucleoside triphosphat |
| *DTT* | Dithiothreitol |
| *ECO* | Enforcement of cytokinesis order |
| *FIR1* | Factor inhibiting Ref2 1 |
| *GAL1* | Galactose metabolism 1 |
| *GAP* | GTPase-activating protein |
| *GCR* | Gross chromosomal arrangements |
| *GEF* | Guanine exchange factor |
| *GTP* | Guanosintriphosphate |
| *HA* | Human influenza hemagglutinin |
| *HECT* | Homologous to E6-AP Carboxyl Terminus |
| *HIS* | Histidine |
| *HMW* | High molecular weight conjugates |
| *Hsp42* | Heat shoch protein 42 |
| *Hsp90* | Heat shock protein 90 |
| *HU* | Hydroxyurea |
| *INQ* | Intranuclear quality control site |
| *IPOD* | Insoluable protein deposits |
| *IR1-M-IR2* | Internal Repeat 1 – Middle – Internal Repeat 2 |
| *JUNQ* | Juxtanuclear quality control site |
| *LRB* | Laemmli Running Buffer |
| *Mms21* | Methyl methanesulfonate sensitivity |
| *MS* | Mass spectrometry |
| *Nap1* | Nucleosome assembly protein |
| *Nba1* | Nap1 and bud neck associated |
| *Nis1* | Neck protein interacting with septins 1 |
| *NLS* | Nuclear localization signal |
| *OD* | Optical density |
| *PAGE* | Polyacrylamide gel electrophoresis |
| *PCNA* | Proliferating cell nuclear antigen |
| *PIAS* | Protein inhibitor of activated STAT |
| *PML* | Promyelocytic leukemia |
| *POD* | Peroxidase |

| | |
|---|---|
| *PTM* | Posttranslational Modification |
| *QC* | Quality control |
| *Rad18* | Radiation sensitive |
| *RanBP* | Ran binding protein |
| *RanGAP* | Ran GTPase activating protein |
| *Rax1/2* | Revert to axial 1/2 |
| *RING* | Really interesting new gene |
| *Rpn* | Regulatory Particle Non-ATPase |
| *Rpt* | Regulatory Particle Triple-A protein |
| *Rub1* | Related to ubiquitin |
| *Sae1/2* | SUMO-activating enzyme subunit 1/2 |
| *SDS* | Sodiumdodecylsulfate |
| *SIM* | SUMO interaction motif |
| *Siz1* | SAP and mIZ-finger domain |
| *Skt5* | Sensitivity to *K. lactis* protein |
| *Slx5/8* | Synthetic lethal gene 5/8 |
| *Smt3* | Suppressor of MIF2 |
| *Sod2* | Superoxide dismutase 2 |
| *Spa2* | Spindle pole antigen |
| *SP-RING* | Siz/PIAS – Really interesting new gene |
| *STUbL* | SUMO-targeted Ubiquitin Ligase |
| *SUMO* | Small Ubiquitin-related modifier |
| *SWI/SNF* | SWItch/Sucrose Non-Fermentable |
| *TCA* | Trichlorocacetic acid |
| *TCE* | Trichlorethylene |
| *TEMED* | Tetramethxlethylenediamine |
| *Uba1* | Ubiquitin activating enzyme 1 |
| *Uba2* | Ubiquitin activating enzyme 2 |
| *Ubc9* | Ubiquitin conjugating enzyme 9 |
| *UBE2I* | Ubiquitin conjugating enzyme E2I |
| *Ubl* | Ubiquitin-like modifier |
| *Ulp1* | Ubl-specific protease 1 |
| *Ulp2* | Ubl-specific protease 1 |
| *Uls1* | Ubiquitin ligase for SUMOylated proteins 1 |
| *Uls2* | Ubiquitin ligase for SUMOylated proteins 2 |
| *UPS* | Ubiquitin Proteasoem System |
| *WT* | Wild-type |
| *YP* | Yeast peptone |
| *YPGlu* | Yeast peptone glucose |
| *YPGal* | Yeast peptone galactose |
| *YPRaf* | Yeast peptone raffinose |

# 6 References


Abramson, J., Adler, J., Dunger, J., Evans, R., Green, T., Pritzel, A., Ronneberger, O., Willmore, L., Ballard, A. J., Bambrick, J., Bodenstein, S. W., Evans, D. A., Hung, C. C., O'Neill, M., Reiman, D., Tunyasuvunakool, K., Wu, Z., Zemgulyte, A., Arvaniti, E., . . . Jumper, J. M. (2024). Accurate structure prediction of biomolecular interactions with AlphaFold 3. *Nature*, *630*(8016), 493-500. https://doi.org/10.1038/s41586-024-07487-w

Agrata, R., & Komander, D. (2025). Ubiquitin-A structural perspective. *Mol Cell*, *85*(2), 323-346. https://doi.org/10.1016/j.molcel.2024.12.015

Albuquerque, C. P., Smolka, M. B., Payne, S. H., Bafna, V., Eng, J., & Zhou, H. (2008). A multidimensional chromatography technology for in-depth phosphoproteome analysis. *Mol Cell Proteomics*, *7*(7), 1389-1396. https://doi.org/10.1074/mcp.M700468-MCP200

Albuquerque, C. P., Wang, G., Lee, N. S., Kolodner, R. D., Putnam, C. D., & Zhou, H. (2013). Distinct SUMO ligases cooperate with Esc2 and Slx5 to suppress duplication-mediated genome rearrangements. *PLoS Genet*, *9*(8), e1003670. https://doi.org/10.1371/journal.pgen.1003670

Bachant, J., Alcasabas, A., Blat, Y., Kleckner, N., & Elledge, S. J. (2002). The SUMO-1 isopeptidase Smt4 is linked to centromeric cohesion through SUMO-1 modification of DNA topoisomerase II. *Mol Cell*, *9*(6), 1169-1182. https://doi.org/10.1016/s1097-2765(02)00543-9

Bauer, S. L., Chen, J., & Astrom, S. U. (2019). Helicase/SUMO-targeted ubiquitin ligase Uls1 interacts with the Holliday junction resolvase Yen1. *PLoS One*, *14*(3), e0214102. https://doi.org/10.1371/journal.pone.0214102

Baugh, J. M., Viktorova, E. G., & Pilipenko, E. V. (2009). Proteasomes can degrade a significant proportion of cellular proteins independent of ubiquitination. *J Mol Biol*, *386*(3), 814-827. https://doi.org/10.1016/j.jmb.2008.12.081

Bhagwat, N. R., Owens, S. N., Ito, M., Boinapalli, J. V., Poa, P., Ditzel, A., Kopparapu, S., Mahalawat, M., Davies, O. R., Collins, S. R., Johnson, J. R., Krogan, N. J., & Hunter, N. (2021). SUMO is a pervasive regulator of meiosis. *Elife*, *10*. https://doi.org/10.7554/eLife.57720

Blaszczak, E., Pasquier, E., Le Dez, G., Odrzywolski, A., Lazarewicz, N., Brossard, A., Fornal, E., Moskalek, P., Wysocki, R., & Rabut, G. (2024). Dissecting Ubiquitylation and DNA Damage Response Pathways in the Yeast Saccharomyces cerevisiae Using a Proteome-Wide Approach. *Mol Cell Proteomics*, *23*(1), 100695. https://doi.org/10.1016/j.mcpro.2023.100695

Bohren, K. M., Nadkarni, V., Song, J. H., Gabbay, K. H., & Owerbach, D. (2004). A M55V polymorphism in a novel SUMO gene (SUMO-4) differentially activates heat shock transcription factors and is associated with susceptibility to type I diabetes mellitus. *J Biol Chem*, *279*(26), 27233-27238. https://doi.org/10.1074/jbc.M402273200

Boorsma, A., de Nobel, H., ter Riet, B., Bargmann, B., Brul, S., Hellingwerf, K. J., & Klis, F. M. (2004). Characterization of the transcriptional response to cell wall stress in Saccharomyces cerevisiae. *Yeast*, *21*(5), 413-427. https://doi.org/10.1002/yea.1109

Borgert, L., Mishra, S., & den Brave, F. (2022). Quality control of cytoplasmic proteins inside the nucleus. *Comput Struct Biotechnol J*, *20*, 4618-4625. https://doi.org/10.1016/j.csbj.2022.08.033

Borkovich, K. A., Farrelly, F. W., Finkelstein, D. B., Taulien, J., & Lindquist, S. (1989). hsp82 is an essential protein that is required in higher concentrations for growth of cells at higher temperatures. *Mol Cell Biol*, *9*(9), 3919-3930. https://doi.org/10.1128/mcb.9.9.3919-3930.1989

Boschetti, E., & Righetti, P. G. (2023). Low-Abundance Protein Enrichment for Medical Applications: The Involvement of Combinatorial Peptide Library Technique. *Int J Mol Sci*, *24*(12). https://doi.org/10.3390/ijms241210329

Brace, J. L., Doerfler, M. D., & Weiss, E. L. (2019). A cell separation checkpoint that enforces the proper order of late cytokinetic events. *J Cell Biol*, *218*(1), 150-170. https://doi.org/10.1083/jcb.201805100

Buchner, J. (2019). Molecular chaperones and protein quality control: an introduction to the JBC Reviews thematic series. *J Biol Chem*, *294*(6), 2074-2075. https://doi.org/10.1074/jbc.REV118.006739

Bylebyl, G. R., Belichenko, I., & Johnson, E. S. (2003). The SUMO isopeptidase Ulp2 prevents accumulation of SUMO chains in yeast. *J Biol Chem*, *278*(45), 44113-44120. https://doi.org/10.1074/jbc.M308357200

Cappadocia, L., & Lima, C. D. (2018). Ubiquitin-like Protein Conjugation: Structures, Chemistry, and Mechanism. *Chem Rev*, *118*(3), 889-918. https://doi.org/10.1021/acs.chemrev.6b00737

Chen, Z., Luo, J., Zhang, Y., Zheng, S., Zhang, H., Huang, Y., Wong, J., & Li, J. (2024). SUMOylation is enriched in the nuclear matrix and required for chromosome segregation. *J Biol Chem*, *300*(1), 105547. https://doi.org/10.1016/j.jbc.2023.105547

Cheng, C. H., Lo, Y. H., Liang, S. S., Ti, S. C., Lin, F. M., Yeh, C. H., Huang, H. Y., & Wang, T. F. (2006). SUMO modifications control assembly of synaptonemal complex and polycomplex in meiosis of Saccharomyces cerevisiae. *Genes Dev*, *20*(15), 2067-2081. https://doi.org/10.1101/gad.1430406

Cohen-Kaplan, V., Livneh, I., Avni, N., Cohen-Rosenzweig, C., & Ciechanover, A. (2016). The ubiquitin-proteasome system and autophagy: Coordinated and independent activities. *Int J Biochem Cell Biol*, *79*, 403-418. https://doi.org/10.1016/j.biocel.2016.07.019

Cook, C. E., Hochstrasser, M., & Kerscher, O. (2009). The SUMO-targeted ubiquitin ligase subunit Slx5 resides in nuclear foci and at sites of DNA breaks. *Cell Cycle*, *8*(7), 1080-1089. https://doi.org/10.4161/cc.8.7.8123

Cox, J., Hein, M. Y., Luber, C. A., Paron, I., Nagaraj, N., & Mann, M. (2014). Accurate proteome-wide label-free quantification by delayed normalization and maximal peptide ratio extraction, termed MaxLFQ. *Mol Cell Proteomics*, *13*(9), 2513-2526. https://doi.org/10.1074/mcp.M113.031591

D'Silva, P. R., Schilke, B., Walter, W., & Craig, E. A. (2005). Role of Pam16's degenerate J domain in protein import across the mitochondrial inner membrane. *Proc Natl Acad Sci U S A*, *102*(35), 12419-12424. https://doi.org/10.1073/pnas.0505969102

Danish, M., & Ahmad, R. (2023). Functional pleiotropy of calcium binding protein Regucalcin in signaling and diseases. *Cell Signal*, *102*, 110533. https://doi.org/10.1016/j.cellsig.2022.110533

Day, A., Schneider, C., & Schneider, B. L. (2004). Yeast cell synchronization. *Methods Mol Biol*, *241*, 55-76. https://doi.org/10.1385/1-59259-646-0:55

De Napoli, C., Schmidt, L., Montesel, M., Cussonneau, L., Sanniti, S., Marcucci, L., Germinario, E., Kindberg, J., Evans, A. L., Gauquelin-Koch, G., Narici, M., Bertile, F., Lefai, E., Kruger, M., Nogara, L., & Blaauw, B. (2025). Reduced ATP

turnover during hibernation in relaxed skeletal muscle. *Nat Commun*, *16*(1), 80. https://doi.org/10.1038/s41467-024-55565-4

Demichev, V., Messner, C. B., Vernardis, S. I., Lilley, K. S., & Ralser, M. (2020). DIA-NN: neural networks and interference correction enable deep proteome coverage in high throughput. *Nat Methods*, *17*(1), 41-44. https://doi.org/10.1038/s41592-019-0638-x

Dohmen, R. J., Stappen, R., McGrath, J. P., Forrova, H., Kolarov, J., Goffeau, A., & Varshavsky, A. (1995). An essential yeast gene encoding a homolog of ubiquitin-activating enzyme. *J Biol Chem*, *270*(30), 18099-18109. https://doi.org/10.1074/jbc.270.30.18099

Eckhoff, J., & Dohmen, R. J. (2015). In Vitro Studies Reveal a Sequential Mode of Chain Processing by the Yeast SUMO (Small Ubiquitin-related Modifier)-specific Protease Ulp2. *J Biol Chem*, *290*(19), 12268-12281. https://doi.org/10.1074/jbc.M114.622217

Finley, D., Ulrich, H. D., Sommer, T., & Kaiser, P. (2012). The ubiquitin-proteasome system of Saccharomyces cerevisiae. *Genetics*, *192*(2), 319-360. https://doi.org/10.1534/genetics.112.140467

Frazier, A. E., Dudek, J., Guiard, B., Voos, W., Li, Y., Lind, M., Meisinger, C., Geissler, A., Sickmann, A., Meyer, H. E., Bilanchone, V., Cumsky, M. G., Truscott, K. N., Pfanner, N., & Rehling, P. (2004). Pam16 has an essential role in the mitochondrial protein import motor. *Nat Struct Mol Biol*, *11*(3), 226-233. https://doi.org/10.1038/nsmb735

French, M. E., Koehler, C. F., & Hunter, T. (2021). Emerging functions of branched ubiquitin chains. *Cell Discov*, *7*(1), 6. https://doi.org/10.1038/s41421-020-00237-y

Gao, Y., Ping, L., Duong, D., Zhang, C., Dammer, E. B., Li, Y., Chen, P., Chang, L., Gao, H., Wu, J., & Xu, P. (2021). Mass-Spectrometry-Based Near-Complete Draft of the Saccharomyces cerevisiae Proteome. *J Proteome Res*, *20*(2), 1328-1340. https://doi.org/10.1021/acs.jproteome.0c00721

Gareau, J. R., & Lima, C. D. (2010). The SUMO pathway: emerging mechanisms that shape specificity, conjugation and recognition. *Nat Rev Mol Cell Biol*, *11*(12), 861-871. https://doi.org/10.1038/nrm3011

Gietz, R. D., & Schiestl, R. H. (2007). High-efficiency yeast transformation using the LiAc/SS carrier DNA/PEG method. *Nat Protoc*, *2*(1), 31-34. https://doi.org/10.1038/nprot.2007.13

Girstmair, H., Tippel, F., Lopez, A., Tych, K., Stein, F., Haberkant, P., Schmid, P. W. N., Helm, D., Rief, M., Sattler, M., & Buchner, J. (2019). The Hsp90 isoforms from S. cerevisiae differ in structure, function and client range. *Nat Commun*, *10*(1), 3626. https://doi.org/10.1038/s41467-019-11518-w

Glickman, M. H., Rubin, D. M., Fried, V. A., & Finley, D. (1998). The regulatory particle of the Saccharomyces cerevisiae proteasome. *Mol Cell Biol*, *18*(6), 3149-3162. https://doi.org/10.1128/MCB.18.6.3149

Hannich, J. T., Lewis, A., Kroetz, M. B., Li, S. J., Heide, H., Emili, A., & Hochstrasser, M. (2005). Defining the SUMO-modified proteome by multiple approaches in Saccharomyces cerevisiae. *J Biol Chem*, *280*(6), 4102-4110. https://doi.org/10.1074/jbc.M413209200

Hegde, R. S., & Zavodszky, E. (2019). Recognition and Degradation of Mislocalized Proteins in Health and Disease. *Cold Spring Harb Perspect Biol*, *11*(11). https://doi.org/10.1101/cshperspect.a033902

Holt, L. J., Tuch, B. B., Villen, J., Johnson, A. D., Gygi, S. P., & Morgan, D. O. (2009). Global analysis of Cdk1 substrate phosphorylation sites provides insights into

evolution. *Science*, *325*(5948), 1682-1686. https://doi.org/10.1126/science.1172867

Hopfler, M., Kern, M. J., Straub, T., Prytuliak, R., Habermann, B. H., Pfander, B., & Jentsch, S. (2019). Slx5/Slx8-dependent ubiquitin hotspots on chromatin contribute to stress tolerance. *EMBO J*, *38*(11). https://doi.org/10.15252/embj.2018100368

Hostettler, L., Grundy, L., Kaser-Pebernard, S., Wicky, C., Schafer, W. R., & Glauser, D. A. (2017). The Bright Fluorescent Protein mNeonGreen Facilitates Protein Expression Analysis In Vivo. *G3 (Bethesda)*, *7*(2), 607-615. https://doi.org/10.1534/g3.116.038133

Huang, X., Luan, B., Wu, J., & Shi, Y. (2016). An atomic structure of the human 26S proteasome. *Nat Struct Mol Biol*, *23*(9), 778-785. https://doi.org/10.1038/nsmb.3273

Hughes, C. S., Moggridge, S., Muller, T., Sorensen, P. H., Morin, G. B., & Krijgsveld, J. (2019). Single-pot, solid-phase-enhanced sample preparation for proteomics experiments. *Nat Protoc*, *14*(1), 68-85. https://doi.org/10.1038/s41596-018-0082-x

Ii, T., Mullen, J. R., Slagle, C. E., & Brill, S. J. (2007). Stimulation of in vitro sumoylation by Slx5-Slx8: evidence for a functional interaction with the SUMO pathway. *DNA Repair (Amst)*, *6*(11), 1679-1691. https://doi.org/10.1016/j.dnarep.2007.06.004

Iwase, M., & Toh-e, A. (2001). Nis1 encoded by YNL078W: a new neck protein of Saccharomyces cerevisiae. *Genes Genet Syst*, *76*(5), 335-343. https://doi.org/10.1266/ggs.76.335

Johnson, D. I., & Pringle, J. R. (1990). Molecular characterization of CDC42, a Saccharomyces cerevisiae gene involved in the development of cell polarity. *J Cell Biol*, *111*(1), 143-152. https://doi.org/10.1083/jcb.111.1.143

Johnson, E. S. (2004). Protein modification by SUMO. *Annu Rev Biochem*, *73*, 355-382. https://doi.org/10.1146/annurev.biochem.73.011303.074118

Johnson, E. S., & Blobel, G. (1997). Ubc9p is the conjugating enzyme for the ubiquitin-like protein Smt3p. *J Biol Chem*, *272*(43), 26799-26802. https://doi.org/10.1074/jbc.272.43.26799

Johnson, E. S., & Blobel, G. (1999). Cell cycle-regulated attachment of the ubiquitin-related protein SUMO to the yeast septins. *J Cell Biol*, *147*(5), 981-994. https://doi.org/10.1083/jcb.147.5.981

Johnson, E. S., & Gupta, A. A. (2001). An E3-like factor that promotes SUMO conjugation to the yeast septins. *Cell*, *106*(6), 735-744. https://doi.org/10.1016/s0092-8674(01)00491-3

Johnson, E. S., Schwienhorst, I., Dohmen, R. J., & Blobel, G. (1997). The ubiquitin-like protein Smt3p is activated for conjugation to other proteins by an Aos1p/Uba2p heterodimer. *EMBO J*, *16*(18), 5509-5519. https://doi.org/10.1093/emboj/16.18.5509

Kamitani, T., Kito, K., Nguyen, H. P., Fukuda-Kamitani, T., & Yeh, E. T. (1998). Characterization of a second member of the sentrin family of ubiquitin-like proteins. *J Biol Chem*, *273*(18), 11349-11353. https://doi.org/10.1074/jbc.273.18.11349

Kang, Y., He, Y. X., Zhao, M. X., & Li, W. F. (2011). Structures of native and Fe-substituted SOD2 from Saccharomyces cerevisiae. *Acta Crystallogr Sect F Struct Biol Cryst Commun*, *67*(Pt 10), 1173-1178. https://doi.org/10.1107/S1744309111029186

Keiten-Schmitz, J., Wagner, K., Piller, T., Kaulich, M., Alberti, S., & Muller, S. (2020). The Nuclear SUMO-Targeted Ubiquitin Quality Control Network Regulates the

Dynamics of Cytoplasmic Stress Granules. *Mol Cell*, *79*(1), 54-67 e57. https://doi.org/10.1016/j.molcel.2020.05.017

Kerscher, O. (2007). SUMO junction-what's your function? New insights through SUMO-interacting motifs. *EMBO Rep*, *8*(6), 550-555. https://doi.org/10.1038/sj.embor.7400980

Knop, M., Siegers, K., Pereira, G., Zachariae, W., Winsor, B., Nasmyth, K., & Schiebel, E. (1999). Epitope tagging of yeast genes using a PCR-based strategy: more tags and improved practical routines. *Yeast*, *15*(10B), 963-972. https://doi.org/10.1002/(SICI)1097-0061(199907)15:10B<963::AID-YEA399>3.0.CO;2-W

Kolhe, J. A., Babu, N. L., & Freeman, B. C. (2023). The Hsp90 molecular chaperone governs client proteins by targeting intrinsically disordered regions. *Mol Cell*, *83*(12), 2035-2044 e2037. https://doi.org/10.1016/j.molcel.2023.05.021

Kramarz, K., Mucha, S., Litwin, I., Barg-Wojas, A., Wysocki, R., & Dziadkowiec, D. (2017). DNA Damage Tolerance Pathway Choice Through Uls1 Modulation of Srs2 SUMOylation in Saccharomyces cerevisiae. *Genetics*, *206*(1), 513-525. https://doi.org/10.1534/genetics.116.196568

Kroetz, M. B., Su, D., & Hochstrasser, M. (2009). Essential role of nuclear localization for yeast Ulp2 SUMO protease function. *Mol Biol Cell*, *20*(8), 2196-2206. https://doi.org/10.1091/mbc.e08-10-1090

Krukenberg, K. A., Street, T. O., Lavery, L. A., & Agard, D. A. (2011). Conformational dynamics of the molecular chaperone Hsp90. *Q Rev Biophys*, *44*(2), 229-255. https://doi.org/10.1017/S0033583510000314

Kumar, A., Mathew, V., & Stirling, P. C. (2022). Nuclear protein quality control in yeast: The latest INQuiries. *J Biol Chem*, *298*(8), 102199. https://doi.org/10.1016/j.jbc.2022.102199

Kunjappu, M. J., & Hochstrasser, M. (2014). Assembly of the 20S proteasome. *Biochim Biophys Acta*, *1843*(1), 2-12. https://doi.org/10.1016/j.bbamcr.2013.03.008

Kushnirov, V. V. (2000). Rapid and reliable protein extraction from yeast. *Yeast*, *16*(9), 857-860. https://doi.org/10.1002/1097-0061(20000630)16:9<857::AID-YEA561>3.0.CO;2-B

Ladner, C. L., Yang, J., Turner, R. J., & Edwards, R. A. (2004). Visible fluorescent detection of proteins in polyacrylamide gels without staining. *Anal Biochem*, *326*(1), 13-20. https://doi.org/10.1016/j.ab.2003.10.047

Laemmli, U. K. (1970). Cleavage of structural proteins during the assembly of the head of bacteriophage T4. *Nature*, *227*(5259), 680-685. https://doi.org/10.1038/227680a0

Lander, G. C., Estrin, E., Matyskiela, M. E., Bashore, C., Nogales, E., & Martin, A. (2012). Complete subunit architecture of the proteasome regulatory particle. *Nature*, *482*(7384), 186-191. https://doi.org/10.1038/nature10774

Lanz, M. C., Yugandhar, K., Gupta, S., Sanford, E. J., Faca, V. M., Vega, S., Joiner, A. M. N., Fromme, J. C., Yu, H., & Smolka, M. B. (2021). In-depth and 3-dimensional exploration of the budding yeast phosphoproteome. *EMBO Rep*, *22*(2), e51121. https://doi.org/10.15252/embr.202051121

Lascorz, J., Codina-Fabra, J., Reverter, D., & Torres-Rosell, J. (2022). SUMO-SIM interactions: From structure to biological functions. *Semin Cell Dev Biol*, *132*, 193-202. https://doi.org/10.1016/j.semcdb.2021.11.007

Lescasse, R., Pobiega, S., Callebaut, I., & Marcand, S. (2013). End-joining inhibition at telomeres requires the translocase and polySUMO-dependent ubiquitin ligase Uls1. *Embo Journal*, *32*(6), 805-815. https://doi.org/10.1038/emboj.2013.24

Leutert, M., Barente, A. S., Fukuda, N. K., Rodriguez-Mias, R. A., & Villen, J. (2023). The regulatory landscape of the yeast phosphoproteome. *Nat Struct Mol Biol*, *30*(11), 1761-1773. https://doi.org/10.1038/s41594-023-01115-3

Li, S. J., & Hochstrasser, M. (1999). A new protease required for cell-cycle progression in yeast. *Nature*, *398*(6724), 246-251. https://doi.org/10.1038/18457

Li, S. J., & Hochstrasser, M. (2000). The yeast ULP2 (SMT4) gene encodes a novel protease specific for the ubiquitin-like Smt3 protein. *Mol Cell Biol*, *20*(7), 2367-2377. https://doi.org/10.1128/mcb.20.7.2367-2377.2000

Li, S. J., & Hochstrasser, M. (2003). The Ulp1 SUMO isopeptidase: distinct domains required for viability, nuclear envelope localization, and substrate specificity. *J Cell Biol*, *160*(7), 1069-1081. https://doi.org/10.1083/jcb.200212052

Liao, Y., Zhang, W., Liu, Y., Zhu, C., & Zou, Z. (2024). The role of ubiquitination in health and disease. *MedComm (2020)*, *5*(10), e736. https://doi.org/10.1002/mco2.736

Liu, X., Li, J., Gygi, S. P., & Paulo, J. A. (2022). Profiling Yeast Deletion Strains Using Sample Multiplexing and Network-Based Analyses. *J Proteome Res*, *21*(6), 1525-1536. https://doi.org/10.1021/acs.jproteome.2c00137

MacGilvray, M. E., Shishkova, E., Place, M., Wagner, E. R., Coon, J. J., & Gasch, A. P. (2020). Phosphoproteome Response to Dithiothreitol Reveals Unique Versus Shared Features of Saccharomyces cerevisiae Stress Responses. *J Proteome Res*, *19*(8), 3405-3417. https://doi.org/10.1021/acs.jproteome.0c00253

Maga, G., & Hubscher, U. (2003). Proliferating cell nuclear antigen (PCNA): a dancer with many partners. *J Cell Sci*, *116*(Pt 15), 3051-3060. https://doi.org/10.1242/jcs.00653

Mahajan, R., Delphin, C., Guan, T., Gerace, L., & Melchior, F. (1997). A small ubiquitin-related polypeptide involved in targeting RanGAP1 to nuclear pore complex protein RanBP2. *Cell*, *88*(1), 97-107. https://doi.org/10.1016/s0092-8674(00)81862-0

Malinovska, L., Kroschwald, S., Munder, M. C., Richter, D., & Alberti, S. (2012). Molecular chaperones and stress-inducible protein-sorting factors coordinate the spatiotemporal distribution of protein aggregates. *Mol Biol Cell*, *23*(16), 3041-3056. https://doi.org/10.1091/mbc.E12-03-0194

Mascle, X. H., Lussier-Price, M., Cappadocia, L., Estephan, P., Raiola, L., Omichinski, J. G., & Aubry, M. (2013). Identification of a non-covalent ternary complex formed by PIAS1, SUMO1, and UBC9 proteins involved in transcriptional regulation. *J Biol Chem*, *288*(51), 36312-36327. https://doi.org/10.1074/jbc.M113.486845

Matias, A. C., Ramos, P. C., & Dohmen, R. J. (2010). Chaperone-assisted assembly of the proteasome core particle. *Biochem Soc Trans*, *38*(Pt 1), 29-33. https://doi.org/10.1042/BST0380029

Matunis, M. J., Coutavas, E., & Blobel, G. (1996). A novel ubiquitin-like modification modulates the partitioning of the Ran-GTPase-activating protein RanGAP1 between the cytosol and the nuclear pore complex. *J Cell Biol*, *135*(6 Pt 1), 1457-1470. https://doi.org/10.1083/jcb.135.6.1457

McGrath, J. P., Jentsch, S., & Varshavsky, A. (1991). UBA 1: an essential yeast gene encoding ubiquitin-activating enzyme. *EMBO J*, *10*(1), 227-236. https://doi.org/10.1002/j.1460-2075.1991.tb07940.x

Meitinger, F., Khmelinskii, A., Morlot, S., Kurtulmus, B., Palani, S., Andres-Pons, A., Hub, B., Knop, M., Charvin, G., & Pereira, G. (2014). A memory system of negative polarity cues prevents replicative aging. *Cell*, *159*(5), 1056-1069. https://doi.org/10.1016/j.cell.2014.10.014

Melchior, F. (2000). SUMO--nonclassical ubiquitin. *Annu Rev Cell Dev Biol*, *16*, 591-626. https://doi.org/10.1146/annurev.cellbio.16.1.591

Meluh, P. B., & Koshland, D. (1995). Evidence that the MIF2 gene of Saccharomyces cerevisiae encodes a centromere protein with homology to the mammalian centromere protein CENP-C. *Mol Biol Cell*, *6*(7), 793-807. https://doi.org/10.1091/mbc.6.7.793

Messner, C. B., Demichev, V., Muenzner, J., Aulakh, S. K., Barthel, N., Rohl, A., Herrera-Dominguez, L., Egger, A. S., Kamrad, S., Hou, J., Tan, G., Lemke, O., Calvani, E., Szyrwiel, L., Mulleder, M., Lilley, K. S., Boone, C., Kustatscher, G., & Ralser, M. (2023). The proteomic landscape of genome-wide genetic perturbations. *Cell*, *186*(9), 2018-2034 e2021. https://doi.org/10.1016/j.cell.2023.03.026

Miller, S. B., Ho, C. T., Winkler, J., Khokhrina, M., Neuner, A., Mohamed, M. Y., Guilbride, D. L., Richter, K., Lisby, M., Schiebel, E., Mogk, A., & Bukau, B. (2015). Compartment-specific aggregases direct distinct nuclear and cytoplasmic aggregate deposition. *EMBO J*, *34*(6), 778-797. https://doi.org/10.15252/embj.201489524

Mokranjac, D., Bourenkov, G., Hell, K., Neupert, W., & Groll, M. (2006). Structure and function of Tim14 and Tim16, the J and J-like components of the mitochondrial protein import motor. *EMBO J*, *25*(19), 4675-4685. https://doi.org/10.1038/sj.emboj.7601334

Mollapour, M., Bourboulia, D., Beebe, K., Woodford, M. R., Polier, S., Hoang, A., Chelluri, R., Li, Y., Guo, A., Lee, M. J., Fotooh-Abadi, E., Khan, S., Prince, T., Miyajima, N., Yoshida, S., Tsutsumi, S., Xu, W., Panaretou, B., Stetler-Stevenson, W. G., . . . Neckers, L. (2014). Asymmetric Hsp90 N domain SUMOylation recruits Aha1 and ATP-competitive inhibitors. *Mol Cell*, *53*(2), 317-329. https://doi.org/10.1016/j.molcel.2013.12.007

Moreno-Gonzalez, I., & Soto, C. (2011). Misfolded protein aggregates: mechanisms, structures and potential for disease transmission. *Semin Cell Dev Biol*, *22*(5), 482-487. https://doi.org/10.1016/j.semcdb.2011.04.002

Mosley, A. L., Florens, L., Wen, Z., & Washburn, M. P. (2009). A label free quantitative proteomic analysis of the Saccharomyces cerevisiae nucleus. *J Proteomics*, *72*(1), 110-120. https://doi.org/10.1016/j.jprot.2008.10.008

Mullen, J. R., Kaliraman, V., Ibrahim, S. S., & Brill, S. J. (2001). Requirement for three novel protein complexes in the absence of the Sgs1 DNA helicase in Saccharomyces cerevisiae. *Genetics*, *157*(1), 103-118. https://www.ncbi.nlm.nih.gov/pubmed/11139495

Müller, J., Furlan, M., Settele, D., Grupp, B., & Johnsson, N. (2024). Transient septin sumoylation steers a Fir1-Skt5 protein complex between the split septin ring. *J Cell Biol*, *223*(1). https://doi.org/10.1083/jcb.202301027

Neiman, A. M. (2011). Sporulation in the budding yeast Saccharomyces cerevisiae. *Genetics*, *189*(3), 737-765. https://doi.org/10.1534/genetics.111.127126

Niskanen, E. A., Malinen, M., Sutinen, P., Toropainen, S., Paakinaho, V., Vihervaara, A., Joutsen, J., Kaikkonen, M. U., Sistonen, L., & Palvimo, J. J. (2015). Global SUMOylation on active chromatin is an acute heat stress response restricting transcription. *Genome Biol*, *16*(1), 153. https://doi.org/10.1186/s13059-015-0717-y

Nolte, H., MacVicar, T. D., Tellkamp, F., & Kruger, M. (2018). Instant Clue: A Software Suite for Interactive Data Visualization and Analysis. *Sci Rep*, *8*(1), 12648. https://doi.org/10.1038/s41598-018-31154-6

Ohkuni, K., Takahashi, Y., Fulp, A., Lawrimore, J., Au, W. C., Pasupala, N., Levy-Myers, R., Warren, J., Strunnikov, A., Baker, R. E., Kerscher, O., Bloom, K., & Basrai, M. A. (2016). SUMO-Targeted Ubiquitin Ligase (STUbL) Slx5 regulates proteolysis of centromeric histone H3 variant Cse4 and prevents its mislocalization to euchromatin. *Mol Biol Cell*, *27*(9), 1500-1510. https://doi.org/10.1091/mbc.E15-12-0827

Ostapenko, D., Burton, J. L., & Solomon, M. J. (2012). Identification of anaphase promoting complex substrates in S. cerevisiae. *PLoS One*, *7*(9), e45895. https://doi.org/10.1371/journal.pone.0045895

Paasch, F., den Brave, F., Psakhye, I., Pfander, B., & Jentsch, S. (2018). Failed mitochondrial import and impaired proteostasis trigger SUMOylation of mitochondrial proteins. *J Biol Chem*, *293*(2), 599-609. https://doi.org/10.1074/jbc.M117.817833

Palma, F. R., He, C. X., Danes, J. M., Paviani, V., Coelho, D. R., Gantner, B. N., & Bonini, M. G. (2020). Mitochondrial Superoxide Dismutase: What the Established, the Intriguing, and the Novel Reveal About a Key Cellular Redox Switch. *Antioxidants & Redox Signaling*, *32*(10), 701-714. https://doi.org/10.1089/ars.2019.7962

Parker, J. L., & Ulrich, H. D. (2012). A SUMO-interacting motif activates budding yeast ubiquitin ligase Rad18 towards SUMO-modified PCNA. *Nucleic Acids Res*, *40*(22), 11380-11388. https://doi.org/10.1093/nar/gks892

Peng, B., Williams, T. C., Henry, M., Nielsen, L. K., & Vickers, C. E. (2015). Controlling heterologous gene expression in yeast cell factories on different carbon substrates and across the diauxic shift: a comparison of yeast promoter activities. *Microb Cell Fact*, *14*, 91. https://doi.org/10.1186/s12934-015-0278-5

Perez, A. M., & Thorner, J. (2019). Septin-associated proteins Aim44 and Nis1 traffic between the bud neck and the nucleus in the yeast Saccharomyces cerevisiae. *Cytoskeleton (Hoboken)*, *76*(1), 15-32. https://doi.org/10.1002/cm.21500

Pichler, A., Gast, A., Seeler, J. S., Dejean, A., & Melchior, F. (2002). The nucleoporin RanBP2 has SUMO1 E3 ligase activity. *Cell*, *108*(1), 109-120. https://doi.org/10.1016/s0092-8674(01)00633-x

Pichler, A., Knipscheer, P., Saitoh, H., Sixma, T. K., & Melchior, F. (2004). The RanBP2 SUMO E3 ligase is neither HECT- nor RING-type. *Nat Struct Mol Biol*, *11*(10), 984-991. https://doi.org/10.1038/nsmb834

Pickart, C. M., & Fushman, D. (2004). Polyubiquitin chains: polymeric protein signals. *Curr Opin Chem Biol*, *8*(6), 610-616. https://doi.org/10.1016/j.cbpa.2004.09.009

Pohl, C., & Dikic, I. (2019). Cellular quality control by the ubiquitin-proteasome system and autophagy. *Science*, *366*(6467), 818-822. https://doi.org/10.1126/science.aax3769

Praefcke, G. J., Hofmann, K., & Dohmen, R. J. (2012). SUMO playing tag with ubiquitin. *Trends Biochem Sci*, *37*(1), 23-31. https://doi.org/10.1016/j.tibs.2011.09.002

Ramazi, S., & Zahiri, J. (2021). Posttranslational modifications in proteins: resources, tools and prediction methods. *Database (Oxford)*, *2021*. https://doi.org/10.1093/database/baab012

Reverter, D., & Lima, C. D. (2005). Insights into E3 ligase activity revealed by a SUMO-RanGAP1-Ubc9-Nup358 complex. *Nature*, *435*(7042), 687-692. https://doi.org/10.1038/nature03588

Rolli, S., Langridge, C. A., & Sontag, E. M. (2024). Clearing the JUNQ: the molecular machinery for sequestration, localization, and degradation of the JUNQ

compartment. *Front Mol Biosci*, *11*, 1427542. https://doi.org/10.3389/fmolb.2024.1427542

Rothe, S., Prakash, A., & Tyedmers, J. (2018). The Insoluble Protein Deposit (IPOD) in Yeast. *Front Mol Neurosci*, *11*, 237. https://doi.org/10.3389/fnmol.2018.00237

Rytinki, M. M., Kaikkonen, S., Pehkonen, P., Jaaskelainen, T., & Palvimo, J. J. (2009). PIAS proteins: pleiotropic interactors associated with SUMO. *Cell Mol Life Sci*, *66*(18), 3029-3041. https://doi.org/10.1007/s00018-009-0061-z

Saeki, Y., & Tanaka, K. (2012). Assembly and function of the proteasome. *Methods Mol Biol*, *832*, 315-337. https://doi.org/10.1007/978-1-61779-474-2_22

Schmidt, L. M. (2024). *Advanced Proteomics of Skeletal Muscles: Spatial and Single Fiber Insights into Metabolic Diversity* University of Cologne].

Schweiggert, J., Stevermann, L., Panigada, D., Kammerer, D., & Liakopoulos, D. (2016). Regulation of a Spindle Positioning Factor at Kinetochores by SUMO-Targeted Ubiquitin Ligases. *Dev Cell*, *36*(4), 415-427. https://doi.org/10.1016/j.devcel.2016.01.011

Schwienhorst, I., Johnson, E. S., & Dohmen, R. J. (2000). SUMO conjugation and deconjugation. *Mol Gen Genet*, *263*(5), 771-786. https://doi.org/10.1007/s004380000254

Sengupta, S., & Pick, E. (2023). The Ubiquitin-like Proteins of Saccharomyces cerevisiae. *Biomolecules*, *13*(5). https://doi.org/10.3390/biom13050734

Shah, P. P., Zheng, X., Epshtein, A., Carey, J. N., Bishop, D. K., & Klein, H. L. (2010). Swi2/Snf2-related translocases prevent accumulation of toxic Rad51 complexes during mitotic growth. *Mol Cell*, *39*(6), 862-872. https://doi.org/10.1016/j.molcel.2010.08.028

Shakya, V. P., Barbeau, W. A., Xiao, T., Knutson, C. S., Schuler, M. H., & Hughes, A. L. (2021). A nuclear-based quality control pathway for non-imported mitochondrial proteins. *Elife*, *10*. https://doi.org/10.7554/eLife.61230

Shen, Z., Pardington-Purtymun, P. E., Comeaux, J. C., Moyzis, R. K., & Chen, D. J. (1996). Associations of UBE2I with RAD52, UBL1, p53, and RAD51 proteins in a yeast two-hybrid system. *Genomics*, *37*(2), 183-186. https://doi.org/10.1006/geno.1996.0540

Soares Rodrigues, C. I., den Ridder, M., Pabst, M., Gombert, A. K., & Wahl, S. A. (2023). Comparative proteome analysis of different Saccharomyces cerevisiae strains during growth on sucrose and glucose. *Sci Rep*, *13*(1), 2126. https://doi.org/10.1038/s41598-023-29172-0

Sriramachandran, A. M., & Dohmen, R. J. (2014). SUMO-targeted ubiquitin ligases. *Biochim Biophys Acta*, *1843*(1), 75-85. https://doi.org/10.1016/j.bbamcr.2013.08.022

Stade, K., Vogel, F., Schwienhorst, I., Meusser, B., Volkwein, C., Nentwig, B., Dohmen, R. J., & Sommer, T. (2002). A lack of SUMO conjugation affects cNLS-dependent nuclear protein import in yeast. *J Biol Chem*, *277*(51), 49554-49561. https://doi.org/10.1074/jbc.M207991200

Stehmeier, P., & Muller, S. (2009). Phospho-regulated SUMO interaction modules connect the SUMO system to CK2 signaling. *Mol Cell*, *33*(3), 400-409. https://doi.org/10.1016/j.molcel.2009.01.013

Sternsdorf, T., Jensen, K., & Will, H. (1997). Evidence for covalent modification of the nuclear dot-associated proteins PML and Sp100 by PIC1/SUMO-1. *J Cell Biol*, *139*(7), 1621-1634. https://doi.org/10.1083/jcb.139.7.1621

Stockwell, S. R., Landry, C. R., & Rifkin, S. A. (2015). The yeast galactose network as a quantitative model for cellular memory. *Mol Biosyst*, *11*(1), 28-37. https://doi.org/10.1039/c4mb00448e

Sun, Y., Miller Jenkins, L. M., Su, Y. P., Nitiss, K. C., Nitiss, J. L., & Pommier, Y. (2020). A conserved SUMO pathway repairs topoisomerase DNA-protein cross-links by engaging ubiquitin-mediated proteasomal degradation. *Sci Adv*, *6*(46). https://doi.org/10.1126/sciadv.aba6290

Swaney, D. L., Beltrao, P., Starita, L., Guo, A., Rush, J., Fields, S., Krogan, N. J., & Villen, J. (2013). Global analysis of phosphorylation and ubiquitylation cross-talk in protein degradation. *Nat Methods*, *10*(7), 676-682. https://doi.org/10.1038/nmeth.2519

Takahashi, Y., Toh-e, A., & Kikuchi, Y. (2001). A novel factor required for the SUMO1/Smt3 conjugation of yeast septins. *Gene*, *275*(2), 223-231. https://doi.org/10.1016/s0378-1119(01)00662-x

Talhaoui, I., Bernal, M., Mullen, J. R., Dorison, H., Palancade, B., Brill, S. J., & Mazon, G. (2018). Slx5-Slx8 ubiquitin ligase targets active pools of the Yen1 nuclease to limit crossover formation. *Nat Commun*, *9*(1), 5016. https://doi.org/10.1038/s41467-018-07364-x

Tatham, M. H., Jaffray, E., Vaughan, O. A., Desterro, J. M., Botting, C. H., Naismith, J. H., & Hay, R. T. (2001). Polymeric chains of SUMO-2 and SUMO-3 are conjugated to protein substrates by SAE1/SAE2 and Ubc9. *J Biol Chem*, *276*(38), 35368-35374. https://doi.org/10.1074/jbc.M104214200

Thu, Y. M., Van Riper, S. K., Higgins, L., Zhang, T., Becker, J. R., Markowski, T. W., Nguyen, H. D., Griffin, T. J., & Bielinsky, A. K. (2016). Slx5/Slx8 Promotes Replication Stress Tolerance by Facilitating Mitotic Progression. *Cell Rep*, *15*(6), 1254-1265. https://doi.org/10.1016/j.celrep.2016.04.017

Timney, B. L., Raveh, B., Mironska, R., Trivedi, J. M., Kim, S. J., Russel, D., Wente, S. R., Sali, A., & Rout, M. P. (2016). Simple rules for passive diffusion through the nuclear pore complex. *J Cell Biol*, *215*(1), 57-76. https://doi.org/10.1083/jcb.201601004

Tomimoto, N., Takasaki, T., & Sugiura, R. (2024). Arsenite treatment induces Hsp90 aggregatesdistinct from conventional stress granules in fission yeast. *Microb Cell*, *11*, 242-253. https://doi.org/10.15698/mic2024.07.829

Uzunova, K., Gottsche, K., Miteva, M., Weisshaar, S. R., Glanemann, C., Schnellhardt, M., Niessen, M., Scheel, H., Hofmann, K., Johnson, E. S., Praefcke, G. J., & Dohmen, R. J. (2007). Ubiquitin-dependent proteolytic control of SUMO conjugates. *J Biol Chem*, *282*(47), 34167-34175. https://doi.org/10.1074/jbc.M706505200

Vlastaridis, P., Kyriakidou, P., Chaliotis, A., Van de Peer, Y., Oliver, S. G., & Amoutzias, G. D. (2017). Estimating the total number of phosphoproteins and phosphorylation sites in eukaryotic proteomes. *Gigascience*, *6*(2), 1-11. https://doi.org/10.1093/gigascience/giw015

Wang, Z., & Prelich, G. (2009). Quality control of a transcriptional regulator by SUMO-targeted degradation. *Mol Cell Biol*, *29*(7), 1694-1706. https://doi.org/10.1128/MCB.01470-08

Wedlich-Soldner, R. (2014). A longer life for yeast with good memory. *Dev Cell*, *31*(4), 391-392. https://doi.org/10.1016/j.devcel.2014.11.011

Weiss, E. L. (2012). Mitotic exit and separation of mother and daughter cells. *Genetics*, *192*(4), 1165-1202. https://doi.org/10.1534/genetics.112.145516

Westerbeck, J. W., Pasupala, N., Guillotte, M., Szymanski, E., Matson, B. C., Esteban, C., & Kerscher, O. (2014). A SUMO-targeted ubiquitin ligase is involved in the

degradation of the nuclear pool of the SUMO E3 ligase Siz1. *Mol Biol Cell*, *25*(1), 1-16. https://doi.org/10.1091/mbc.E13-05-0291

Xiao, Y., Pollack, D., Nieves, E., Winchell, A., Callaway, M., & Vigodner, M. (2015). Can your protein be sumoylated? A quick summary and important tips to study SUMO-modified proteins. *Anal Biochem*, *477*, 95-97. https://doi.org/10.1016/j.ab.2014.11.006

Xie, Y., Rubenstein, E. M., Matt, T., & Hochstrasser, M. (2010). SUMO-independent in vivo activity of a SUMO-targeted ubiquitin ligase toward a short-lived transcription factor. *Genes Dev*, *24*(9), 893-903. https://doi.org/10.1101/gad.1906510

Xu, P., Duong, D. M., Seyfried, N. T., Cheng, D., Xie, Y., Robert, J., Rush, J., Hochstrasser, M., Finley, D., & Peng, J. (2009). Quantitative proteomics reveals the function of unconventional ubiquitin chains in proteasomal degradation. *Cell*, *137*(1), 133-145. https://doi.org/10.1016/j.cell.2009.01.041

Xu, Z., Yaguchi, S., & Tsurugi, K. (2004). Gts1p stabilizes oscillations in energy metabolism by activating the transcription of TPS1 encoding trehalose-6-phosphate synthase 1 in the yeast Saccharomyces cerevisiae. *Biochem J*, *383*(Pt 1), 171-178. https://doi.org/10.1042/BJ20040967

Yaguchi, S., & Tsurugi, K. (2003). Gts1p activates SNF1-dependent derepression of HSP104 and TPS1 in the stationary phase of yeast growth. *J Biol Chem*, *278*(32), 29760-29768. https://doi.org/10.1074/jbc.M301441200

Zhang, C., Roberts, T. M., Yang, J., Desai, R., & Brown, G. W. (2006). Suppression of genomic instability by SLX5 and SLX8 in Saccharomyces cerevisiae. *DNA Repair (Amst)*, *5*(3), 336-346. https://doi.org/10.1016/j.dnarep.2005.10.010

Zhang, Z., & Buchman, A. R. (1997). Identification of a member of a DNA-dependent ATPase family that causes interference with silencing. *Mol Cell Biol*, *17*(9), 5461-5472. https://doi.org/10.1128/MCB.17.9.5461

Zhao, X., & Blobel, G. (2005). A SUMO ligase is part of a nuclear multiprotein complex that affects DNA repair and chromosomal organization. *Proc Natl Acad Sci U S A*, *102*(13), 4777-4782. https://doi.org/10.1073/pnas.0500537102

Zhong, Q., Xiao, X., Qiu, Y., Xu, Z., Chen, C., Chong, B., Zhao, X., Hai, S., Li, S., An, Z., & Dai, L. (2023). Protein posttranslational modifications in health and diseases: Functions, regulatory mechanisms, and therapeutic implications. *MedComm (2020)*, *4*(3), e261. https://doi.org/10.1002/mco2.261

Zhou, W., Ryan, J. J., & Zhou, H. (2004). Global analyses of sumoylated proteins in Saccharomyces cerevisiae. Induction of protein sumoylation by cellular stresses. *J Biol Chem*, *279*(31), 32262-32268. https://doi.org/10.1074/jbc.M404173200

Zhou, X., Li, W., Liu, Y., & Amon, A. (2021). Cross-compartment signal propagation in the mitotic exit network. *Elife*, *10*. https://doi.org/10.7554/eLife.63645

# 7 Acknowledgments

First and foremost, I want to thank my supervisor Jürgen. During my whole PhD Jürgen was always happily available to discuss any problems and provided helpful advice. Every time I entered the office with a small question, it turned into a fruitful three-hour discussion, and I left with many new ideas. I am very thankful that you were such a supportive supervisor.

Next I want to thank my TAC and disputation committee. Kay Hofmann and Jan Riemer. Thank you very much for taking the time to listen to my progress and provide valuable feedback and advice. What I most enjoyed about the TAC meetings is that I always left them more motivated than before.

Also, a whole-hearted thank you to Luisa Schmidt who helped me with the preparation of my proteomics and carried out the bioinformatics. Without you this thesis would not be here in this form.

Then I want to thank all members of the Dohmen lab, active as well as graduated. You made this PhD so special for me. We are not only colleagues but friends. This transformed this journey into a very special one for me. I want to thank Paula, Kerstin, Tanja and Merle for always assisting me with any questions I had, as well as with emotional support when experiments were frustrating. I enjoyed the coffee breaks, the brunches and birthday cakes.

Furthermore, I want to specially thank the graduated PhD students in our lab. Jessica, Lenny and Stefan. You were there in the beginning, taught me everything in the lab and supported me when I needed help. But you did not only support me in the lab, but also throughout corona pandemic, when colleagues were the only people you could see I was so happy that you guys were my colleagues and friends. One of course must mention our rounds of kicker with an honorable mention of Kai who taught me how to improve my Kicker game quite a lot. Even though I find myself a little bit sad that now that I spend my whole time finishing my PhD instead of improving my kicker game, he will now never suggest me for their kicker team.

Now onto the current members of our lab Max and Lucie. You guys really made the second half of my PhD so special that I could not imagine doing it without you and it really feels like you were here from the beginning. We share so many memories, a lot of them include Mensa and criticizing Max' near complete vegan plate. But I also treasure our Kicker phase followed by our Pokémon card collection. I am also thankful that you guys took the time and collected a whole binder of Hello Kitty cards just for Linus. Also thank you so much for taking the time to read my thesis and listening to all my troubles during western blotting, writing, and just general Monday tiredness or Friday exhaustion.

Of course, I also want to thank my lab friends, André and Dennis, for all the fun times we had. In the social room, in Mensa or in meet ups after work and providing protocol suggestions or advice along the way.

Last but not least, I want to thank my family without whom I would not have been here. My parents who supported me throughout my whole life in every way either with

advice, financially or with babysitting Linus (a lot). Thank you for enabling me to take such a long time to study and do something I enjoy doing. Next, I want to thank my sister, because it makes life so much more enjoyable of you have somebody who was along your side (nearly) your whole life and who also shares the same values (No, I don’t want to know the answer to puzzle, I want to figure it out myself’) and misses the same things (Why did they get rid of the Schoko-Kirsch-Müsli).

I want to thank my husband Moritz, who is now by my side for half my life and who supported me through all my highs and lows during my PhD and my life and who reminds me that often it’s not that serious and that I worry too much.

Finally, I want to thank my son Linus even though you did not help me with my PhD, one could even say you slowed it down quite a bit, you made it so much more fun and when experiments did not work or everybody was stressed, you were the one always smiling and enjoying every garbage truck and excavator!

# 8 Supplements

**Supplements I**

**Description of Mass spectrometry protocol and bioinformatics provided by Luisa Schmidt (Schmidt, 2024)**

Samples were digested following the standard SP3 protocol (Hughes et al., 2019). Briefly, 20 µg of each washed SP3 beads were added to each well followed by immediately adding one sample volume of acetonitrile (ACN). After the incubation period of 8 min and 2 min on a magnet, supernatant was discarded and magnetic beads were washed 2x with 70% EtOH, 1x with 100% ACN. Samples were digested with 10 µl of 20 ng LysC and 40 ng trypsin dissolved in 50 mM ammonium bicarbonate at 37 °C, 750 rpm overnight. Samples were acidified by using 100 µl 0.1% FA followed by a clean-up with house-made SDB-RPS tips. (De Napoli et al., 2025)

Desalted peptides were reconstituted in 5% FA, 2% ACN in HPLC water. Peptide separation was performed on an nanoElute (upgraded, Bruker) equipped with a 10 cm PepSep column (150 µm inner diameter, 1.5 µm particle size) with an applied 50 min gradient. Mobile phases were compromised of 0.1% FA as solvent A and 0.1% FA in ACN as solvent B. The HPLC system was coupled to a timsTOF pro 2 using a CaptiveSpray source (both Bruker). Samples were measured in dia-PASEF mode with automatized ion mobility calibrated using three ions of Agilent ESI-Low Tuning Mix following vendor specifications. The dia-PASEF window was ranging in dimension 1/k0 0.7-1.45, with 16x2 Th windows and in dimension m/z from 350 to 1250.

Acquired spectra were analyzed with DIA-NN 1.8.1 using library free search against UniProt *S. cerevisiae* database (April 2024). Mass ranges were set according to the settings of the mass spectrometer; mass deviation was set to 15. Data was further processed using R (V 4.2.2), with the libraries: tidyverse, diann, data.table, magrittr, FactoMineR, factoextra and ggplot2, gprofiler, missForest, ggplot2. An in-house modified R-script based on the version by V. Demichev was used to calculate MaxLFQ values (Github page, cit MaxLFQ) (Cox et al., 2014; Demichev et al., 2020). Data input was filtered for unique peptides, q-Value <0.01, Lib.Q.Value <0.01, PG.Q.Value < 0.01, Global.Q.Value < 0.01, Quantity.Quality > 0.7, Fragment.count >= 4. Statistical analysis was performed on the MaxLFQ normalised data with R (V 4.2.2), and Perseus (V.1.6.5.0) and visualized with Instant clue (V 0.10.10.20210315). Data completeness of 70% was calculated on each group. Missing values were imputed by

random forest algorithm for groups with 70% data completeness, with more than 30% missing values random forest algorithm was downshifted of 0.3, width 1.5. Further analysis was performed in perseus (V 1.6.5.0) and InstantClue (V 0.10.10.20211105) (Nolte et al., 2018). ANOVA analysis and Student's T-test analysis was performed with an FDR with less than 0.05 and 500 randomizations. Quality control of iRT peptides were performed in Skyline-Daily (V 22.21.391). (Schmidt, 2024)

# Supplemental Literature


Abramson, J., Adler, J., Dunger, J., Evans, R., Green, T., Pritzel, A., Ronneberger, O., Willmore, L., Ballard, A. J., Bambrick, J., Bodenstein, S. W., Evans, D. A., Hung, C. C., O'Neill, M., Reiman, D., Tunyasuvunakool, K., Wu, Z., Zemgulyte, A., Arvaniti, E., . . . Jumper, J. M. (2024). Accurate structure prediction of biomolecular interactions with AlphaFold 3. *Nature*, *630*(8016), 493-500. https://doi.org/10.1038/s41586-024-07487-w

Agrata, R., & Komander, D. (2025). Ubiquitin-A structural perspective. *Mol Cell*, *85*(2), 323-346. https://doi.org/10.1016/j.molcel.2024.12.015

Albuquerque, C. P., Smolka, M. B., Payne, S. H., Bafna, V., Eng, J., & Zhou, H. (2008). A multidimensional chromatography technology for in-depth phosphoproteome analysis. *Mol Cell Proteomics*, *7*(7), 1389-1396. https://doi.org/10.1074/mcp.M700468-MCP200

Albuquerque, C. P., Wang, G., Lee, N. S., Kolodner, R. D., Putnam, C. D., & Zhou, H. (2013). Distinct SUMO ligases cooperate with Esc2 and Slx5 to suppress duplication-mediated genome rearrangements. *PLoS Genet*, *9*(8), e1003670. https://doi.org/10.1371/journal.pgen.1003670

Bachant, J., Alcasabas, A., Blat, Y., Kleckner, N., & Elledge, S. J. (2002). The SUMO-1 isopeptidase Smt4 is linked to centromeric cohesion through SUMO-1 modification of DNA topoisomerase II. *Mol Cell*, *9*(6), 1169-1182. https://doi.org/10.1016/s1097-2765(02)00543-9

Bauer, S. L., Chen, J., & Astrom, S. U. (2019). Helicase/SUMO-targeted ubiquitin ligase Uls1 interacts with the Holliday junction resolvase Yen1. *PLoS One*, *14*(3), e0214102. https://doi.org/10.1371/journal.pone.0214102

Baugh, J. M., Viktorova, E. G., & Pilipenko, E. V. (2009). Proteasomes can degrade a significant proportion of cellular proteins independent of ubiquitination. *J Mol Biol*, *386*(3), 814-827. https://doi.org/10.1016/j.jmb.2008.12.081

Bhagwat, N. R., Owens, S. N., Ito, M., Boinapalli, J. V., Poa, P., Ditzel, A., Kopparapu, S., Mahalawat, M., Davies, O. R., Collins, S. R., Johnson, J. R., Krogan, N. J., & Hunter, N. (2021). SUMO is a pervasive regulator of meiosis. *Elife*, *10*. https://doi.org/10.7554/eLife.57720

Blaszczak, E., Pasquier, E., Le Dez, G., Odrzywolski, A., Lazarewicz, N., Brossard, A., Fornal, E., Moskalek, P., Wysocki, R., & Rabut, G. (2024). Dissecting Ubiquitylation and DNA Damage Response Pathways in the Yeast Saccharomyces cerevisiae Using a Proteome-Wide Approach. *Mol Cell Proteomics*, *23*(1), 100695. https://doi.org/10.1016/j.mcpro.2023.100695

Bohren, K. M., Nadkarni, V., Song, J. H., Gabbay, K. H., & Owerbach, D. (2004). A M55V polymorphism in a novel SUMO gene (SUMO-4) differentially activates heat shock transcription factors and is associated with susceptibility to type I diabetes mellitus. *J Biol Chem*, *279*(26), 27233-27238. https://doi.org/10.1074/jbc.M402273200

Boorsma, A., de Nobel, H., ter Riet, B., Bargmann, B., Brul, S., Hellingwerf, K. J., & Klis, F. M. (2004). Characterization of the transcriptional response to cell wall stress in Saccharomyces cerevisiae. *Yeast*, *21*(5), 413-427. https://doi.org/10.1002/yea.1109

Borgert, L., Mishra, S., & den Brave, F. (2022). Quality control of cytoplasmic proteins inside the nucleus. *Comput Struct Biotechnol J*, *20*, 4618-4625. https://doi.org/10.1016/j.csbj.2022.08.033

Borkovich, K. A., Farrelly, F. W., Finkelstein, D. B., Taulien, J., & Lindquist, S. (1989). hsp82 is an essential protein that is required in higher concentrations for growth of cells at higher temperatures. *Mol Cell Biol*, *9*(9), 3919-3930. https://doi.org/10.1128/mcb.9.9.3919-3930.1989

Boschetti, E., & Righetti, P. G. (2023). Low-Abundance Protein Enrichment for Medical Applications: The Involvement of Combinatorial Peptide Library Technique. *Int J Mol Sci*, *24*(12). https://doi.org/10.3390/ijms241210329

Brace, J. L., Doerfler, M. D., & Weiss, E. L. (2019). A cell separation checkpoint that enforces the proper order of late cytokinetic events. *J Cell Biol*, *218*(1), 150-170. https://doi.org/10.1083/jcb.201805100

Buchner, J. (2019). Molecular chaperones and protein quality control: an introduction to the JBC Reviews thematic series. *J Biol Chem*, *294*(6), 2074-2075. https://doi.org/10.1074/jbc.REV118.006739

Bylebyl, G. R., Belichenko, I., & Johnson, E. S. (2003). The SUMO isopeptidase Ulp2 prevents accumulation of SUMO chains in yeast. *J Biol Chem*, *278*(45), 44113-44120. https://doi.org/10.1074/jbc.M308357200

Cappadocia, L., & Lima, C. D. (2018). Ubiquitin-like Protein Conjugation: Structures, Chemistry, and Mechanism. *Chem Rev*, *118*(3), 889-918. https://doi.org/10.1021/acs.chemrev.6b00737

Chen, Z., Luo, J., Zhang, Y., Zheng, S., Zhang, H., Huang, Y., Wong, J., & Li, J. (2024). SUMOylation is enriched in the nuclear matrix and required for chromosome segregation. *J Biol Chem*, *300*(1), 105547. https://doi.org/10.1016/j.jbc.2023.105547

Cheng, C. H., Lo, Y. H., Liang, S. S., Ti, S. C., Lin, F. M., Yeh, C. H., Huang, H. Y., & Wang, T. F. (2006). SUMO modifications control assembly of synaptonemal complex and polycomplex in meiosis of Saccharomyces cerevisiae. *Genes Dev*, *20*(15), 2067-2081. https://doi.org/10.1101/gad.1430406

Cohen-Kaplan, V., Livneh, I., Avni, N., Cohen-Rosenzweig, C., & Ciechanover, A. (2016). The ubiquitin-proteasome system and autophagy: Coordinated and independent activities. *Int J Biochem Cell Biol*, *79*, 403-418. https://doi.org/10.1016/j.biocel.2016.07.019

Cook, C. E., Hochstrasser, M., & Kerscher, O. (2009). The SUMO-targeted ubiquitin ligase subunit Slx5 resides in nuclear foci and at sites of DNA breaks. *Cell Cycle*, *8*(7), 1080-1089. https://doi.org/10.4161/cc.8.7.8123

Cox, J., Hein, M. Y., Luber, C. A., Paron, I., Nagaraj, N., & Mann, M. (2014). Accurate proteome-wide label-free quantification by delayed normalization and maximal peptide ratio extraction, termed MaxLFQ. *Mol Cell Proteomics*, *13*(9), 2513-2526. https://doi.org/10.1074/mcp.M113.031591

D'Silva, P. R., Schilke, B., Walter, W., & Craig, E. A. (2005). Role of Pam16's degenerate J domain in protein import across the mitochondrial inner membrane. *Proc Natl Acad Sci U S A*, *102*(35), 12419-12424. https://doi.org/10.1073/pnas.0505969102

Danish, M., & Ahmad, R. (2023). Functional pleiotropy of calcium binding protein Regucalcin in signaling and diseases. *Cell Signal*, *102*, 110533. https://doi.org/10.1016/j.cellsig.2022.110533

Day, A., Schneider, C., & Schneider, B. L. (2004). Yeast cell synchronization. *Methods Mol Biol*, *241*, 55-76. https://doi.org/10.1385/1-59259-646-0:55

De Napoli, C., Schmidt, L., Montesel, M., Cussonneau, L., Sanniti, S., Marcucci, L., Germinario, E., Kindberg, J., Evans, A. L., Gauquelin-Koch, G., Narici, M., Bertile, F., Lefai, E., Kruger, M., Nogara, L., & Blaauw, B. (2025). Reduced ATP turnover during hibernation in relaxed skeletal muscle. *Nat Commun*, *16*(1), 80. https://doi.org/10.1038/s41467-024-55565-4

Demichev, V., Messner, C. B., Vernardis, S. I., Lilley, K. S., & Ralser, M. (2020). DIA-NN: neural networks and interference correction enable deep proteome coverage in high throughput. *Nat Methods*, *17*(1), 41-44. https://doi.org/10.1038/s41592-019-0638-x

Dohmen, R. J., Stappen, R., McGrath, J. P., Forrova, H., Kolarov, J., Goffeau, A., & Varshavsky, A. (1995). An essential yeast gene encoding a homolog of ubiquitin-activating enzyme. *J Biol Chem*, *270*(30), 18099-18109. https://doi.org/10.1074/jbc.270.30.18099

Eckhoff, J., & Dohmen, R. J. (2015). In Vitro Studies Reveal a Sequential Mode of Chain Processing by the Yeast SUMO (Small Ubiquitin-related Modifier)-specific Protease Ulp2. *J Biol Chem*, *290*(19), 12268-12281. https://doi.org/10.1074/jbc.M114.622217

Finley, D., Ulrich, H. D., Sommer, T., & Kaiser, P. (2012). The ubiquitin-proteasome system of Saccharomyces cerevisiae. *Genetics*, *192*(2), 319-360. https://doi.org/10.1534/genetics.112.140467

Frazier, A. E., Dudek, J., Guiard, B., Voos, W., Li, Y., Lind, M., Meisinger, C., Geissler, A., Sickmann, A., Meyer, H. E., Bilanchone, V., Cumsky, M. G., Truscott, K. N., Pfanner, N., & Rehling, P. (2004). Pam16 has an essential role in the mitochondrial protein import motor. *Nat Struct Mol Biol*, *11*(3), 226-233. https://doi.org/10.1038/nsmb735

French, M. E., Koehler, C. F., & Hunter, T. (2021). Emerging functions of branched ubiquitin chains. *Cell Discov*, *7*(1), 6. https://doi.org/10.1038/s41421-020-00237-y

Gao, Y., Ping, L., Duong, D., Zhang, C., Dammer, E. B., Li, Y., Chen, P., Chang, L., Gao, H., Wu, J., & Xu, P. (2021). Mass-Spectrometry-Based Near-Complete Draft of the Saccharomyces cerevisiae Proteome. *J Proteome Res*, *20*(2), 1328-1340. https://doi.org/10.1021/acs.jproteome.0c00721

Gareau, J. R., & Lima, C. D. (2010). The SUMO pathway: emerging mechanisms that shape specificity, conjugation and recognition. *Nat Rev Mol Cell Biol*, *11*(12), 861-871. https://doi.org/10.1038/nrm3011

Gietz, R. D., & Schiestl, R. H. (2007). High-efficiency yeast transformation using the LiAc/SS carrier DNA/PEG method. *Nat Protoc*, *2*(1), 31-34. https://doi.org/10.1038/nprot.2007.13

Girstmair, H., Tippel, F., Lopez, A., Tych, K., Stein, F., Haberkant, P., Schmid, P. W. N., Helm, D., Rief, M., Sattler, M., & Buchner, J. (2019). The Hsp90 isoforms from S. cerevisiae differ in structure, function and client range. *Nat Commun*, *10*(1), 3626. https://doi.org/10.1038/s41467-019-11518-w

Glickman, M. H., Rubin, D. M., Fried, V. A., & Finley, D. (1998). The regulatory particle of the Saccharomyces cerevisiae proteasome. *Mol Cell Biol*, *18*(6), 3149-3162. https://doi.org/10.1128/MCB.18.6.3149

Hannich, J. T., Lewis, A., Kroetz, M. B., Li, S. J., Heide, H., Emili, A., & Hochstrasser, M. (2005). Defining the SUMO-modified proteome by multiple approaches in Saccharomyces cerevisiae. *J Biol Chem*, *280*(6), 4102-4110. https://doi.org/10.1074/jbc.M413209200

Hegde, R. S., & Zavodszky, E. (2019). Recognition and Degradation of Mislocalized Proteins in Health and Disease. *Cold Spring Harb Perspect Biol*, *11*(11). https://doi.org/10.1101/cshperspect.a033902

Holt, L. J., Tuch, B. B., Villen, J., Johnson, A. D., Gygi, S. P., & Morgan, D. O. (2009). Global analysis of Cdk1 substrate phosphorylation sites provides insights into evolution. *Science*, *325*(5948), 1682-1686. https://doi.org/10.1126/science.1172867

Hopfler, M., Kern, M. J., Straub, T., Prytuliak, R., Habermann, B. H., Pfander, B., & Jentsch, S. (2019). Slx5/Slx8-dependent ubiquitin hotspots on chromatin contribute to stress tolerance. *EMBO J*, *38*(11). https://doi.org/10.15252/embj.2018100368

Hostettler, L., Grundy, L., Kaser-Pebernard, S., Wicky, C., Schafer, W. R., & Glauser, D. A. (2017). The Bright Fluorescent Protein mNeonGreen Facilitates Protein Expression Analysis In Vivo. *G3 (Bethesda)*, *7*(2), 607-615. https://doi.org/10.1534/g3.116.038133

Huang, X., Luan, B., Wu, J., & Shi, Y. (2016). An atomic structure of the human 26S proteasome. *Nat Struct Mol Biol*, *23*(9), 778-785. https://doi.org/10.1038/nsmb.3273

Hughes, C. S., Moggridge, S., Muller, T., Sorensen, P. H., Morin, G. B., & Krijgsveld, J. (2019). Single-pot, solid-phase-enhanced sample preparation for proteomics experiments. *Nat Protoc*, *14*(1), 68-85. https://doi.org/10.1038/s41596-018-0082-x

Ii, T., Mullen, J. R., Slagle, C. E., & Brill, S. J. (2007). Stimulation of in vitro sumoylation by Slx5-Slx8: evidence for a functional interaction with the SUMO pathway. *DNA Repair (Amst)*, *6*(11), 1679-1691. https://doi.org/10.1016/j.dnarep.2007.06.004

Iwase, M., & Toh-e, A. (2001). Nis1 encoded by YNL078W: a new neck protein of Saccharomyces cerevisiae. *Genes Genet Syst*, *76*(5), 335-343. https://doi.org/10.1266/ggs.76.335

Johnson, D. I., & Pringle, J. R. (1990). Molecular characterization of CDC42, a Saccharomyces cerevisiae gene involved in the development of cell polarity. *J Cell Biol*, *111*(1), 143-152. https://doi.org/10.1083/jcb.111.1.143

Johnson, E. S. (2004). Protein modification by SUMO. *Annu Rev Biochem*, *73*, 355-382. https://doi.org/10.1146/annurev.biochem.73.011303.074118

Johnson, E. S., & Blobel, G. (1997). Ubc9p is the conjugating enzyme for the ubiquitin-like protein Smt3p. *J Biol Chem*, *272*(43), 26799-26802. https://doi.org/10.1074/jbc.272.43.26799

Johnson, E. S., & Blobel, G. (1999). Cell cycle-regulated attachment of the ubiquitin-related protein SUMO to the yeast septins. *J Cell Biol*, *147*(5), 981-994. https://doi.org/10.1083/jcb.147.5.981

Johnson, E. S., & Gupta, A. A. (2001). An E3-like factor that promotes SUMO conjugation to the yeast septins. *Cell*, *106*(6), 735-744. https://doi.org/10.1016/s0092-8674(01)00491-3

Johnson, E. S., Schwienhorst, I., Dohmen, R. J., & Blobel, G. (1997). The ubiquitin-like protein Smt3p is activated for conjugation to other proteins by an Aos1p/Uba2p

heterodimer. *EMBO J*, *16*(18), 5509-5519. https://doi.org/10.1093/emboj/16.18.5509

Kamitani, T., Kito, K., Nguyen, H. P., Fukuda-Kamitani, T., & Yeh, E. T. (1998). Characterization of a second member of the sentrin family of ubiquitin-like proteins. *J Biol Chem*, *273*(18), 11349-11353. https://doi.org/10.1074/jbc.273.18.11349

Kang, Y., He, Y. X., Zhao, M. X., & Li, W. F. (2011). Structures of native and Fe-substituted SOD2 from Saccharomyces cerevisiae. *Acta Crystallogr Sect F Struct Biol Cryst Commun*, *67*(Pt 10), 1173-1178. https://doi.org/10.1107/S1744309111029186

Keiten-Schmitz, J., Wagner, K., Piller, T., Kaulich, M., Alberti, S., & Muller, S. (2020). The Nuclear SUMO-Targeted Ubiquitin Quality Control Network Regulates the Dynamics of Cytoplasmic Stress Granules. *Mol Cell*, *79*(1), 54-67 e57. https://doi.org/10.1016/j.molcel.2020.05.017

Kerscher, O. (2007). SUMO junction-what's your function? New insights through SUMO-interacting motifs. *EMBO Rep*, *8*(6), 550-555. https://doi.org/10.1038/sj.embor.7400980

Knop, M., Siegers, K., Pereira, G., Zachariae, W., Winsor, B., Nasmyth, K., & Schiebel, E. (1999). Epitope tagging of yeast genes using a PCR-based strategy: more tags and improved practical routines. *Yeast*, *15*(10B), 963-972. https://doi.org/10.1002/(SICI)1097-0061(199907)15:10B<963::AID-YEA399>3.0.CO;2-W

Kolhe, J. A., Babu, N. L., & Freeman, B. C. (2023). The Hsp90 molecular chaperone governs client proteins by targeting intrinsically disordered regions. *Mol Cell*, *83*(12), 2035-2044 e2037. https://doi.org/10.1016/j.molcel.2023.05.021

Kramarz, K., Mucha, S., Litwin, I., Barg-Wojas, A., Wysocki, R., & Dziadkowiec, D. (2017). DNA Damage Tolerance Pathway Choice Through Uls1 Modulation of Srs2 SUMOylation in Saccharomyces cerevisiae. *Genetics*, *206*(1), 513-525. https://doi.org/10.1534/genetics.116.196568

Kroetz, M. B., Su, D., & Hochstrasser, M. (2009). Essential role of nuclear localization for yeast Ulp2 SUMO protease function. *Mol Biol Cell*, *20*(8), 2196-2206. https://doi.org/10.1091/mbc.e08-10-1090

Krukenberg, K. A., Street, T. O., Lavery, L. A., & Agard, D. A. (2011). Conformational dynamics of the molecular chaperone Hsp90. *Q Rev Biophys*, *44*(2), 229-255. https://doi.org/10.1017/S0033583510000314

Kumar, A., Mathew, V., & Stirling, P. C. (2022). Nuclear protein quality control in yeast: The latest INQuiries. *J Biol Chem*, *298*(8), 102199. https://doi.org/10.1016/j.jbc.2022.102199

Kunjappu, M. J., & Hochstrasser, M. (2014). Assembly of the 20S proteasome. *Biochim Biophys Acta*, *1843*(1), 2-12. https://doi.org/10.1016/j.bbamcr.2013.03.008

Kushnirov, V. V. (2000). Rapid and reliable protein extraction from yeast. *Yeast*, *16*(9), 857-860. https://doi.org/10.1002/1097-0061(20000630)16:9<857::AID-YEA561>3.0.CO;2-B

Ladner, C. L., Yang, J., Turner, R. J., & Edwards, R. A. (2004). Visible fluorescent detection of proteins in polyacrylamide gels without staining. *Anal Biochem*, *326*(1), 13-20. https://doi.org/10.1016/j.ab.2003.10.047

Laemmli, U. K. (1970). Cleavage of structural proteins during the assembly of the head of bacteriophage T4. *Nature*, *227*(5259), 680-685. https://doi.org/10.1038/227680a0

Lander, G. C., Estrin, E., Matyskiela, M. E., Bashore, C., Nogales, E., & Martin, A. (2012). Complete subunit architecture of the proteasome regulatory particle. *Nature*, *482*(7384), 186-191. https://doi.org/10.1038/nature10774

Lanz, M. C., Yugandhar, K., Gupta, S., Sanford, E. J., Faca, V. M., Vega, S., Joiner, A. M. N., Fromme, J. C., Yu, H., & Smolka, M. B. (2021). In-depth and 3-dimensional exploration of the budding yeast phosphoproteome. *EMBO Rep*, *22*(2), e51121. https://doi.org/10.15252/embr.202051121

Lascorz, J., Codina-Fabra, J., Reverter, D., & Torres-Rosell, J. (2022). SUMO-SIM interactions: From structure to biological functions. *Semin Cell Dev Biol*, *132*, 193-202. https://doi.org/10.1016/j.semcdb.2021.11.007

Lescasse, R., Pobiega, S., Callebaut, I., & Marcand, S. (2013). End-joining inhibition at telomeres requires the translocase and polySUMO-dependent ubiquitin ligase Uls1. *Embo Journal*, *32*(6), 805-815. https://doi.org/10.1038/emboj.2013.24

Leutert, M., Barente, A. S., Fukuda, N. K., Rodriguez-Mias, R. A., & Villen, J. (2023). The regulatory landscape of the yeast phosphoproteome. *Nat Struct Mol Biol*, *30*(11), 1761-1773. https://doi.org/10.1038/s41594-023-01115-3

Li, S. J., & Hochstrasser, M. (1999). A new protease required for cell-cycle progression in yeast. *Nature*, *398*(6724), 246-251. https://doi.org/10.1038/18457

Li, S. J., & Hochstrasser, M. (2000). The yeast ULP2 (SMT4) gene encodes a novel protease specific for the ubiquitin-like Smt3 protein. *Mol Cell Biol*, *20*(7), 2367-2377. https://doi.org/10.1128/mcb.20.7.2367-2377.2000

Li, S. J., & Hochstrasser, M. (2003). The Ulp1 SUMO isopeptidase: distinct domains required for viability, nuclear envelope localization, and substrate specificity. *J Cell Biol*, *160*(7), 1069-1081. https://doi.org/10.1083/jcb.200212052

Liao, Y., Zhang, W., Liu, Y., Zhu, C., & Zou, Z. (2024). The role of ubiquitination in health and disease. *MedComm (2020)*, *5*(10), e736. https://doi.org/10.1002/mco2.736

Liu, X., Li, J., Gygi, S. P., & Paulo, J. A. (2022). Profiling Yeast Deletion Strains Using Sample Multiplexing and Network-Based Analyses. *J Proteome Res*, *21*(6), 1525-1536. https://doi.org/10.1021/acs.jproteome.2c00137

MacGilvray, M. E., Shishkova, E., Place, M., Wagner, E. R., Coon, J. J., & Gasch, A. P. (2020). Phosphoproteome Response to Dithiothreitol Reveals Unique Versus Shared Features of Saccharomyces cerevisiae Stress Responses. *J Proteome Res*, *19*(8), 3405-3417. https://doi.org/10.1021/acs.jproteome.0c00253

Maga, G., & Hubscher, U. (2003). Proliferating cell nuclear antigen (PCNA): a dancer with many partners. *J Cell Sci*, *116*(Pt 15), 3051-3060. https://doi.org/10.1242/jcs.00653

Mahajan, R., Delphin, C., Guan, T., Gerace, L., & Melchior, F. (1997). A small ubiquitin-related polypeptide involved in targeting RanGAP1 to nuclear pore complex protein RanBP2. *Cell*, *88*(1), 97-107. https://doi.org/10.1016/s0092-8674(00)81862-0

Malinovska, L., Kroschwald, S., Munder, M. C., Richter, D., & Alberti, S. (2012). Molecular chaperones and stress-inducible protein-sorting factors coordinate the spatiotemporal distribution of protein aggregates. *Mol Biol Cell*, *23*(16), 3041-3056. https://doi.org/10.1091/mbc.E12-03-0194

Mascle, X. H., Lussier-Price, M., Cappadocia, L., Estephan, P., Raiola, L., Omichinski, J. G., & Aubry, M. (2013). Identification of a non-covalent ternary complex formed by PIAS1, SUMO1, and UBC9 proteins involved in transcriptional regulation. *J Biol Chem*, *288*(51), 36312-36327. https://doi.org/10.1074/jbc.M113.486845

Matias, A. C., Ramos, P. C., & Dohmen, R. J. (2010). Chaperone-assisted assembly of the proteasome core particle. *Biochem Soc Trans*, *38*(Pt 1), 29-33. https://doi.org/10.1042/BST0380029

Matunis, M. J., Coutavas, E., & Blobel, G. (1996). A novel ubiquitin-like modification modulates the partitioning of the Ran-GTPase-activating protein RanGAP1 between the cytosol and the nuclear pore complex. *J Cell Biol*, *135*(6 Pt 1), 1457-1470. https://doi.org/10.1083/jcb.135.6.1457

McGrath, J. P., Jentsch, S., & Varshavsky, A. (1991). UBA 1: an essential yeast gene encoding ubiquitin-activating enzyme. *EMBO J*, *10*(1), 227-236. https://doi.org/10.1002/j.1460-2075.1991.tb07940.x

Meitinger, F., Khmelinskii, A., Morlot, S., Kurtulmus, B., Palani, S., Andres-Pons, A., Hub, B., Knop, M., Charvin, G., & Pereira, G. (2014). A memory system of negative polarity cues prevents replicative aging. *Cell*, *159*(5), 1056-1069. https://doi.org/10.1016/j.cell.2014.10.014

Melchior, F. (2000). SUMO--nonclassical ubiquitin. *Annu Rev Cell Dev Biol*, *16*, 591-626. https://doi.org/10.1146/annurev.cellbio.16.1.591

Meluh, P. B., & Koshland, D. (1995). Evidence that the MIF2 gene of Saccharomyces cerevisiae encodes a centromere protein with homology to the mammalian centromere protein CENP-C. *Mol Biol Cell*, *6*(7), 793-807. https://doi.org/10.1091/mbc.6.7.793

Messner, C. B., Demichev, V., Muenzner, J., Aulakh, S. K., Barthel, N., Rohl, A., Herrera-Dominguez, L., Egger, A. S., Kamrad, S., Hou, J., Tan, G., Lemke, O., Calvani, E., Szyrwiel, L., Mulleder, M., Lilley, K. S., Boone, C., Kustatscher, G., & Ralser, M. (2023). The proteomic landscape of genome-wide genetic perturbations. *Cell*, *186*(9), 2018-2034 e2021. https://doi.org/10.1016/j.cell.2023.03.026

Miller, S. B., Ho, C. T., Winkler, J., Khokhrina, M., Neuner, A., Mohamed, M. Y., Guilbride, D. L., Richter, K., Lisby, M., Schiebel, E., Mogk, A., & Bukau, B. (2015). Compartment-specific aggregases direct distinct nuclear and cytoplasmic aggregate deposition. *EMBO J*, *34*(6), 778-797. https://doi.org/10.15252/embj.201489524

Mokranjac, D., Bourenkov, G., Hell, K., Neupert, W., & Groll, M. (2006). Structure and function of Tim14 and Tim16, the J and J-like components of the mitochondrial protein import motor. *EMBO J*, *25*(19), 4675-4685. https://doi.org/10.1038/sj.emboj.7601334

Mollapour, M., Bourboulia, D., Beebe, K., Woodford, M. R., Polier, S., Hoang, A., Chelluri, R., Li, Y., Guo, A., Lee, M. J., Fotooh-Abadi, E., Khan, S., Prince, T., Miyajima, N., Yoshida, S., Tsutsumi, S., Xu, W., Panaretou, B., Stetler-Stevenson, W. G., . . . Neckers, L. (2014). Asymmetric Hsp90 N domain SUMOylation recruits Aha1 and ATP-competitive inhibitors. *Mol Cell*, *53*(2), 317-329. https://doi.org/10.1016/j.molcel.2013.12.007

Moreno-Gonzalez, I., & Soto, C. (2011). Misfolded protein aggregates: mechanisms, structures and potential for disease transmission. *Semin Cell Dev Biol*, *22*(5), 482-487. https://doi.org/10.1016/j.semcdb.2011.04.002

Mosley, A. L., Florens, L., Wen, Z., & Washburn, M. P. (2009). A label free quantitative proteomic analysis of the Saccharomyces cerevisiae nucleus. *J Proteomics*, *72*(1), 110-120. https://doi.org/10.1016/j.jprot.2008.10.008

Mullen, J. R., Kaliraman, V., Ibrahim, S. S., & Brill, S. J. (2001). Requirement for three novel protein complexes in the absence of the Sgs1 DNA helicase in Saccharomyces cerevisiae. *Genetics*, *157*(1), 103-118. https://www.ncbi.nlm.nih.gov/pubmed/11139495

Müller, J., Furlan, M., Settele, D., Grupp, B., & Johnsson, N. (2024). Transient septin sumoylation steers a Fir1-Skt5 protein complex between the split septin ring. *J Cell Biol*, *223*(1). https://doi.org/10.1083/jcb.202301027

Neiman, A. M. (2011). Sporulation in the budding yeast Saccharomyces cerevisiae. *Genetics*, *189*(3), 737-765. https://doi.org/10.1534/genetics.111.127126

Niskanen, E. A., Malinen, M., Sutinen, P., Toropainen, S., Paakinaho, V., Vihervaara, A., Joutsen, J., Kaikkonen, M. U., Sistonen, L., & Palvimo, J. J. (2015). Global SUMOylation on active chromatin is an acute heat stress response restricting transcription. *Genome Biol*, *16*(1), 153. https://doi.org/10.1186/s13059-015-0717-y

Nolte, H., MacVicar, T. D., Tellkamp, F., & Kruger, M. (2018). Instant Clue: A Software Suite for Interactive Data Visualization and Analysis. *Sci Rep*, *8*(1), 12648. https://doi.org/10.1038/s41598-018-31154-6

Ohkuni, K., Takahashi, Y., Fulp, A., Lawrimore, J., Au, W. C., Pasupala, N., Levy-Myers, R., Warren, J., Strunnikov, A., Baker, R. E., Kerscher, O., Bloom, K., & Basrai, M. A. (2016). SUMO-Targeted Ubiquitin Ligase (STUbL) Slx5 regulates proteolysis of centromeric histone H3 variant Cse4 and prevents its mislocalization to euchromatin. *Mol Biol Cell*, *27*(9), 1500-1510. https://doi.org/10.1091/mbc.E15-12-0827

Ostapenko, D., Burton, J. L., & Solomon, M. J. (2012). Identification of anaphase promoting complex substrates in S. cerevisiae. *PLoS One*, *7*(9), e45895. https://doi.org/10.1371/journal.pone.0045895

Paasch, F., den Brave, F., Psakhye, I., Pfander, B., & Jentsch, S. (2018). Failed mitochondrial import and impaired proteostasis trigger SUMOylation of mitochondrial proteins. *J Biol Chem*, *293*(2), 599-609. https://doi.org/10.1074/jbc.M117.817833

Palma, F. R., He, C. X., Danes, J. M., Paviani, V., Coelho, D. R., Gantner, B. N., & Bonini, M. G. (2020). Mitochondrial Superoxide Dismutase: What the Established, the Intriguing, and the Novel Reveal About a Key Cellular Redox Switch. *Antioxidants & Redox Signaling*, *32*(10), 701-714. https://doi.org/10.1089/ars.2019.7962

Parker, J. L., & Ulrich, H. D. (2012). A SUMO-interacting motif activates budding yeast ubiquitin ligase Rad18 towards SUMO-modified PCNA. *Nucleic Acids Res*, *40*(22), 11380-11388. https://doi.org/10.1093/nar/gks892

Peng, B., Williams, T. C., Henry, M., Nielsen, L. K., & Vickers, C. E. (2015). Controlling heterologous gene expression in yeast cell factories on different carbon substrates and across the diauxic shift: a comparison of yeast promoter activities. *Microb Cell Fact*, *14*, 91. https://doi.org/10.1186/s12934-015-0278-5

Perez, A. M., & Thorner, J. (2019). Septin-associated proteins Aim44 and Nis1 traffic between the bud neck and the nucleus in the yeast Saccharomyces cerevisiae. *Cytoskeleton (Hoboken)*, *76*(1), 15-32. https://doi.org/10.1002/cm.21500

Pichler, A., Gast, A., Seeler, J. S., Dejean, A., & Melchior, F. (2002). The nucleoporin RanBP2 has SUMO1 E3 ligase activity. *Cell*, *108*(1), 109-120. https://doi.org/10.1016/s0092-8674(01)00633-x

Pichler, A., Knipscheer, P., Saitoh, H., Sixma, T. K., & Melchior, F. (2004). The RanBP2 SUMO E3 ligase is neither HECT- nor RING-type. *Nat Struct Mol Biol*, *11*(10), 984-991. https://doi.org/10.1038/nsmb834

Pickart, C. M., & Fushman, D. (2004). Polyubiquitin chains: polymeric protein signals. *Curr Opin Chem Biol*, *8*(6), 610-616. https://doi.org/10.1016/j.cbpa.2004.09.009

Pohl, C., & Dikic, I. (2019). Cellular quality control by the ubiquitin-proteasome system and autophagy. *Science*, *366*(6467), 818-822. https://doi.org/10.1126/science.aax3769

Praefcke, G. J., Hofmann, K., & Dohmen, R. J. (2012). SUMO playing tag with ubiquitin. *Trends Biochem Sci*, *37*(1), 23-31. https://doi.org/10.1016/j.tibs.2011.09.002

Ramazi, S., & Zahiri, J. (2021). Posttranslational modifications in proteins: resources, tools and prediction methods. *Database (Oxford)*, *2021*. https://doi.org/10.1093/database/baab012

Reverter, D., & Lima, C. D. (2005). Insights into E3 ligase activity revealed by a SUMO-RanGAP1-Ubc9-Nup358 complex. *Nature*, *435*(7042), 687-692. https://doi.org/10.1038/nature03588

Rolli, S., Langridge, C. A., & Sontag, E. M. (2024). Clearing the JUNQ: the molecular machinery for sequestration, localization, and degradation of the JUNQ compartment. *Front Mol Biosci*, *11*, 1427542. https://doi.org/10.3389/fmolb.2024.1427542

Rothe, S., Prakash, A., & Tyedmers, J. (2018). The Insoluble Protein Deposit (IPOD) in Yeast. *Front Mol Neurosci*, *11*, 237. https://doi.org/10.3389/fnmol.2018.00237

Rytinki, M. M., Kaikkonen, S., Pehkonen, P., Jaaskelainen, T., & Palvimo, J. J. (2009). PIAS proteins: pleiotropic interactors associated with SUMO. *Cell Mol Life Sci*, *66*(18), 3029-3041. https://doi.org/10.1007/s00018-009-0061-z

Saeki, Y., & Tanaka, K. (2012). Assembly and function of the proteasome. *Methods Mol Biol*, *832*, 315-337. https://doi.org/10.1007/978-1-61779-474-2_22

Schmidt, L. M. (2024). *Advanced Proteomics of Skeletal Muscles: Spatial and Single Fiber Insights into Metabolic Diversity* University of Cologne].

Schweiggert, J., Stevermann, L., Panigada, D., Kammerer, D., & Liakopoulos, D. (2016). Regulation of a Spindle Positioning Factor at Kinetochores by SUMO-Targeted Ubiquitin Ligases. *Dev Cell*, *36*(4), 415-427. https://doi.org/10.1016/j.devcel.2016.01.011

Schwienhorst, I., Johnson, E. S., & Dohmen, R. J. (2000). SUMO conjugation and deconjugation. *Mol Gen Genet*, *263*(5), 771-786. https://doi.org/10.1007/s004380000254

Sengupta, S., & Pick, E. (2023). The Ubiquitin-like Proteins of Saccharomyces cerevisiae. *Biomolecules*, *13*(5). https://doi.org/10.3390/biom13050734

Shah, P. P., Zheng, X., Epshtein, A., Carey, J. N., Bishop, D. K., & Klein, H. L. (2010). Swi2/Snf2-related translocases prevent accumulation of toxic Rad51 complexes during mitotic growth. *Mol Cell*, *39*(6), 862-872. https://doi.org/10.1016/j.molcel.2010.08.028

Shakya, V. P., Barbeau, W. A., Xiao, T., Knutson, C. S., Schuler, M. H., & Hughes, A. L. (2021). A nuclear-based quality control pathway for non-imported mitochondrial proteins. *Elife*, *10*. https://doi.org/10.7554/eLife.61230

Shen, Z., Pardington-Purtymun, P. E., Comeaux, J. C., Moyzis, R. K., & Chen, D. J. (1996). Associations of UBE2I with RAD52, UBL1, p53, and RAD51 proteins in a yeast two-hybrid system. *Genomics*, *37*(2), 183-186. https://doi.org/10.1006/geno.1996.0540

Soares Rodrigues, C. I., den Ridder, M., Pabst, M., Gombert, A. K., & Wahl, S. A. (2023). Comparative proteome analysis of different Saccharomyces cerevisiae strains during growth on sucrose and glucose. *Sci Rep*, *13*(1), 2126. https://doi.org/10.1038/s41598-023-29172-0

Sriramachandran, A. M., & Dohmen, R. J. (2014). SUMO-targeted ubiquitin ligases. *Biochim Biophys Acta*, *1843*(1), 75-85. https://doi.org/10.1016/j.bbamcr.2013.08.022

Stade, K., Vogel, F., Schwienhorst, I., Meusser, B., Volkwein, C., Nentwig, B., Dohmen, R. J., & Sommer, T. (2002). A lack of SUMO conjugation affects cNLS-dependent nuclear protein import in yeast. *J Biol Chem*, *277*(51), 49554-49561. https://doi.org/10.1074/jbc.M207991200

Stehmeier, P., & Muller, S. (2009). Phospho-regulated SUMO interaction modules connect the SUMO system to CK2 signaling. *Mol Cell*, *33*(3), 400-409. https://doi.org/10.1016/j.molcel.2009.01.013

Sternsdorf, T., Jensen, K., & Will, H. (1997). Evidence for covalent modification of the nuclear dot-associated proteins PML and Sp100 by PIC1/SUMO-1. *J Cell Biol*, *139*(7), 1621-1634. https://doi.org/10.1083/jcb.139.7.1621

Stockwell, S. R., Landry, C. R., & Rifkin, S. A. (2015). The yeast galactose network as a quantitative model for cellular memory. *Mol Biosyst*, *11*(1), 28-37. https://doi.org/10.1039/c4mb00448e

Sun, Y., Miller Jenkins, L. M., Su, Y. P., Nitiss, K. C., Nitiss, J. L., & Pommier, Y. (2020). A conserved SUMO pathway repairs topoisomerase DNA-protein cross-links by engaging ubiquitin-mediated proteasomal degradation. *Sci Adv*, *6*(46). https://doi.org/10.1126/sciadv.aba6290

Swaney, D. L., Beltrao, P., Starita, L., Guo, A., Rush, J., Fields, S., Krogan, N. J., & Villen, J. (2013). Global analysis of phosphorylation and ubiquitylation cross-talk in protein degradation. *Nat Methods*, *10*(7), 676-682. https://doi.org/10.1038/nmeth.2519

Takahashi, Y., Toh-e, A., & Kikuchi, Y. (2001). A novel factor required for the SUMO1/Smt3 conjugation of yeast septins. *Gene*, *275*(2), 223-231. https://doi.org/10.1016/s0378-1119(01)00662-x

Talhaoui, I., Bernal, M., Mullen, J. R., Dorison, H., Palancade, B., Brill, S. J., & Mazon, G. (2018). Slx5-Slx8 ubiquitin ligase targets active pools of the Yen1 nuclease to limit crossover formation. *Nat Commun*, *9*(1), 5016. https://doi.org/10.1038/s41467-018-07364-x

Tatham, M. H., Jaffray, E., Vaughan, O. A., Desterro, J. M., Botting, C. H., Naismith, J. H., & Hay, R. T. (2001). Polymeric chains of SUMO-2 and SUMO-3 are conjugated to protein substrates by SAE1/SAE2 and Ubc9. *J Biol Chem*, *276*(38), 35368-35374. https://doi.org/10.1074/jbc.M104214200

Thu, Y. M., Van Riper, S. K., Higgins, L., Zhang, T., Becker, J. R., Markowski, T. W., Nguyen, H. D., Griffin, T. J., & Bielinsky, A. K. (2016). Slx5/Slx8 Promotes Replication Stress Tolerance by Facilitating Mitotic Progression. *Cell Rep*, *15*(6), 1254-1265. https://doi.org/10.1016/j.celrep.2016.04.017

Timney, B. L., Raveh, B., Mironska, R., Trivedi, J. M., Kim, S. J., Russel, D., Wente, S. R., Sali, A., & Rout, M. P. (2016). Simple rules for passive diffusion through the nuclear pore complex. *J Cell Biol*, *215*(1), 57-76. https://doi.org/10.1083/jcb.201601004

Tomimoto, N., Takasaki, T., & Sugiura, R. (2024). Arsenite treatment induces Hsp90 aggregatesdistinct from conventional stress granules in fission yeast. *Microb Cell*, *11*, 242-253. https://doi.org/10.15698/mic2024.07.829

Uzunova, K., Gottsche, K., Miteva, M., Weisshaar, S. R., Glanemann, C., Schnellhardt, M., Niessen, M., Scheel, H., Hofmann, K., Johnson, E. S., Praefcke, G. J., & Dohmen, R. J. (2007). Ubiquitin-dependent proteolytic control of SUMO conjugates. *J Biol Chem*, *282*(47), 34167-34175. https://doi.org/10.1074/jbc.M706505200

Vlastaridis, P., Kyriakidou, P., Chaliotis, A., Van de Peer, Y., Oliver, S. G., & Amoutzias, G. D. (2017). Estimating the total number of phosphoproteins and phosphorylation sites in eukaryotic proteomes. *Gigascience*, *6*(2), 1-11. https://doi.org/10.1093/gigascience/giw015

Wang, Z., & Prelich, G. (2009). Quality control of a transcriptional regulator by SUMO-targeted degradation. *Mol Cell Biol*, *29*(7), 1694-1706. https://doi.org/10.1128/MCB.01470-08

Wedlich-Soldner, R. (2014). A longer life for yeast with good memory. *Dev Cell*, *31*(4), 391-392. https://doi.org/10.1016/j.devcel.2014.11.011

Weiss, E. L. (2012). Mitotic exit and separation of mother and daughter cells. *Genetics*, *192*(4), 1165-1202. https://doi.org/10.1534/genetics.112.145516

Westerbeck, J. W., Pasupala, N., Guillotte, M., Szymanski, E., Matson, B. C., Esteban, C., & Kerscher, O. (2014). A SUMO-targeted ubiquitin ligase is involved in the degradation of the nuclear pool of the SUMO E3 ligase Siz1. *Mol Biol Cell*, *25*(1), 1-16. https://doi.org/10.1091/mbc.E13-05-0291

Xiao, Y., Pollack, D., Nieves, E., Winchell, A., Callaway, M., & Vigodner, M. (2015). Can your protein be sumoylated? A quick summary and important tips to study SUMO-modified proteins. *Anal Biochem*, *477*, 95-97. https://doi.org/10.1016/j.ab.2014.11.006

Xie, Y., Rubenstein, E. M., Matt, T., & Hochstrasser, M. (2010). SUMO-independent in vivo activity of a SUMO-targeted ubiquitin ligase toward a short-lived transcription factor. *Genes Dev*, *24*(9), 893-903. https://doi.org/10.1101/gad.1906510

Xu, P., Duong, D. M., Seyfried, N. T., Cheng, D., Xie, Y., Robert, J., Rush, J., Hochstrasser, M., Finley, D., & Peng, J. (2009). Quantitative proteomics reveals the function of unconventional ubiquitin chains in proteasomal degradation. *Cell*, *137*(1), 133-145. https://doi.org/10.1016/j.cell.2009.01.041

Xu, Z., Yaguchi, S., & Tsurugi, K. (2004). Gts1p stabilizes oscillations in energy metabolism by activating the transcription of TPS1 encoding trehalose-6-phosphate synthase 1 in the yeast Saccharomyces cerevisiae. *Biochem J*, *383*(Pt 1), 171-178. https://doi.org/10.1042/BJ20040967

Yaguchi, S., & Tsurugi, K. (2003). Gts1p activates SNF1-dependent derepression of HSP104 and TPS1 in the stationary phase of yeast growth. *J Biol Chem*, *278*(32), 29760-29768. https://doi.org/10.1074/jbc.M301441200

Zhang, C., Roberts, T. M., Yang, J., Desai, R., & Brown, G. W. (2006). Suppression of genomic instability by SLX5 and SLX8 in Saccharomyces cerevisiae. *DNA Repair (Amst)*, *5*(3), 336-346. https://doi.org/10.1016/j.dnarep.2005.10.010

Zhang, Z., & Buchman, A. R. (1997). Identification of a member of a DNA-dependent ATPase family that causes interference with silencing. *Mol Cell Biol*, *17*(9), 5461-5472. https://doi.org/10.1128/MCB.17.9.5461

Zhao, X., & Blobel, G. (2005). A SUMO ligase is part of a nuclear multiprotein complex that affects DNA repair and chromosomal organization. *Proc Natl Acad Sci U S A*, *102*(13), 4777-4782. https://doi.org/10.1073/pnas.0500537102

Zhong, Q., Xiao, X., Qiu, Y., Xu, Z., Chen, C., Chong, B., Zhao, X., Hai, S., Li, S., An, Z., & Dai, L. (2023). Protein posttranslational modifications in health and diseases: Functions, regulatory mechanisms, and therapeutic implications. *MedComm (2020)*, *4*(3), e261. https://doi.org/10.1002/mco2.261

Zhou, W., Ryan, J. J., & Zhou, H. (2004). Global analyses of sumoylated proteins in Saccharomyces cerevisiae. Induction of protein sumoylation by cellular stresses. *J Biol Chem*, *279*(31), 32262-32268. https://doi.org/10.1074/jbc.M404173200

Zhou, X., Li, W., Liu, Y., & Amon, A. (2021). Cross-compartment signal propagation in the mitotic exit network. *Elife*, *10*. https://doi.org/10.7554/eLife.63645